Universidad Autónoma de San Luis Potosí
Facultad de Ingeniería
Centro de Investigación y Estudios de Posgrado

Modelado y Control de Sistemas de Orden Fraccionario. El Caso de Sistemas Lineales

T E S I S

Que para obtener el grado de:

Maestro en Ingeniería Eléctrica
Opción en Control Automático

Presenta:
Adrián Josué Guel Cortez

Asesor:
Dr. Emilio Jorge González Galván

Co-asesor:
Dr. César Fernando Francisco Méndez Barrios

San Luis Potosí, S. L. P. Octubre de 2018

Índice general

UASLP
Universidad Autónoma
de San Luis Potosí

21 de junio de 2018

ING. ADRIÁN JOSUÉ GUEL CORTEZ
P R E S E N T E.

En atención a su solicitud de Temario, presentada por los **Dres. Emilio Jorge González Galván y César Fernando Francisco Méndez Barrios**, Asesor y Co-asesor de la Tesis que desarrollará Usted con el objeto de obtener el Grado de **Maestro en Ingeniería Eléctrica**, me es grato comunicarle que en la Sesión del H. Consejo Técnico Consultivo celebrada el día 21 de junio del presente, fue aprobado el Temario propuesto:

TEMARIO:

"Modelado y Control de Sistemas de Orden Fraccionario. El caso de Sistemas Lineales"

Introducción.
1. Preliminares sobre sistemas de orden fraccionario.
2. Modelado matemático de sistemas de orden fraccionario.
3. Estabilidad de sistemas de orden fraccionario.
4. Diseño de controladores PD^{μ} y PI^{λ} de orden fraccionario
5. Aplicaciones prácticas de controladores de orden fraccionario.

Conclusiones.
Referencias.

"MODOS ET CUNCTARUM RERUM MENSURAS AUDEBO"

A T E N T A M E N T E

M. I. JORGE ALBERTO PÉREZ GONZÁLEZ
DIRECTOR.

UNIVERSIDAD AUTONOMA
DE SAN LUIS POTOSI
FACULTAD DE INGENIERIA
DIRECCION

FACULTAD DE
INGENIERÍA
Av. Manuel Nava 8
Zona Universitaria • CP 78290
San Luis Potosí, S.L.P.
tel. (444) 826 2330 al39
fax (444) 826 2336
www.uaslp.mx

Copia. Archivo.
*etn.

ADRIÁN JOSUÉ GUEL CORTEZ

MODELING AND CONTROL OF FRACTIONAL ORDER SYSTEMS. THE LINEAR SYSTEMS CASE

CENTRO DE INVESTIGACIÓN Y ESTUDIOS DE POSGRADO, UASLP-FACULTAD DE INGENIERÍA.

PUBLISHED BY CENTRO DE INVESTIGACIÓN Y ESTUDIOS DE POSGRADO, UASLP-FACULTAD DE INGENIERÍA.

http://ciep.ing.uaslp.mx/electrica/

First printing, October 2018

Agradecimientos

A lo largo de estos dos años he pasado momentos difíciles que me han exigido sobrepasar mis límites, momentos de completa incertidumbre y sobre todo de una constante duda. Una duda que me ha hecho experimentar esa curiosidad que da energía para seguir a pesar de estar completamente exhausto.

Ha sido en este proceso cuando he tenido la fortuna de conocer y estar cerca de gente increíble. Agradezco primeramente al Dr. César M. quien me ha formado en gran medida en los campos de matemáticas y teoría de control y que gracias a él he podido desarrollar este trabajo en el área del *Cálculo Fraccionario*, al Dr. *Emilio G.* por el apoyo, las diversas atenciones y por creer en mi trabajo. Agradezco al equipo de *Control automático* (como yo lo llamo) que con ayuda de nuestras discusiones y encuentros enriquecí mi experiencia a: *Enrique D.*, *Carlos C.*, *David N.*, *Alex M.*, Carmen L. & *Alfredo A.*. A mis amigos y compañeros del laboratorio de *Robótica* y de generación, en especial a *Yuniel L.* y *M. Cobian.*

A todo el equipo de *profesores* con los que tomé alguna materia en el *Centro de Investigación y Estudios de Posgrado* de la Universidad Autónoma de San Luis Potosí (incluyendo su Facultad de Ingeniería) o en el *Instituto Potosino de Investigación Científica y Tecnológica*. Menciono especialmente a los Drs. *Homero M.*, *R. Salas*, *A. Salas*, *E. Carbajal*, *L. Félix*, *A. Cárdenas*, *D. Langarica* y *Azahel R.*. Además, es obvio mi agradecimiento a CONACyT y COPOCyT por el apoyo económico que me brindaron para poder cumplir con esta meta y al Dr. *Morales Saldaña* por su apoyo como coordinador de mi posgrado.

Agradezco a los Drs. *Mihir Sen* y *Bill Goodwine* de la *Universidad de Notre Dame*, por su colaboración en el desarrollo de algunos resultados de esta tesis, la invitación y éxito en la estancia de colaboración que realicé en su universidad, el interés en mi trabajo y las largas discusiones sobre la *Física* detrás del *Cálculo Fraccionario*.

Para finalizar, es infinito el agradecimiento que debo a mi familia en especial a mi madre *María C.* a quien debo todo, a mi amada *Zareth M.* que complementa mi vida y finalmente a mi segunda familia la *Sociedad Teosófica* cuyos objetivos enriquecen mi vida.

Contents

List of Figures

List of Symbols

$\forall$	Universal quantification which is interpreted as *given any* or *for all*.
$\exists$	Existential quantification which is interpreted as *there exists*, *there is at least one*, or *for some*.
$\in$	Set membership which is interpreted as *is an element of*.
$\mathbb{C}$	Field of complex numbers.
$\mathbb{R}$	Field of real numbers.
$\mathbb{R}^-$	Negative real numbers.
$\mathbb{R}^+$	Positive real numbers.
$j := \sqrt{-1}$	Imaginary number.
$\Re[z]$	Real part of $z \in \mathbb{C}$.
$\Im[z]$	Imaginary part of z.
$\mathscr{L}$	Laplace transformation.
$\mathscr{L}^{-1}$	Inverse Laplace transformation.
$\mathbb{N}$	The set of natural numbers.
$\mathbb{Q}$	The set of rational numbers.
t	Independent real variable, in engineering problems time.
$\mathbb{Z}$	The set of integer numbers.
$\Gamma(x)$	Gamma function.
ω	Angular frequency (in rad/s).
$\binom{a}{b}$	Newton Binomial.
$\lfloor x \rfloor$	Floor of $x \in \mathbb{R}$, that is to say, $\max\{n \in \mathbb{Z} : n \leq x\}$.
$\lceil x \rceil$	Ceiling of $x \in \mathbb{R}$, that is to say, $\min\{n \in \mathbb{Z} : n \geq x\}$.
$E_{\alpha,\beta}(t)$	Two parameter Mittag-Leffler function.
$\mathbb{X}^+$	Set of positive elements of $\mathbb{X}$ (which may be $\mathbb{Z}$, $\mathbb{Q}$ or $\mathbb{R}$).
$\mathbb{X}^-$	Set of negative elements of $\mathbb{X}$ (which may be $\mathbb{Z}$, $\mathbb{Q}$ or $\mathbb{R}$).
$\bigcup$	Union set.
$\mathbb{X}_0^+$	$\mathbb{X}^+ \bigcup \{0\}$.
$\mathbb{X}_0^-$	$\mathbb{X}^- \bigcup \{0\}$.
$\blacksquare$	Marks the end of proofs.
s	Complex numbers , usually transform of t in the Laplace domain.
$\bar{z}$	Complex conjugate of $z \in \mathbb{C}$.
$\arg(z)$	Main argument of $z \in \mathbb{C}$ i.e. $\arg(z) \in (-\pi, \pi)$.
$\lvert x \rvert$	Absolute value $x \in \mathbb{R}$.
$\langle x, y \rangle$	Scalar product of $x, y \in \mathbb{C}^n$ which is denoted by $\langle x, y \rangle = y^H x$, where y^H is the complex conjugate transpose of y.
$\mathrm{lcm}(a, b)$	Least common multiple of the pair (a, b) with $a, b \in \mathbb{N}$.
$\mathrm{den}\left(\frac{a}{b}\right)$	Denominator of the pair (a, b) with $a, b \in \mathbb{N}$.
$\mathcal{L}$	Linear laplace transformed operator.
$\mathbf{L}$	Linear operator.
$\mathbb{C} \setminus \mathbb{R}^-$	Set of complex numbers less the negative real numbers.
$\mathcal{D}$	Derivative operator $\mathcal{D} = \frac{d}{dt}$.
$\parallel x \parallel$	Euclidean norm of a vector x, with n elements, given by $\sqrt{\sum_{k=1}^{n} a_k^2}$.
$\mathbf{I}$	Identity operator.
$J_0(\cdot)$	Bessel function.
$I_0(\cdot)$	Modified Bessel function.

Abbreviations

FIR	Finite Impulse Response (filter).
IIR	Infinite Impulse Response (filter).
SISO	Single-Input, Single-Output (system).
LTI	Linear Time Invariant (system).
BC	Branch Cut.
BP	Branch Point.
ILT	Inverse Laplace Transform.
RHP	Right Half Plane, refers to the set of complex numbers with strictly positive real part.
LHP	Left Half Plane, refers to the set of complex numbers with strictly negative real part.
BIBO	Bounded-Input, Bounded-Output.

Introduction

Automatic control is a branch of scientific research that deals, amongst other things, with automatons. In our daily lives, we keep surrounded by automated systems, such as battery chargers, cruise control mechanisms in cars, automatic pilots for aircrafts and rockets, and so on. These dynamic systems require continuous control to ensure that their function in question is maintained. Engineers in automatic control work in the fields of domestic appliances, automobiles, aerospace, chemical process, wastewater management, 3D printers and so on.

Automatic control implies different problems to solve (see, Fig. 1). In fact automatic control can be seen as natural conclusion of systems analysis. Nowadays, the study of complex system dynamics theory implies that we are actually studying simplifications of the real-physical systems and that we need techniques to simplify the analysis but to improve the accuracy of our models (Bar-Yam, 1997). The diagram shown in Fig. 2 (Based on a diagram created by Hiroki Sayama, D.Sc., Collective Dynamics of Complex Systems (CoCo) Research Group at Binghamton University, State University of New York, 26 November 2010.) allow us to appreciate some of the multiple areas of research that try to find depeer understanding to the physical phenomena.

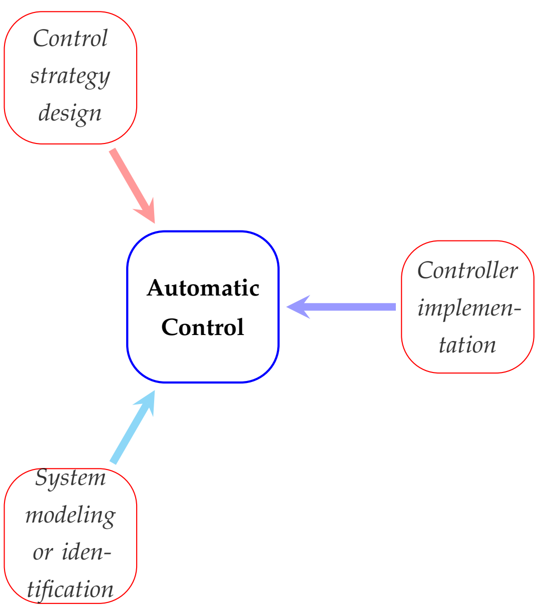

Figure 1: Automatic control principal steps.

In an interview at the 20th world Congress of the Internation Federation of Automatic Control (IFAC 2017), Dimitri Peaucelle, a researcher at the *LAAS* (Laboratory of Analysis and Architecture of Systems) mentioned that one of the future problems that we expect automatic control systems will have the ability to overcome the problem of controlling distributed systems (Mussat, 2017). Hence, automatic control future results expect to consider large-scale systems, multi-agent systems and networks which involve high nonlinear dynamics, collective behavior and evolution.

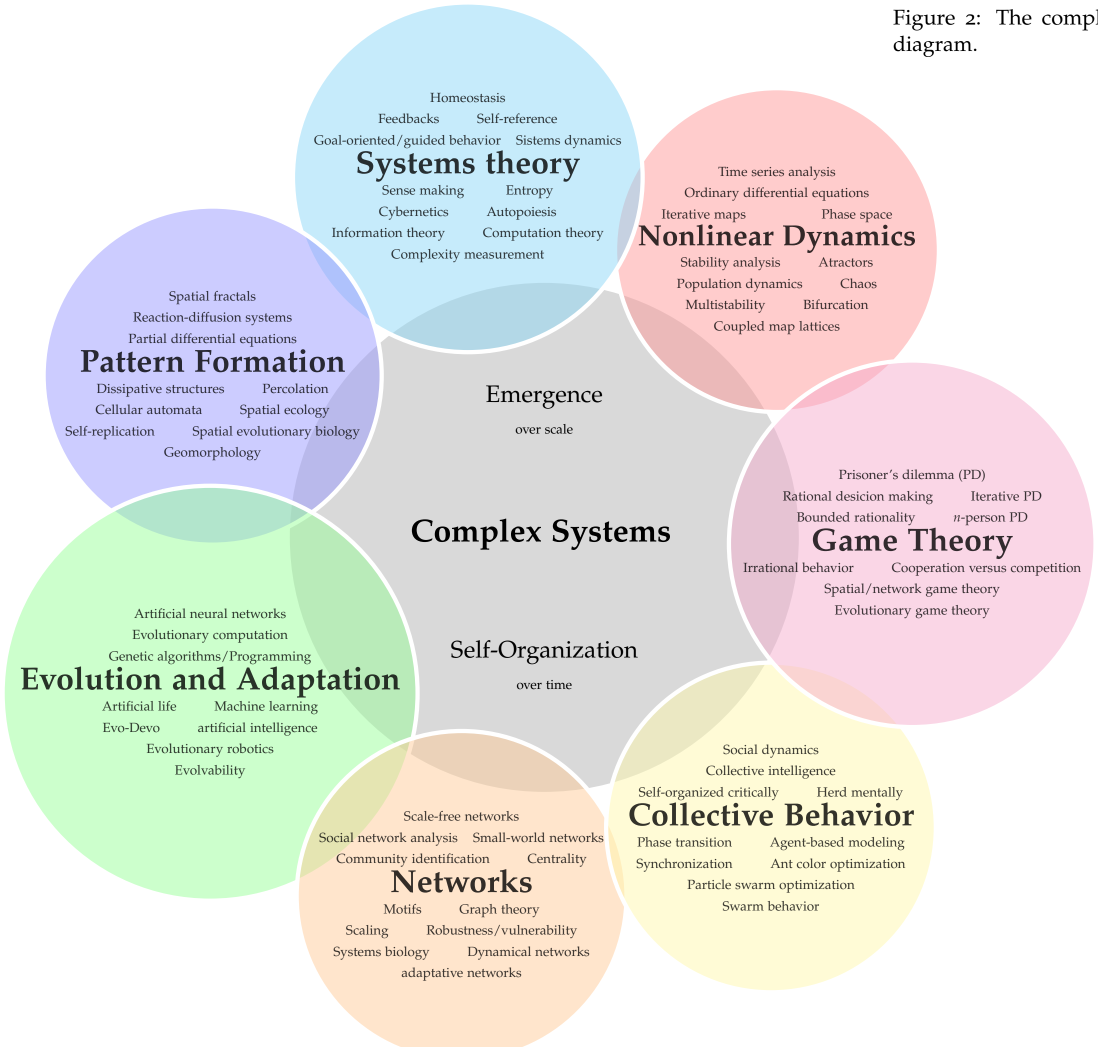

Figure 2: The complex systems topics diagram.

Essentialy the most basic but still highly used scheme to analyze dynamical systems is using linear models. This field of linear systems has been declared many times to be "*mature*", but interest has repeatedly been renewed due to new viewpoints and introduction of new theories (Astrom and Kumar, 2014).

Within this general perspective of the automatic control area, in this work a nothing new, but freshly theory is used for automatic control: *Fractional Calculus*.

Fractional calculus is used to add up new solutions to the problematics presented in automation, but considering the basiest case: *The linear systems case*. This case, even though considered as "*mature*", enable us to find new possibilities due to the generalization of calculus definitions of integrals and derivatives to the real or even complex order case.

Fractional calculus will be used in this work as a tool to design a control feedback algorithm for linear fractional and non fractional order, time-invariant systems with time-delay and as a mathematical modeling tool for large-scale mechanical systems. The feedback control algorithm considered consists of a fractional PD and a fractional PI called: PD^{μ} and PI^{λ}, respectively. These new type of controllers allow us to have more degrees of freedom and new dynamical characteristics due to the fractional-operator properties. Besides, we search for practical applications and implications of using fractional-order controllers.

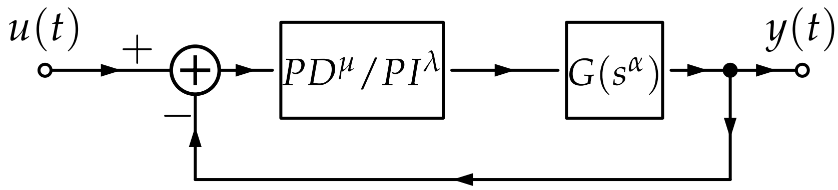

Figure 3: General control diagram

As seen in Fig. 3 when talking about fractional order plants, we will consider commensurate order systems with rational degree α. Furthermore, we do not consider the general $PI^{\lambda}D^{\mu}$ general controller algorithm in our theoretical analysis, nonetheless we make use of it in some practical applications.

An important contribution of this work lies on the proposal and analysis of new mathematical models for a type of distributed parameters systems with special geometrical physical constructions implying a multivalued complex function analysis.

We acknowledge that the results presented in the following pages embody a contribution to the *Fractional Calculus* area and a contribution to the *Automatic Control* theory and practice.

Some publications derived from this work are:

1.- A.-J. Guel-Cortez, C.-F. Méndez-Barrios, V. Ramírez-Rivera, J.G. Romero, E.J. González-Galván. Fractional$-PD^{\mu}$ controllers design for LTI-systems with time-delay. A geometric approach. In *5th International Conference on Control, Desicion and Information Technologies*, 2018.

2.- A.-J. Guel Cortez and C.-F. Méndez-Barrios and E. González-Galván. Geometrical design of fractional PD^{μ} controllers for LTI-fractional order systems with time delay. Submitted to *Journal of Systems and Control Engineering*, 2018.

Hence, we can outline the thesis general and particular objectives as follows:

Thesis general objective

Developing stability criteria to synthesize fractional order controllers of $PD^{\mu}$and PI^{λ}-type. Besides, to study mathematical fractional order models describing infinite mechanical networks.

Thesis particular objectives

- To study the stability of fractional order systems with time-delay of commensurate order.
- To design fractional order PD^{μ} and PI^{λ} controllers for integer and non-integer time-delay linear systems.
- To implement the fractional PD^{μ} controller in a teleoperated system. Based on a bilateral control scheme formed by two Omni Phantom haptic units.
- To analyze proposed mathematical models for infinte mechanical networks.

1 Preliminaries on fractional order systems

Historical Notes

In 1695 L'Hopital asked Leibniz what meaning could be ascribed to $\frac{d^n f(t)}{dt^n}$ if n were a fraction. But it was not until 1884 that the theory of generalized operators achieved such a level in its development to make it a subject in modern mathematics.

> God made the integers; all else is the work of man
>
> *Leopold Kronecker (1886)*

The earliest more or less systematic studies in the subject seem to have been made in the begining and middle of the 19th century by Liouville (Liouville, 1832), Riemann (Riemann, 1847), Holmgren (Holmgren, 1867) (to mention some of them) and others who made contributions even earlier.
A complete survey on the history of the fractional calculus can be found at (Miller and Ross, 1993; Oldham and Spanier, 2006).

Fundamental definitions

Fractional calculus is a generalization of the integration and differentiation to non-integer order fundamental operator ${}_cD_t^\alpha$, where c and t are the limits of the operation and $c \in \mathbb{R}$. There are several alternative definitions of fractional derivatives, of which the three main ones are considered in this work. The existence of different definitions is similar to that of integrals of real-valued functions of a real variable that may be defined according to Riemman or Lebesgue.

Let us first define the especial function Γ as

Definition 1.0.1: Gamma function

We define the Gamma function as

$$\Gamma(n) = \int_0^\infty t^{n-1} e^{-t} dt$$

This function is a generalization of the factorial in the following form:

$$\Gamma(n) = (n-1)! \tag{1.1}$$

Definition 1.0.2: Riemann-Liouville fractional derivatives

$$
{}_cD_t^\alpha = \begin{cases} \int_c^t \frac{(t-\tau)^{-\alpha-1}}{\Gamma(-\alpha)} f(\tau)d\tau, & \text{if } \alpha \in \mathbb{R}^- \\ f(t), & \text{if } \alpha = 0 \\ \frac{d^{\lceil\alpha\rceil}}{dt^{\lceil\alpha\rceil}} {}_cD_t^{\alpha-\lceil\alpha\rceil} f(t), & \text{if } \alpha \in \mathbb{R}^+ \end{cases} \tag{1.2}
$$

$$
{}_tD_c^\alpha = \begin{cases} \int_t^c \frac{(t-\tau)^{-\alpha-1}}{\Gamma(-\alpha)} f(\tau)d\tau, & \text{if } \alpha \in \mathbb{R}^- \\ f(t), & \text{if } \alpha = 0 \\ (-1)^{\lceil\alpha\rceil} \frac{d^{\lceil\alpha\rceil}}{dt^{\lceil\alpha\rceil}} {}_tD_c^{\alpha-\lceil\alpha\rceil} f(t), & \text{if } \alpha \in \mathbb{R}^+ \end{cases} \tag{1.3}
$$

where $\Gamma(\cdot)$ is the *Gamma* function.

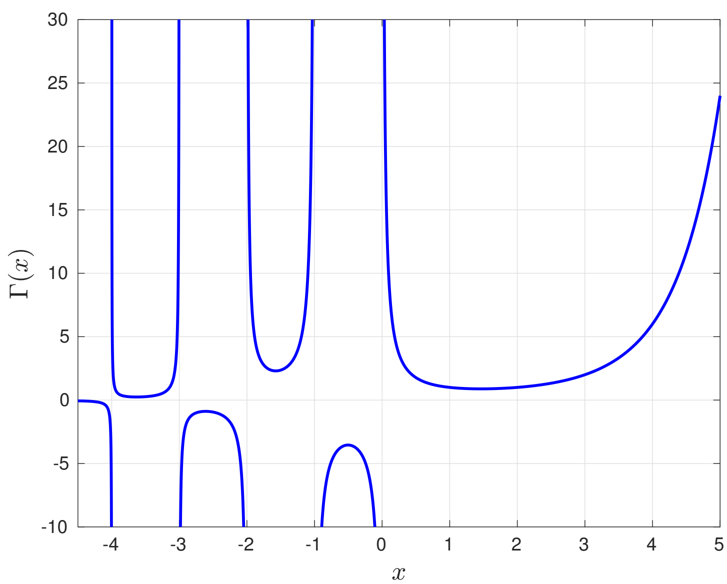

Figure 1.1: The Γ function.

Definition 1.0.3: Caputo fractional derivatives

$$
{}_cD_t^{\alpha} = \begin{cases} \int_c^t \frac{(t-\tau)^{-\alpha-1}}{\Gamma(-\alpha)} f(\tau)d\tau, & \text{if } \alpha \in \mathbb{R}^- \\ f(t), & \text{if } \alpha = 0 \\ {}_cD_t^{\alpha-\lceil\alpha\rceil} \frac{d^{\lceil\alpha\rceil}}{dt^{\lceil\alpha\rceil}} f(t), & \text{if } \alpha \in \mathbb{R}^+ \end{cases} \tag{1.4}
$$

$$
{}_tD_c^{\alpha} = \begin{cases} \int_t^c \frac{(t-\tau)^{-\alpha-1}}{\Gamma(-\alpha)} f(\tau)d\tau, & \text{if } \alpha \in \mathbb{R}^- \\ f(t), & \text{if } \alpha = 0 \\ (-1)^{\lceil\alpha\rceil} {}_tD_c^{\alpha-\lceil\alpha\rceil} \frac{d^{\lceil\alpha\rceil}}{dt^{\lceil\alpha\rceil}} f(t), & \text{if } \alpha \in \mathbb{R}^+ \end{cases} \tag{1.5}
$$

where $\Gamma(\cdot)$ is the *Gamma* function.

It is important to notice the difference between Definitions 1.0.2 and 1.0.3 stands for $\alpha \in \mathbb{R}^+$ which corresponds to the fractional differentation. The Caputo definition of the fractional-derivative integrates after deriving. In the Caputo case, the derivative of a constant is zero and the initial conditions for the fractional-order differential equations are in the same form as for the integer-order differential equations. It is an advantage, because applied problems require definitions of fractional derivatives, where there are clear interpretations of initial conditions, which contain $f(a), f'(a), f''(a)$, etc. To see more about the Riemann-Liouville and Caputo definitions see (Li et al., 2011)

Definition 1.0.4: Grünwald-Letnikoff fractional derivatives

$$
{}_cD_t^{\alpha} = \lim_{h\to 0^+} \frac{\sum_{j=0}^{\lfloor\frac{t-c}{h}\rfloor} (-1)^j \binom{\alpha}{j} f(t-jh)}{h^{\alpha}} \tag{1.6}
$$

$$
{}_tD_c^{\alpha} = \lim_{h\to 0^+} \frac{\sum_{j=0}^{\lfloor\frac{t-c}{h}\rfloor} (-1)^j \binom{\alpha}{j} f(t+jh)}{h^{\alpha}} \tag{1.7}
$$

As we will see in further sections the Grünwald-Letnikoff (GL) definition is commonly used when fractional derivatives and integrals are implemented in digital platforms.

The definitions depicted above are not the unique ones. In fact it is of contemporary interest to find a general definition for what it would be a fractional integral or derivative. Some other definitions are studied in (Ortigueira and Machado, 2015; de Oliveira and Machado, 2014).

Geometrical and physical meaning of the fractional derivative

Commonly asked questions in the literature of *Fractional Calculus* are: **What is the meaning of a fractional derivative?**, **How can we interpret it geometrically?** and some others in the same sense.

When we talk of a half-derivative or a α-derivative we are actually generalizing the concepts of *Calculus*. It is known that the integer order derivative represents the scope of a tangent line of some given curve. Nontheless, in *Fractional Calculus* there is not a concise geometrical interpretation, because each of them relies on the definiton being used. Some geometrical interpretations can be found at (Podlubny, 2001; Karci, 2015; Zhao and Luo, 2017; Tavassoli et al., 2013).

Now, in terms of the physical interpretation of the *Fractional Calculus*. Let us consider the popular differential equations of theoretical physics of the form

$$a\frac{\partial^m f(x,t)}{\partial t^m} + b\frac{\partial^n f(x,t)}{\partial x^n} = F, \tag{1.8}$$

where x, t are the space-time variables, a, b and F are given functions of x and t, and $m, n = 0, 1, 2, \ldots$ are integer numbers. Some popular versions of equations of mathematical physics are represented in the following table (see, for instance (Uchaikin, 2013)):

> The fractional calculus is the calculus of the XXI century
>
> *K. Nishimoto (1989)*

m,n	1D-equations	3D-equations	Phys. sense	Math. type
1,0	$\lvert a\rvert\frac{dv}{dt} + bv = F$	$\lvert a\rvert\frac{d\mathbf{v}}{dt} + b\mathbf{v} = F$	Damped motion	-
2,0	$\lvert a\rvert\frac{d^2x}{dt^2} + bx = F$	$\lvert a\rvert\frac{d^2\mathbf{r}}{dt^2} + b\mathbf{r} = F$	Oscillation	-
1,1	$\lvert a\rvert\frac{\partial f}{\partial t} + \frac{\partial(bf)}{\partial x} = F$	$\lvert a\rvert\frac{\partial f(t)}{\partial t} + \nabla(\mathbf{b}f) = F$	Continuity	-
1,2	$\lvert a\rvert\frac{\partial f}{\partial t} - \lvert b\rvert\frac{\partial^2 f}{\partial^2 x} = F$	$\lvert a\rvert\frac{\partial f(t)}{\partial t} - \lvert b\rvert\nabla^2 f = F$	Diffusion	Parabolic
2,2	$\lvert a\rvert\frac{\partial^2 f}{\partial^2 t} - \lvert b\rvert\frac{\partial^2 f}{\partial^2 x} = F$	$\lvert a\rvert\frac{\partial^2 f(t)}{\partial^2 t} - \lvert b\rvert\nabla^2 f = F$	Waves	Hyperbolic
0,2	$af + b\frac{\partial^2 f}{\partial^2 x} = F$	$af + b\nabla^2 f = F$	Static fields	Elliptic
μ, v **non-integers**	$a\frac{\partial^\mu f}{\partial^\mu t} + b\frac{\partial^2}{\partial^2 x}^{v/2} f = F$ $t > 0, \infty < x < \infty$	$a\frac{\partial^\mu f(t)}{\partial^\mu t} + b\nabla^{v/2} f = F$	?	Not yet classified

Then, according to this table classification, it is clear that there is not a specific phenomenon already known corresponding to the usage of *Fractional Calculus*.

In spite of such a conclusion, important properties of Nature "*seem*" to underlie the mathematical concept of fractional calculus: Heredity, nonlocality, selfsimilarity, and stochasticity. (see, for more details (Uchaikin, 2013)) when we analyze the mathematical properties of the kernel in the fractional operator ${}_cD_t^\alpha$.

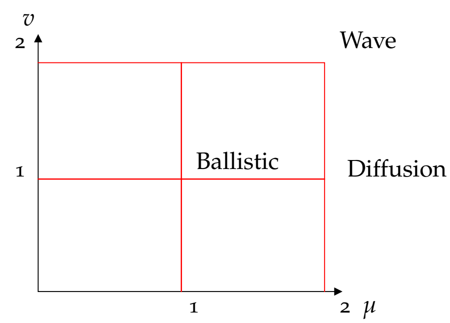

Figure 1.2: Continuous manifold of fractional partial equations

To explain one of the aforementioned properties that may be represented by using *Fractional Calculus*, let us look at the next experiment described by Bird and Curtiss (1984) (Fig. 1.3). A pump leaks a fluid through a tube. At the beginning of the experiment a section of the fluid is marked with a paint. During the stream process the marked surface takes the parabolic form typical for the Poiseuille flow. When the pump is turned off the fluid stops. Herewith the Newtonian liquid keeps being motionless while polymeric liquid streams some distance back, though it does not take its first position. The back motion process reveals the memory of polymeric liquid and the fact that the liquid does not take its initial condition, as a spring does, is the evidence of memory attenuation.

Some steps in the analysis of the physical interpretation of fractional calculus try to study common mechanical or electrical systems by substituting their derivatives or integrals orders in its mathematical models with a real order. In (Gómez-Aguilar et al., 2014), J. Gómez A. an application of fractional calculus for modeling is depicted by using the fractional differential equation for the RC circuit on Fig. 1.4 as

$$\frac{d^\gamma q}{dt^\gamma} + \frac{1}{\tau_\gamma}q(t) = \frac{C}{\tau_\gamma}v(t), \tag{1.9}$$

where

$$\tau_\gamma = \frac{RC}{\sigma^{1-\gamma}}, \tag{1.10}$$

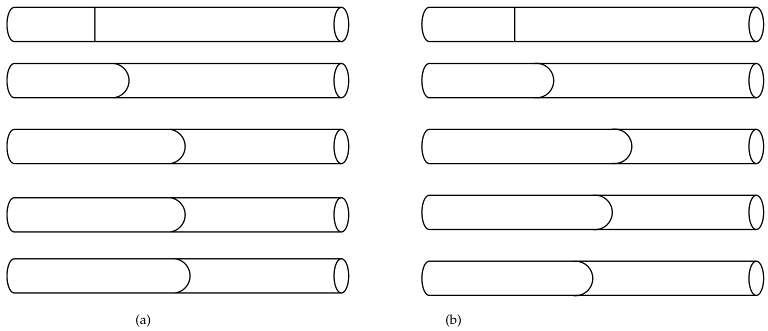

Figure 1.3: Hereditary behavior of a Newtonian liquid (a) versus Polymeric liquid (b).

can be called the fractional time constant due to its dimensionality s^{γ}. When $\gamma = 1$, from (1.10) we have the well known time constant $\tau = RC$.

Given the values, $R = 1M\Omega$, $C = 1\mu F$, we simulate the solution of (1.9) according to (Gómez-Aguilar et al., 2014), obtaining the results shown in Figures 1.5 and 1.6 of the behavior of the charge and voltage using the following fractional exponents $\gamma = 0.25$, $\gamma = 0.5$, $\gamma = 0.75$ and $\gamma = 1$.

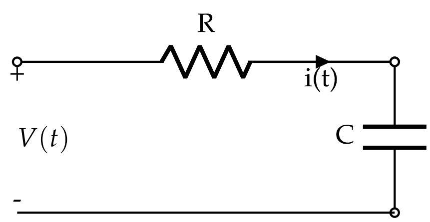

Figure 1.4: RC Circuit.

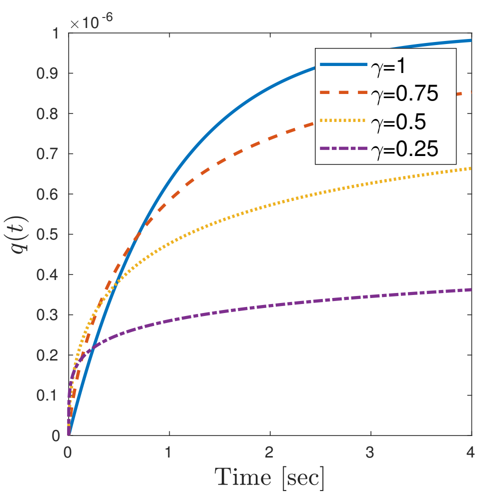

Figure 1.5: Step response of the capacitor's charge.

Now, in (Gómez-Aguilar et al., 2015) a mass-spring system is studied, again by changing the differential equations model order. The equation of the mass-spring-damper system represented in Fig. 1.7 is given by:

$$\frac{m}{\sigma^{2(1-\gamma)}} {}_0^C D_t^{2\gamma} x(t) + \frac{\beta}{\sigma^{1-\gamma}} {}_0^C D_t^{\gamma} x(t) + kx(t) = F(t), \tag{1.11}$$

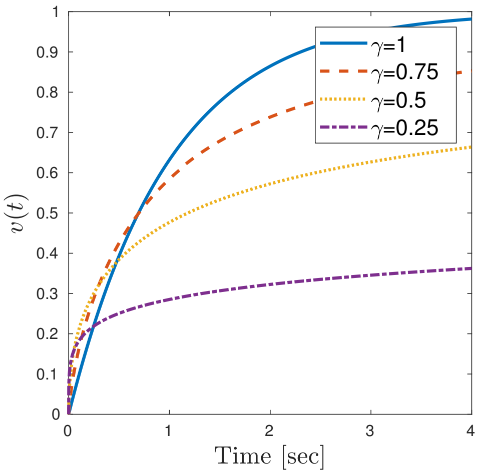

Figure 1.6: Step response of the capacitor's voltage.

and for the Caputo Fabrizio definition (Caputo and Fabrizio, 2015), we have:

$$\frac{m}{\sigma^{2(1-\gamma)}}{}_0^{CF}D_t^{2\gamma}x(t) + \frac{\beta}{\sigma^{1-\gamma}}{}_0^{CF}D_t^{\gamma}x(t) + kx(t) = F(t), \tag{1.12}$$

where the mass is m, the damping coefficient is β, the spring constant is k and $F(t)$ represents the forcing function.

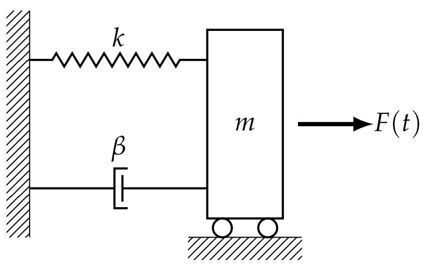

Figure 1.7: Mass-spring-damper system.

Considering the case of a mass-spring system with $\beta = 0$, simulating expressions (1.13) and (1.14) using zero intial conditions we obtain the results on Fig. 1.8.

$$x(t) = \left(x_0 - \frac{f_0}{k}\right) E_{2\gamma}\left\{-\eta^2 t^{2\gamma}\right\} + \frac{f_0}{k}, \tag{1.13}$$

$$x(t) = \left(x_0 - \frac{f_0}{k}\right) E_{2\gamma}\left\{-\gamma^{2(1-\gamma)t^{2\gamma}}\right\} + \frac{f_0}{k}. \tag{1.14}$$

The last examples show how the time response of basics systems behave when we change the derivate orders to some real number. This just gives an insight of which type of behaviours we may model by using *Fractional Calculus*.

In further sections of this work we propose some systems modeled by means of fractional derivatives and analyze some applications.

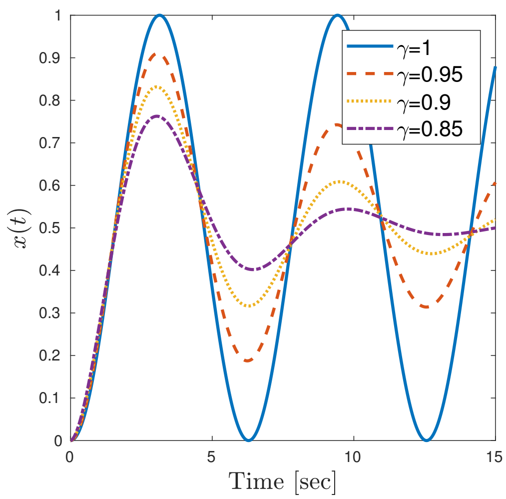

Figure 1.8: Mass-spring system with a constant source, Caputo derivative approach.

Numerical solutions and implementations

Consider the already known Grünwald-Letnikov (GL) definition, given by

$$ {}_aD_t^{\alpha} f(t) \quad = \quad \lim_{h \to 0} h^{-\alpha} \sum_{j=0}^{[\frac{t-a}{h}]} (-1)^j \begin{pmatrix} \alpha \\ j \end{pmatrix} f(t-jh). $$

The relation for explicit numerical approximation of r-th derivative at the points kh, (k=1,2,...) has the following form:

$$ {}_{(k-\frac{L_m}{h})}D_{t_k}^{q} f(t) \approx h^{-q} \sum_{j=0}^{k} (-1)^j \begin{pmatrix} q \\ j \end{pmatrix} f(t_{k-j}) = h^{-q} \sum_{j=0}^{k} c_j^{(q)} f(t_{k-j}) \tag{1.15} $$

where L_m is the memory lenght, $t_k = kh$, h is the time step of the calculation and $c_j^{(q)}$, $(j = 0, 1, \dots)$ are binomial coefficients. For their calculation we can use the following expression:

$$ \begin{aligned} c_o^{(q)} &= 1 \\ c_j^{(q)} &= \left(1 - \frac{1+q}{j}\right) c_{j-1}^{(q)} \end{aligned} $$

Writing the factorial as gamma function, it allows the binomial coefficient to be generalized to non-integer arguments. We can write the relations:

$$ (-1)^j \begin{pmatrix} q \\ j \end{pmatrix} = (-1)^j \frac{\Gamma(q+1)}{\Gamma(j+1)\Gamma(q-j+1)} = \frac{\Gamma(j-q)}{\Gamma(-q)\Gamma(j+1)} $$

Obviously, for this simplification we pay a penalty in the form of some inaccuracy. If $f(t) \leq M$, we can easily establish the following estimate for determining the memory length L_m, providing the required accuracy ϵ:

$$ L_m \geq \left(\frac{M}{\epsilon |\Gamma(1-q)|} \right)^{\frac{1}{q}} $$

This method is named the *Power Series Expansion* (PSE) of a generating function which can be discretized to form a FIR filter. The resulting discrete transfer function, approximating fractional-order operators, can be expressed in the z-domain as follows:

$$ {}_0D_{kT}^{\pm r}G(z) = \frac{Y(z)}{F(z)} = \left(\frac{1}{T}\right)^{\pm r} PSE\{\left(1-z^{-1}\right)^{\pm r}\} \approx T^{\mp r}R_n(z^{-1}) $$

where T is the sample period, $PSE\{u\}$ denote the function resulting from applying the power series expansion to the function u, $Y(z)$ is the Z transform of the output sequence $y(kT)$, $F(z)$ is the Z transform of the input sequence $f(kT)$, n is the order of the approximation, and R is polynomial of degree n, respectively, in the variable z^{-1}, and $k = 1, 2, \ldots$. Using a Matlab function based on relation (1.15) we obtained the result shown in Fig. 1.9 of deriving $f = sin(t)$ from order 0 to 1 on intervals of 0.1.

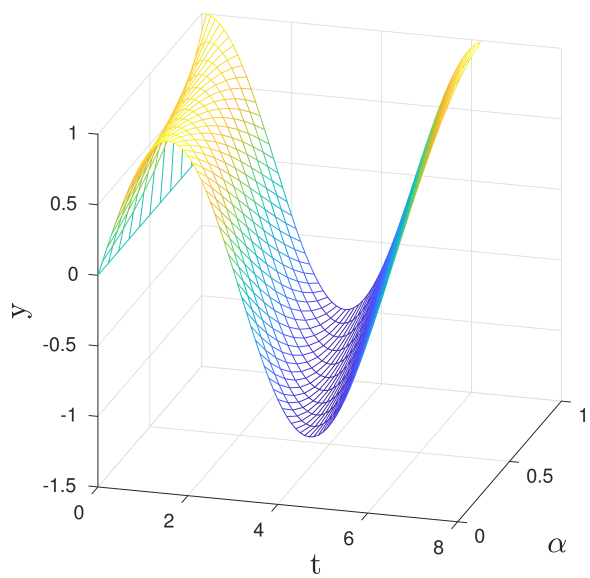

Figure 1.9: Evaluation of the fractional derivative of $sin(t)$ using relation (1.15).

For another example of the use of relation (1.15), consider a three-term differential equation in the form

$$ {}_{a_2}D_t^{\alpha_2}y(t) +_{a_1} D_t^{\alpha_1}y(t) + a_0y(t) = u(t). \tag{1.16} $$

Substituting (1.15) into the equation (1.16), one can write

$$ \frac{a_2}{h^{\alpha_2}}\sum_{j=0}^{k} q_j^{\alpha_2}y(t_k - j) + \frac{a_1}{h^{\alpha_1}}\sum_{j=0}^{k} q_j^{\alpha_1}y(t_k - j) + a_0y(t_k) = u(t_k), \tag{1.17} $$

where $t_k = kh$ $(k = 1, 2, \ldots, N)$ and $q_j^{(\alpha)}$ are binomial coefficients. After some rearrangement of the terms in the relation (1.17), we can obtain the numerical solution depicted in Fig. 1.10 of the fractional differential equation (1.16) in the following form:

$$ y(t_k) = \frac{u(t_k) - \frac{a_2}{h^{\alpha_2}}\sum_{j=1}^{k} q_j^{(\alpha_2)}y(t_k - j) - \frac{a_1}{h^{\alpha_1}}\sum_{j=1}^{k} q_j^{(\alpha_1)}y(t_k - j)}{\frac{a_2}{h^{\alpha_2}} + \frac{a_1}{h^{\alpha_1}} + a_0} \tag{1.18} $$

where $k = 1, 2, \ldots, N$ for $N = T_{sim}/h$ and where T_{sim} is the total time of the calculation. The above approach is general and can be used for n-term fractional differential equation

$$a_n D_t^{\alpha_n} y(t) + a_{n-1} D_t^{\alpha_{n-1}} y(t) + \ldots + a_0 D_t^{\alpha_0} y(t) = b_m D_t^{\beta_m} u(t) + b_{m-1} D_t^{\beta_{m-1} u(t)} + \ldots + b_0 D_t^{\beta_0} u(t).$$

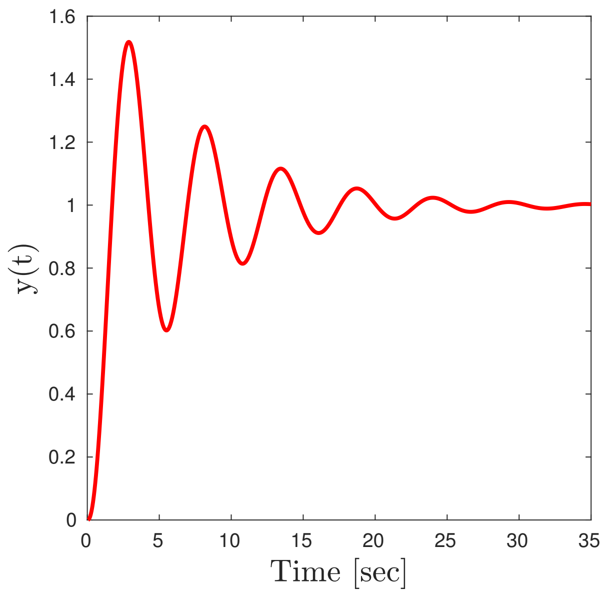

Figure 1.10: Solution of the equation (1.16) for parameters: $a_2 = 0.8$, $a_1 = 0.5$, $a_0 = 1$, $\alpha_2 = 2.2$, $\alpha_1 = 0.9$ for $u(t) = 1$, under zero initial conditions, time step $h = 0.05$ and computation time $T_{sim} =$ 35sec.

Continuous and discrete-time approximation techniques

Continued Fraction Expansion (CFE)

Other approach can be obtained by Continued Fraction Expansion (CFE) of the generating function and then the approximated fractional operator is in the form of IIR filter, which has poles and zeros.

Taking into account that our aim is to obtain equivalents to the fractional integrodifferential operators in the Laplace domain, $s^{\pm r}$, the result of such approximation for an irrational function, $G(s)$, can be expressed into the form:

$$G(s) \backsimeq a_0(s) + \cfrac{b_1(s)}{a_1(s) + \cfrac{b_2(s)}{a_2(s) + \cfrac{b_3(s)}{a_3(s)+\ldots}}} = a_0(s) + \frac{b_1(s)}{a_1(s)+} \; \frac{b_2(s)}{a_2(s)+} \; \frac{b_3(s)}{a_3(s)+} \; \ldots$$

where $a_i s$ and $b_i s$ are rational functions of the variable s, or are constants. The application of the method yields a rational function, which is an approximation of the irrational function $G(s)$. In other words, for evaluation purposes, the rational approximations obtained by CFE frequently converge much more rapidly than the PSE and have a wider domain of convergence in the complex plane. On the other hand, the approximation by PSE and the short memory principle is convenient for dynamical properties consideration.

These techniques are based on the approximations of an irrational function, $G(s)$, by a rational function defined by the quotient of two polynomials in the variable s in frequency s-domain:

$$G(s) \equiv R_{i(i+1)\dots(i+m)} \quad = \quad \frac{P_\mu(s)}{Q_v(s)} = \frac{p_0 + p_1 s + \cdots + p_\mu s^\mu}{q_0 + q_1 s + \cdots + q_v s^v}, \quad (m+1 = \mu + v + 1)$$

passing through the points $(s_i, G(s_i), \dots, (s_{i+m}, G(s_{i+m})))$.

The resulting discrete transfer function, approximating fractional-order operators, can be expressed as:

$$_0D_{kT}^{\pm r} G(z) \quad = \quad \frac{Y(Z)}{F(z)} = \left(\frac{2}{T}\right)^{\pm r} CFE\{\left(\frac{1-z^{-1}}{1+z^{-1}}\right)^{\pm r}\}_{p,n} \approx \left(\frac{2}{T}\right)^{\pm r} \frac{P_p(z^{-1})}{Q_n(z^{-1})}$$

where T is the sample period, CFE$\{u\}$ denotes the function resulting from applying the continued fraction expansion to the function u, $Y(z)$ is the Z transform of the output sequence $y(kT)$, $F(z)$ is the Z transform of the input sequence $f(kT)$, p and n are the orders of the approximation, and P and Q are polynomials of degrees p and n, respectively, in the variable z^{-1}, and $k = 1, 2, \dots$

In general, the discretization of fractional-order differentiatior/integrador $s^{\pm r}$ ($r \in \mathbb{R}$) can be expressed by the generating function $s \approx w(z^{-1})$. This generating function and its expansion determine the form of the approximation and the coeficients.

$$(\omega(z^{-1}))^{\pm r} = \left(\frac{1+a}{T} \frac{1-z^{-1}}{+az^{-1}}\right)^{\pm r}$$

where a is the ratio term and r is the fractional order. The ratio term a is the amount of phase shift and this tuning knob is sufficient for solving most engineering problems.

The result of such approximation for an irrational function, $\hat{G}(z^{-1})$, can be expressed by $G(z^{-1})$ in the CFE form

$$G(z^{-1}) \quad \backsimeq \quad a_0(z^{-1}) + \cfrac{b_1(z^{-1})}{a_1(z^{-1}) + \cfrac{b_2(z^{-1})}{a_2(z^{-1}) + \cfrac{b_3(z^{-1})}{a_3(z^{-1}) + \dots}}} = a_0(z^{-1}) + \frac{b_1(z^{-1})}{a_1(z^{-1})+} \; \frac{b_2(z^{-1})}{a_2(z^{-1})+} \; \frac{b_3(z^{-1})}{a_3(z^{-1})+} \; \cdots$$

where a_i and b_i are either rational functions of variable z^{-1} or constants. The application of the method yields a rational function, $G(z^{-1})$, which is an approximation of the irrational function $\hat{G}(z^{-1})$.

The resulting discrete transfer function, approximating fractional-order operators, ca be expressed as:

$$(w(z^{-1}))^{\pm r} \quad \approx \quad \left(\tfrac{1+a}{T}\right)^{\pm r} CFE\{\left(\tfrac{1-z^{-1}}{1+az^{-1}}\right)^{\pm r}\}_{p,q} = \left(\tfrac{1+a}{T}\right)^{\pm r} \tfrac{P_p(z^{-1})}{Q_q(z^{-1})} = \left(\tfrac{1+a}{T}\right)^{\pm r} \tfrac{p_0 + p_1 z^{-1} + \dots + p_m z^{-1}}{q_0 + q_1 z^{-1} + \dots + q_n z^{-q}} \tag{1.19}$$

where CFE$\{u\}$ denotes the continued fraction expansion of u; p and q are the orders of the approximation and P and Q are polynomials of degrees p and q. Normally, we can set $p = q = n$.

Here we present some results for fractional order $r = 0.5$. The value of approximation order n is truncated to $n = 3$ and weighting factor a is chosen $a = 1/3$. Assuming sampling period $T = 0.001$ sec.

Oustaloups Recursive Approximation

The method is based on the approximation of a function of the form:

$$H(s) = s^r, \quad r \in \mathbb{R}, \quad r \in [-1; 1],$$

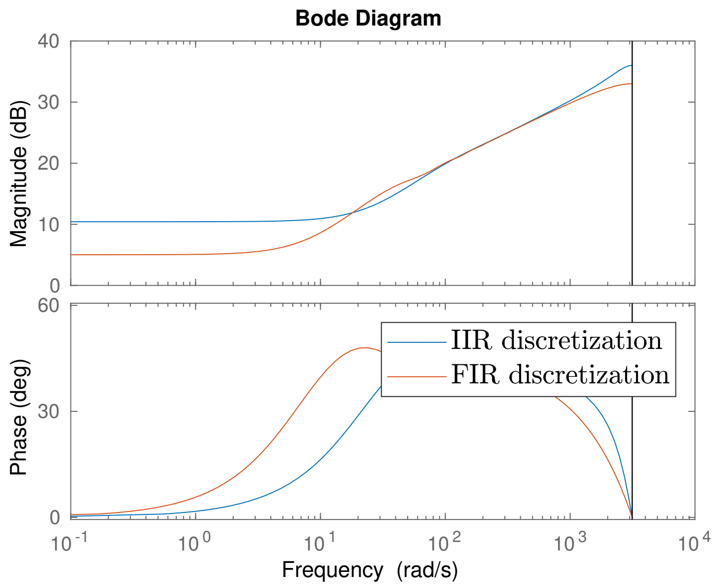

Figure 1.11: Bode diagram comparison of the discretization of $s^{0.5}$ by using a FIR and IIR form.

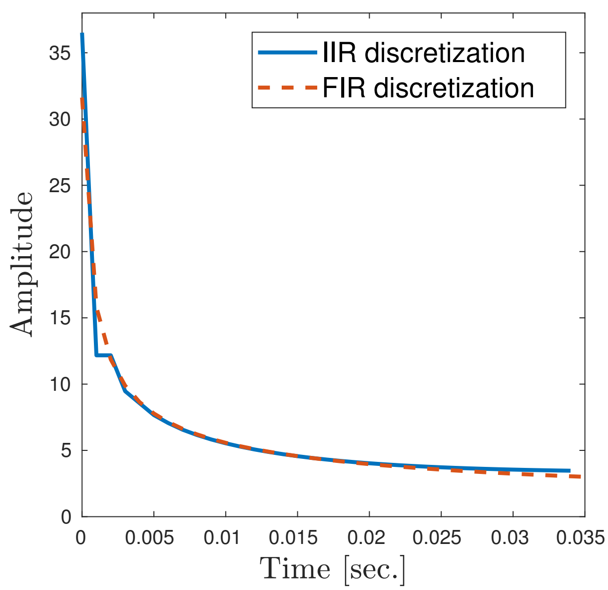

Figure 1.12: Step response comparison of the discretization of $s^{0.5}$ by using a FIR and IIR form

for the frequency range selected as (ω_b, ω_h) by a rational function:

$$\hat{H} = C_o \prod_{k=-N}^{N} \frac{s + \omega'_k}{s + \omega_k}, \tag{1.20}$$

using the following set of synthesis formulas for zeros, poles and the gain:

$$\begin{aligned}
\omega'_k &= \omega_b \left(\frac{\omega_h}{\omega_b}\right)^{\frac{k+N+0.5(1-r)}{2N+1}}, \\
\omega_k &= \omega_b \left(\frac{\omega_h}{\omega_b}\right)^{\frac{k+N+0.5(1-r)}{2N+1}}, \\
C_o &= \left(\frac{\omega_h}{\omega_b}\right)^{\frac{r}{2}} \prod_{k=-N}^{N} \frac{\omega_k}{\omega'_k}.
\end{aligned}$$

where ω_h, ω_b are the high and low transitional frequencies.

Using the described Oustaloups-Recursive-Aproximation (ORA) method with:

$$\omega_b = 10^{-2}, \omega_h = 10^2,$$

the obtained approximation for fractional function $H(s) = s^{\frac{1}{2}}$ for $N = 3$ gives the results shown in Figs. 1.14 and 1.13.

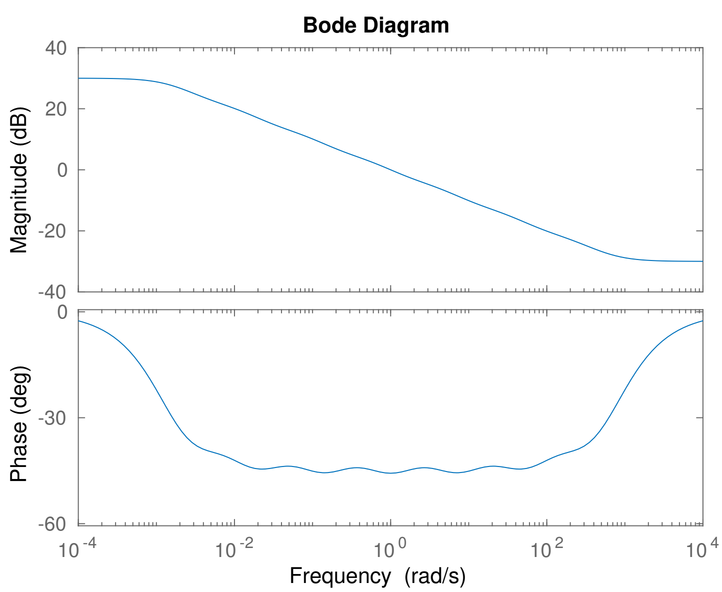

Figure 1.13: Oustaloup's-Recursive-Approximation (ORA) method Bode plot of $s^{-0.5}$, using $\omega_n = 10^{-2}, \omega_h = 10^2$ and $N = 3$.

As we can see from the methods presented, there is not an exact possible implementation to solve a fractional integral or derivative. An approximation is always used, this presents an oportunity area of research.

The methods used in the last sections are disscused widely in (Petráš, 2011a). In (Caponetto, 2010) some implementations of fractional derivates and integrals are presented by using *microprocessors*, *Field Programmable Gate Arrays* and *Field Programmable analog Arrays*. In (Podlubny et al., 2002; Dorčák et al., 2013) posible analogue realizations for fractional order dynamical controllers and systems are presented.

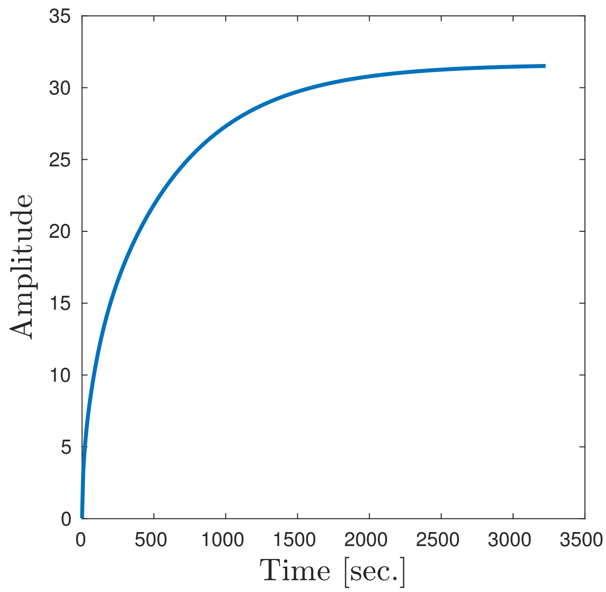

Figure 1.14: Oustaloup's-Recursive-Approximation (ORA) method step response of $s^{-0.5}$, using $\omega_n = 10^{-2}, \omega_h = 10^2$ and $N = 3$.

The Laplace transform in fractional calculus

The *Laplace transform* is one of the most powerful tools used in fractional order systems to stablish criteria for stability, modeling and system identification. This, due to the simpliciy gained in the frequency domain.

In further sections we will discuss practically all our results by taking a frequency domain analysis. Here, it is of great interest to stablish what would be the *Laplace transform* of the most used fractional derivative and integral definitions.

Riemann-Liouville definition

Theorem 1.0.1: Laplace transform of the Riemann-Liouville definition (Valério and da Costa, 2013)

The *Laplace transform* of D when the Riemann-Liouville definition is used is given by

$$\mathscr{L}\left[{}_0D_t^{\alpha} f(t)\right] = \begin{cases} s^{\alpha}F(s), & \text{if } \alpha \in \mathbb{R}^- \\ F(s), & \text{if } \alpha = 0 \\ s^{\alpha}F(s) - \sum_{k=0}^{\lceil\alpha\rceil-1} s^k {}_0D_t^{\alpha-k-1} f(0), & \text{if } \alpha \in \mathbb{R}^+ \end{cases} \tag{1.21}$$

Proof. The result is trivial for $\alpha = 0$. For $\alpha < 0$:

$$\begin{aligned} \mathscr{L}\left[{}_0D_t^{\alpha} f(t)\right] &= \mathscr{L}\left[\tfrac{1}{\Gamma(-\alpha)} \int_0^t (t-\tau)^{-\alpha-1} f(\tau) d\tau\right], \\ &= \tfrac{1}{\Gamma(-\alpha)} \mathscr{L}\left[t^{-\alpha-1}\right] \mathscr{L}\left[f(t)\right], \\ &= \tfrac{1}{\Gamma(-\alpha)} \tfrac{\Gamma(-\alpha)}{s^{-\alpha}} \mathscr{L}\left[f(t)\right]. \end{aligned}$$

For $\alpha > 0$:

$$\begin{aligned}\mathscr{L}\left[{}_0D_t^{\alpha}f(t)\right] &= \mathscr{L}\left[D^{\lceil\alpha\rceil}{}_0D_t^{\alpha-\lceil\alpha\rceil}f(t)\right],\\ &= s^{\lceil\alpha\rceil}s^{\alpha-\lceil\alpha\rceil}F(s)-\sum_{k=0}^{\lceil\alpha\rceil-1}s^kD^{\lceil\alpha\rceil-k-1}{}_0D_t^{\alpha-\lceil\alpha\rceil}f(0)\blacksquare\end{aligned}$$

□

Theorem 1.0.2: Laplace transform of the Caputo definition (Valério and da Costa, 2013)

The *Laplace transform* of D nwhen the Caputo definition is used is given by

$$\mathscr{L}\left[{}_0D_t^{\alpha}f(t)\right]=\begin{cases}s^{\alpha}F(s), & \text{if } \alpha\in\mathbb{R}^-\\ F(s), & \text{if } \alpha=0\\ s^{\alpha}F(s)-\sum_{k=0}^{\lceil\alpha\rceil-1}s^{\alpha-k-1}D^kf(0), & \text{if } \alpha\in\mathbb{R}^+\end{cases}\tag{1.22}$$

Proof. The proof is identical to that of Theorem 1.0.1 save for $\alpha > 0$, when we will have

$$\begin{aligned}\mathscr{L}\left[{}_0D_t^{\alpha}f(t)\right] &= \mathscr{L}\left[{}_0D_t^{\alpha-\lceil\alpha\rceil}D\right]\\ &= s^{\alpha-\lceil\alpha\rceil}\left(s^{\lceil\alpha\rceil}F(s)-\sum_{i=0}^{\lceil\alpha\rceil-1}s^iD^{\lceil\alpha\rceil-i-1}f(0)\right).\end{aligned}$$

Making $k=\lceil\alpha\rceil-1-i$ we obtain the result $\blacksquare$ □

The Laplace transform of fractional order systems

To start analyzing the *Laplace Transform* of fractional order system we need to define the *Mittag-Leffler* function as follows

Definition 1.0.5: Mittag-Leffler function

The one-parameter and the two-parameter Mittag-Leffler functions are defined as

$$E_{\alpha}(t) = \sum_{k=0}^{+\infty}\frac{t^k}{\Gamma(\alpha k+1)}=E_{\alpha,1},\quad \alpha>0 \tag{1.23}$$

$$E_{\alpha,\beta}(t) = \sum_{k=0}^{+\infty}\frac{t^k}{\Gamma(\alpha k+\beta)},\quad \alpha,\beta>0 \tag{1.24}$$

Some particular values of these functions include

$$E_1(t)=E_{1,1}(t) = \sum_{k=0}^{+\infty}\frac{t^k}{\Gamma(k+1)}=\sum_{k=0}^{+\infty}\frac{t^k}{k!}=e^t \tag{1.26}$$

$$E_1(at) = E_{1,1}(at)=e^{at} \tag{1.27}$$

$$E_{2,1}(t^2) = \sum_{k=0}^{+\infty}\frac{t^{2k}}{\Gamma(2k+1)}=\sum_{k=0}^{+\infty}\frac{t^{2k}}{(2k)!}=\cosh(t) \tag{1.28}$$

Remark 1.0.1 (Miller-Ross function). *A generalization of the Mittag-Leffler function is known as the Miller-Ross function which is defined as*

$$\epsilon_t(v,a)=\sum_{k=0}^{+\infty}\frac{a^kt^{k+v}}{\Gamma(v+k+1)}=t^vE_{1,v+1}(at). \tag{1.25}$$

For more details about the Mittag-Leffler function see (Gorenflo et al., 2014).

As we can see, the *Mittag Leffler* function allow us to find a general way of expressing several functions. In this vein, the *Mittag Leffler* function will stablish different decay behaviours.

A powerfull result for finding the *Laplace transform* of the mayority of the systems in the literature is given as follows

Theorem 1.0.3: (Valério and da Costa, 2013)

The Laplace transform of $t^{\alpha k+\beta-1}\frac{d^k E_{\alpha,\beta}(\pm a t^\alpha)}{d(\pm a t^\alpha)^k}$ is

$$\mathcal{L}\left[t^{\alpha k+\beta-1}\frac{d^k E_{\alpha,\beta}(\pm a t^\alpha)}{d(\pm a t^\alpha)^k}\right] = \frac{k! s^{\alpha-\beta}}{(s^\alpha \mp a)^{k+1}} \tag{1.29}$$

Proof. We start by mentioning the following results

Lemma 1.0.2. *The integer derivatives of* $\frac{1}{1\mp t}$ *are given by*

$$D^k \frac{1}{1\mp t} = \frac{k!(\pm 1)^k}{(1\mp t)^{k+1}}, \quad k \in \mathbb{Z}_0^+. \tag{1.30}$$

Corollary 1.0.1

The MacLaurin series of $\frac{1}{1\mp t}$ is $\sum_{k=0}^{+\infty}(\pm t)^k$.

Then, first notice that

$$\begin{aligned}
\int_0^{+\infty} e^{-t} t^{\beta-1} E_{\alpha,\beta} dt &= \int_0^{\infty} e^{-t} t^{\beta-1} \sum_{k=0}^{+\infty} \frac{(\pm z)^k t^{\alpha k}}{\Gamma(\alpha k+\beta)} dt \\
&= \sum_{k=0}^{+\infty} \frac{(\pm)^k}{\Gamma(\alpha k+\beta)} \int_0^{+\infty} e^{-t} t^{\alpha k+\beta-1} dt \\
&= \frac{1}{1\mp z}
\end{aligned} \tag{1.31}$$

Differentiating the rightmost and the leftmost members of (1.31) $k \in \mathbb{Z}_0^+$ times:

$$\begin{aligned}
\frac{k!(\pm 1)^k}{(1\mp t)^{k+1}} &= \frac{d^k}{dz^k} \int_0^{+\infty} e^{-t} t^{\beta-1} E_{\alpha,\beta} dt \\
&= \int_0^{+\infty} e^{-t} t^{\beta-1} (\pm t^\alpha)^k \frac{d^k}{d(\pm z t^\alpha)^k} E_{\alpha,\beta}(\pm z t^\alpha) dt
\end{aligned} \tag{1.32}$$

We now replace t with st (and thus dt with sdt) and get

$$\frac{k!(\pm 1)^k}{(1\mp t)^{k+1}} = \int_0^{+\infty} e^{-st} s^{\beta-1} t^{\beta-1} (\pm 1)^k s^{\alpha k} t^{\alpha k} \frac{d^k E_{\alpha,\beta}(\pm z s^\alpha t^\alpha)}{d(\pm z s^\alpha t^\alpha)^k} s\, dt \tag{1.33}$$

Rearranging the terms and replacing zs^{α} with a (and thus z with $\frac{a}{s^{\alpha}}$):

$$\begin{aligned}
\frac{k!}{s^{\beta}s^{\alpha k}(1 \mp \frac{a}{s^{\alpha}})^{k+1}} &= \int_0^{+\infty} e^{-st}t^{\alpha k+\beta-1}\frac{d^k E_{\alpha,\beta}(\pm at^{\alpha})}{d(\pm at^{\alpha})^k}dt \\
\frac{k!s^{-\beta}s^{\alpha}}{s^{\alpha(k+1)}(1 \mp \frac{a}{s^{\alpha}})^{k+1}} &= \\
\frac{k!s^{\alpha-\beta}}{(s^{\alpha} \mp a)^{k+1}} &= \quad \blacksquare
\end{aligned} \tag{1.34}$$

$\square$

From Theorem 1.0.3 we can stablish the following useful corollaries:

Corollary 1.0.2

$$\mathcal{L}\left[t^{\beta-1}E_{\alpha,\beta}(\pm at^{\alpha})\right] = \frac{s^{\alpha-\beta}}{s^{\alpha} \mp a} \tag{1.35}$$

Proof. The proof follows by making $k = 0$ in (1.29) $\blacksquare$ $\square$

Remark 1.0.3. *A more detailed analysis of the Mittag-Leffler function behaviour can be found in (Podlubny, 1999), (Valério and da Costa, 2013) and specially (Gorenflo et al., 2014).*

Corollary 1.0.3

$$\mathcal{L}\left[t^{\alpha-1}E_{\alpha,\alpha}(\pm at^{\alpha})\right] = \frac{1}{s^{\alpha} \mp a} \tag{1.36}$$

Proof. Making $\alpha = \beta$ in (1.35) $\blacksquare$ $\square$

Corollary 1.0.4

$$\mathcal{L}\left[t^{\beta-1}E_{1,\beta}(\pm at)\right] = \frac{s^{1-\beta}}{s \mp a} \tag{1.37}$$

Proof. Making $\alpha = 1$ in (1.35) $\blacksquare$ $\square$

Corollary 1.0.5

$$\mathcal{L}\left[t^{\beta-1}E_{1,\beta}(0)\right] = \mathcal{L}\left[\frac{t^{\beta-1}}{\Gamma(\beta)}\right] = \frac{1}{s^{\beta}} \tag{1.38}$$

Proof. Making $a = 0$ in (1.37) $\blacksquare$ $\square$

Hence, to obtain the time response of several useful transfer functions to inputs like: impulse ($\delta(t)$), unit step ($H(s)$) and unit ramp (t). Making $\beta = \alpha$, $\alpha + 1$ and $\alpha + 2$ in (1.38), (1.35) and (1.29), we obtain the following responses:

$$\mathcal{L}^{-1}\left[\frac{1}{s^{\alpha}}\mathcal{L}\left[\delta(t)\right]\right] = \frac{t^{\alpha-1}}{\Gamma(\alpha)} \tag{1.39}$$

$$\mathcal{L}^{-1}\left[\frac{1}{s^{\alpha}}\mathcal{L}\left[H(t)\right]\right]=\frac{t^{\alpha}}{\Gamma(\alpha+1)} \tag{1.40}$$

$$\mathcal{L}^{-1}\left[\frac{1}{s^{\alpha}}\mathcal{L}\left[t\right]\right]=\frac{t^{\alpha+1}}{\Gamma(\alpha+2)} \tag{1.41}$$

$$\mathcal{L}^{-1}\left[\frac{1}{s^{\alpha}\mp a}\mathcal{L}\left[\delta(t)\right]\right]=t^{\alpha-1}E_{\alpha,\alpha}(\pm at^{\alpha}) \tag{1.42}$$

$$\mathcal{L}^{-1}\left[\frac{1}{s^{\alpha}\mp a}\mathcal{L}\left[H(t)\right]\right]=t^{\alpha}E_{\alpha,\alpha+1}(\pm at^{\alpha}) \tag{1.43}$$

$$\mathcal{L}^{-1}\left[\frac{1}{s^{\alpha}\mp a}\mathcal{L}\left[t\right]\right]=t^{\alpha+1}E_{\alpha,\alpha+2}(\pm at^{\alpha}) \tag{1.44}$$

$$\mathcal{L}^{-1}\left[\frac{1}{(s^{\alpha}\mp a)^{k+1}}\mathcal{L}\left[\delta(t)\right]\right]=\frac{t^{\alpha(k+1)-1}}{\Gamma(k+1)}\frac{d^{k}E_{\alpha,\alpha}(\pm at^{\alpha})}{d(\pm at^{\alpha})^{k}} \tag{1.45}$$

$$\mathcal{L}^{-1}\left[\frac{1}{(s^{\alpha}\mp a)^{k+1}}\mathcal{L}\left[H(t)\right]\right]=\frac{t^{\alpha(k+1)}}{\Gamma(k+1)}\frac{d^{k}E_{\alpha,\alpha+1}(\pm at^{\alpha})}{d(\pm at^{\alpha})^{k}} \tag{1.46}$$

$$\mathcal{L}^{-1}\left[\frac{1}{(s^{\alpha}\mp a)^{k+1}}\mathcal{L}\left[t\right]\right]=\frac{t^{\alpha(k+1)+1}}{\Gamma(k+1)}\frac{d^{k}E_{\alpha,\alpha+2}(\pm at^{\alpha})}{d(\pm at^{\alpha})^{k}} \tag{1.47}$$

Multivalued functions

One of the concepts that will be of great use in this work, is the idea of *Multivalued functions*. We know that from the stablished concept of *single-valued* functions, $w = f(s)$, we can naturally ask whether such a function can always have an inverse whereby s can be specified as a function of w. In those cases where several values of s yield identical values of w we are in trouble, for then the inverse can not be *single-valued*, and in the true sense of the word an inverse function does not exist, the reason is that such a mapping $s \to f(w)$ is not *single-valued*.

In complex analysis a function that satisfies

$$F\left[z(r,\theta+2\pi)\right]=F\left[z(r,\theta)\right] \tag{1.48}$$

is called a *single-valued function*.

For a better understand of the concept of *multi-valued functions*, perhaps the simplest example is the inverse of

$$w=s^{2}, \tag{1.49}$$

which will be written as,

$$s=w^{1/2}. \tag{1.50}$$

Using s instead of w as the independent variable for convenience then (1.49) is now written with s and w interchanged, as follows:

$$w=s^{1/2}. \tag{1.51}$$

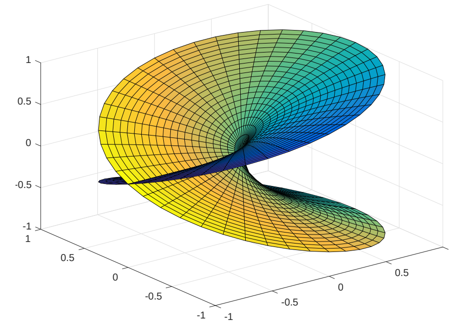
Figure 1.15: $\sqrt{s}$ Riemann-surface.

This function has two s planes which map onto a single w-plane. We exploit the idea of having two s planes. If somehow a distinction can be made between these two s planes, we could then regard overlying points in the two s planes as being different, and the function $w = s^{1/2}$ would appear to be *single-valued*. Refering to Figs. 1.16 and 1.17, we can see a pair of edges (one edge from each plane), where one solid line and one dashed line fit together. The curves such as C and C' do not cross such a cut but pass continuously from one plane to the other. When the two s planes are joined in this way, they form a **Riemann-surface** (for a formal definition of Riemann-surface see (Farkas and Kra, 1980)).

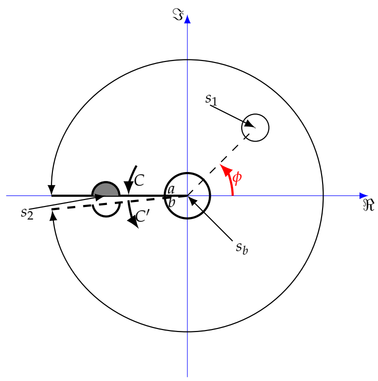

Figure 1.16: Riemann-surface interpretation of the function $w = s^{1/2}$. s-plane, sheet 1

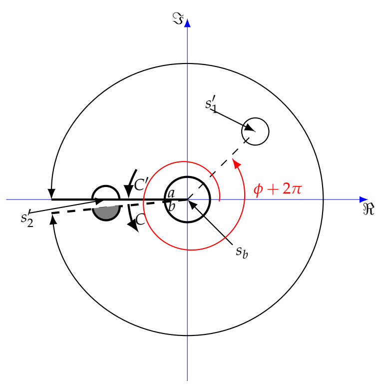

Figure 1.17: Riemann-surface interpretation of the function $w = s^{1/2}$. s-plane, sheet 2

The Riemann surfaces allow us to define a complex function without introducing artificial branches (Marsden and Hoffman, 1999). Each of the s planes is called a **sheet** of the Riemann-surface (RF). Before continuing with our example, there are two basic concepts we have to consider: *Branch points* (BP) and *Branch cuts* (BC).

Definition 1.0.6: Branch points (BP)

The branch point or point of accumulation is defined as the point with the smallest magnitude for which a function is multivalued (Cohen, 2007). Another definition would be: A branch point is a point such that the function is discontinuous when going around an arbitrarily small circuit around this point (see, for further details (Needham, 1997))

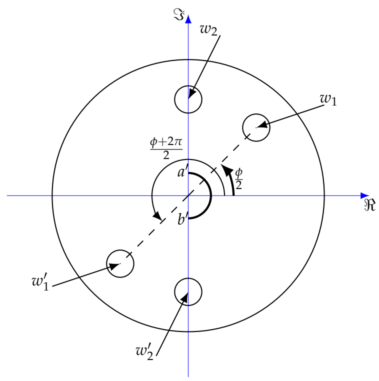

Figure 1.18: Riemann-surface interpretation of the function $w = s^{1/2}$. w-plane

For example, consider the general N^{th} root function written as

$$z^{\frac{M}{N}} = [z(r, \theta + 2k\pi)]^{\frac{M}{N}} = r^{\frac{M}{N}} e^{j\frac{M\theta}{N}} e^{j2\pi k\frac{M}{N}}. \tag{1.52}$$

We see that this function has multiple values for all $0 < r < \infty$. That is, the multivaluedness starts at $r = 0$, and therefore at $z = 0$. As such, the general N^{th} root function is said to have a branch point at $z = 0$. By replacing z by $z - z_0$ in (1.52), the branch point can be translated to the point z_0. Therefore, the expression

$$F_{\frac{M}{N}}(z) = (z - z_0)^{\frac{M}{N}}, \tag{1.53}$$

has a fractional root branch point at z_0.

Definition 1.0.7: Branch cuts

Let $F(z)$ be a multivalued function with a BP at z_0. We let θ increase so that z varies from $z\,[r, \theta + 2\pi k]$ to $z\,[r, \theta + 2\pi(k+1)]$. In doing so, values of $F(z)$ migrate from the k^{th} sheet, defined by $F\,\{z\,[r, \theta + 2\pi k]\}$, to the $(k+1)^{th}$ sheet, defined by $F\,\{z\,[r, \theta + 2\pi(k+1)]\}$. In order for these values of $F(z)$ to vary continuously, we envision the k^{th} sheet to be cut along some line called the *branch line* or *branch cut*, which extends from the branch point to ∞. This branch cut allows access to the $(k+1)^{th}$ sheet from the k^{th} sheet (Cohen, 2007). Hence, a cut in each sheet of a Riemann-surface is called a branch cut (BC) and is always formed by any simple arc connecting two branch points (BP)(Needham, 1997)).

We note from the above definition that the increase of θ by 2π can begin at any value of θ. Therefore, the cut can be oriented at any angle θ_0 to the positive real axis. All sheets are cut in this way to allow access from points on any one sheet to points on any adjacent sheet. The sheet defined by $k = 0$, for which $\theta_0 < \theta < \theta_0 + 2\pi$, is called the principal sheet or the principal branch of $F(z)$. The second sheet is defined by $\theta_0 + 2\pi < \theta < \theta_0 + 4\pi$ and so on.

Then, in our example (1.51) suppose that there are two points s_1 and s'_1 similarly located in the two sheets of Fig. 1.16, 1.17 and 1.18. The Riemann-surface interpretation allows them be regarded as different points. In this way $w_1 = f(s_1)$ and $w'_1 = f(s'_1)$ are clearly distinct because $\angle(s'_1) = 2\pi + \angle(s_1)$. With this interpretation $f(s)$ becomes single-valued. In sheet 1 of Fig. 1.16 the angle ϕ lies in the range $-\pi < \phi \leq \pi$, and in sheet 2 of the RF the range is $\pi < \phi \leq 3\pi$.

Consider the neighborhoods of points s and s', where the unprimed value is always in sheet 1 and the primed one is on sheet 2. Each of these neighborhoods will be transformed into neighborhoods of corresponding points in the w plane. A few particular cases are considered, beginning with points s_1 and s_1'. There is no possibility of neighborhood of s' becoming confused with the neighborhood of s_1. This permits us to use the definition of continuity without being bothered by multivaluedness. A point like s_2 on a solid-line edge of a branch cut can not have a neighborhood completely in one sheet. Its neighborhood must be in two sheets, as indicated by the two shaded areas in Fig. 1.16 and 1.17. This neighborhood goes into a neightborhood of w_2 in the w plane. The corresponding point s_2' has a neighborhood consisting of the two nonshaded circular segments, which transforms into a neighborhood of w_2'. Although the neighborhoods of s_2 and s_2' are each in two sheets, the function is single-valued in each neighborhood.

Now, analyzing the branch point labeled as s_b. If we try to put a small circle around s_b in sheet 1, we find that points a and b cannont be conected; from a point a we must proceed into sheet 2. If points a and b are allowed to approach each other, the corresponding points in the w plane approach a' and b', which are at the ends of a semicircle, as shown in Fig. 1.18. A small circle which encircles a branch point only once can not transform into a closed figure in the function plane. Two or more circuits (two in this example) around a branch point are required to give a closed figure in the function plane. Branch points are designated by an order number. The order is on less than the number of circuits around it required to give a closed figure in the function plane.

The above description brings to light other distinctive features of a branch point. Unlike points such as s_1 and s_2, a branch point can not be assigned to any one sheet of the Riemann-surface, and therefore it can not have a neighborhood lying in only one sheet. That is, it is impossible to define a neighborhood of a branch point in which the function is single-valued.

We can use the fact that encircling a branch point only once does not close the figure traced in the function plane can be used to test wheter or not a given point is a branch point. As an example, we shall test whether $s = 0$ and $s = 1$ are branch points of the function

$$w = s^{1/2}. \tag{1.54}$$

At $s = 0$, we write

$$s = \rho e^{j\phi}, \quad w = re^{j\theta}, \tag{1.55}$$

giving

$$r^2 e^{j2\theta} = \rho e^{j\phi}, \tag{1.56}$$

and

$$r = \sqrt{\rho}, \quad \theta = \frac{\phi}{2} \tag{1.57}$$

If ϕ is increased by 2π, so that point $s = 0$ is encircled once, θ will increase by π, which carry w only halfway around the origin. Thus, $s = 0$ is a branch point. Now, look at the pair of points $s = 1$ and $w = 1$. In their neighborhoods we write

$$s = 1 + \rho e^{j\phi}, \quad w = 1 + re^{j\theta} \tag{1.58}$$

and

$$1 + 2re^{j\theta} + r^2 e^{j2\theta} = 1 + \rho e^{j\phi}, \tag{1.59}$$

as r is made very small, the r^2 term approaches zero faster than r and so the above approaches

$$2re^{j\theta} \approx \rho e^{j\phi}, \tag{1.60}$$

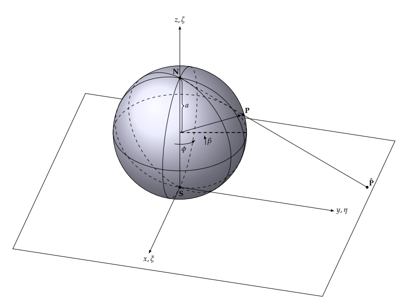

Figure 1.19: The Riemann-sphere. Sthereographic projection of the (ξ, η, ζ) sphere onto the s plane.

showing that point $w = 1$ is encircled only once when $s = 1$ is encircled once by a small circle. Thus, $s = 1$ is not a branch point.

If the Riemann-sphere interpretation is introduced (see, for further details (Cohn, 1967)), we can also identify a branch point at the point infinity. A small circular path enclosing the point at infinity on the Riemann-sphere becomes a large circle in the flat plane. Thus, to test whether the point at infinity is a branch point, we look at the figure traced in the function plane as we follow one circuit around a large circle (approaching infinite radius) in the s plane. If the function-plane does not close, the point at infinity is a branch point.

We conclude that the function $w = s^{1/2}$ has branch points of order 1, at $s = 0$ and at infinity. Then, the BC is the union of such BPs.

Integration around Branch Points

A very powerfull method to identify where the BPs of a multivalued function are, is by menas of the integral. To see why, consider the following function

$$F(s) = \frac{1}{s^{1/2}}, \tag{1.61}$$

from previous discussions we know that this function has a BP at $s = 0$ and at infinity. Although, this function becomes infinite at the BP, this is not a pole of the function. To find the reason, consider the integral

$$\int_C \frac{1}{s^{1/2}} ds, \tag{1.62}$$

where C is a counterclockwise closed curve encircling the origin once. For simplicity, consider the curve as a circle of radius ρ. Assuming $s = \rho e^{j\phi}$, it follows that

Remark 1.0.4. *More details about integration or derivation around BPs can be found at (LePage, 1980)*

$$\int_C \frac{1}{s^{1/2}} = \int_{-\pi}^{\pi} \frac{1}{\sqrt{\rho} e^{j\phi/2}} (j\rho e^{j\phi}) d\phi = j4\sqrt{\rho}. \tag{1.63}$$

It is observed that the integral around BP approaches zero as the radius of integration approaches zero. This would not be true for integration around a pole.

2
Mathematical modeling of fractional order systems

Infinite networks flow dynamics

We may say that Nature works with fractional time derivatives

S. Westerlund (1991)

In previous sections we have seen that *Fractional Calculus* does not have a physical meaning yet. Nontheless, many results trying to represent or identify systems by using *Fractional Calculus* have been published.

In (Coimbra, 2003) the use of fractional operators for modeling viscoeslastic forces is described. For the area of *Capacitor theory*, Svante Westerlund et al. propose a new linear capacitor model making use of the fractional derivative, the model gives arise to a capacitor impedance $Z(j\omega) = \frac{1}{(j\omega)^n C}$ with $0 < n < 1$ and C is the known capacitor constant (see, for further details (Westerlund and Ekstam, 1994)).
A connection of *Fractional Calculus* with the theory of *Viscoelasticity* is shown in (Koeller, 1984) due to the memory or heredity property of fractional operators. *Fractional Calculus* is considered an interesting tool in Biology, Chemistry and Medicine (see, for further details (Magin, 2006)), for some examples see: (Simpson et al., 2012), (Meerschaert et al., 2012), (Neto et al., 2017), (Lundstrom et al., 2008) and (Martínez-García et al., 2017).

One of the considered properties presented in *Fractional Calculus* is the *Self-similarity* property, this means that we can use it as a tool for decribing systems with self-affinity. In (Heymans and Bauwens, 1994) fractal rheological models are discussed and in (Nakagawa and Sorimachi, 1992) the characteristics of a fractance device are analyzed. Both of the mentioned works have something in common: they present the Fig. 2.1 and Fig. 2.2 as basic topologies for systems presenting fractance which can be modeled by means of fractional order differential equations.

Given $\mathbf{L}_i$, $i = 1, 2$ as a linear operator, for example $\mathbf{L} = \mathcal{D}$ where $\mathcal{D}$ is the derivative operator. If we look for a relation between $x_{out}(t)$ and $x_{in}(t)$ in schemes Fig. 2.2 and 2.1 we notice clearly that such a relation is of infinite-order. We mention that infinite order systems in the *Laplace* domain present *Multivalued functions* sometimes involving fractional order operators (see, (Curtain, 1992; Curtain and Zwart, 1995)).

Within these ideas Jason Mayes and Mihir Sen (see, (Mayes and Sen, 2011)) studied the binary tree in Fig. 2.1 to find such a transfer function relating $x_{out}(t)$ and $x_{in}(t)$

$$\mathbf{L}_N^* u(t) = \Delta x(t), \tag{2.1}$$

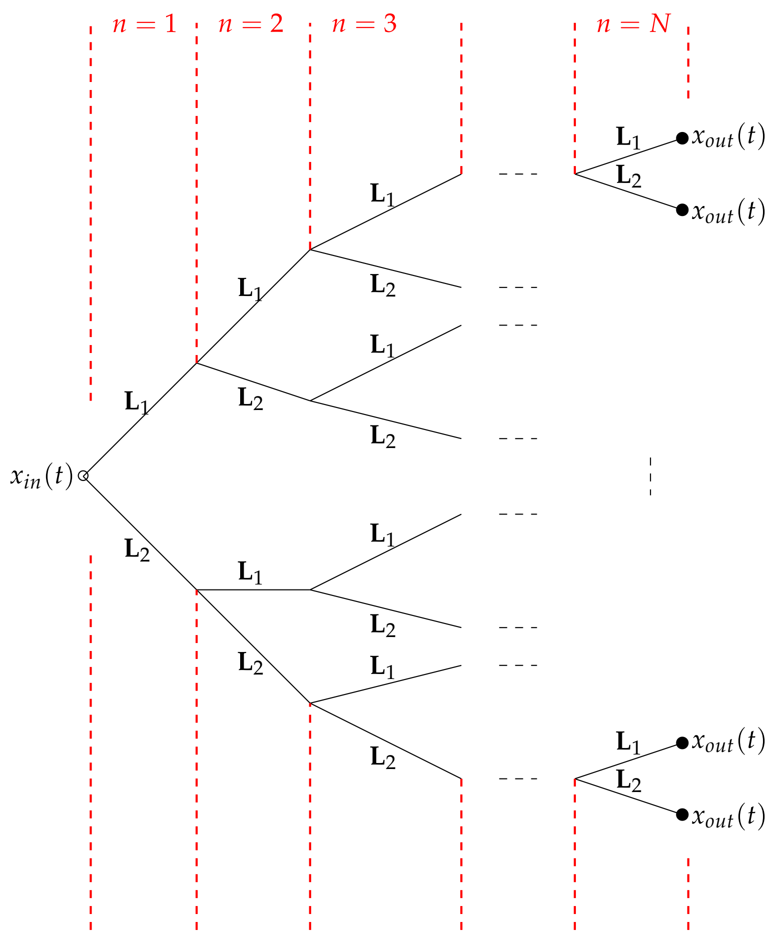

Figure 2.1: Tree configuration (only three generations shown); ◦ is input, • is fixed.

where $u(t)$ is the total transfer through or across the network, $\Delta x(t)$ is the potential difference across the network and $\mathbf{L}_N^*$ is the approximate operator relating the potential difference and induced transfer.

Even though, (Mayes and Sen, 2011) presents the general case analysis. Let us consider the following particular example of a mechanical $N=2$ generation tree network in Fig. 2.3 so that $x_{2,1}=x_{2,2}=x_{2,3}=x_{2,4}=x_{out}$.

According to (Mayes and Sen, 2011), for $N=2$ there are $2^N=4$ possible paths through this network. The six transfer equations for the system (one for each branch) are

$$
\begin{aligned}
\mathbf{L}_1 u_{1,1} &= \Delta x_{1,1} = x_{in} - x_{1,1},\\
\mathbf{L}_2 u_{1,2} &= \Delta x_{1,2} = x_{in} - x_{1,2},\\
\mathbf{L}_1 u_{2,1} &= \Delta x_{2,1} = x_{1,1} - x_{out},\\
\mathbf{L}_2 u_{2,2} &= \Delta x_{2,2} = x_{1,1} - x_{out},\\
\mathbf{L}_1 u_{2,3} &= \Delta x_{2,3} = x_{1,2} - x_{out},\\
\mathbf{L}_2 u_{2,4} &= \Delta x_{2,4} = x_{1,2} - x_{out},
\end{aligned}
$$

where $u_{i,j}$, $\Delta x_{i,j}$ and $x_{i,j}$ are functions of time. Additionally, assuming unit weights the conservation equations

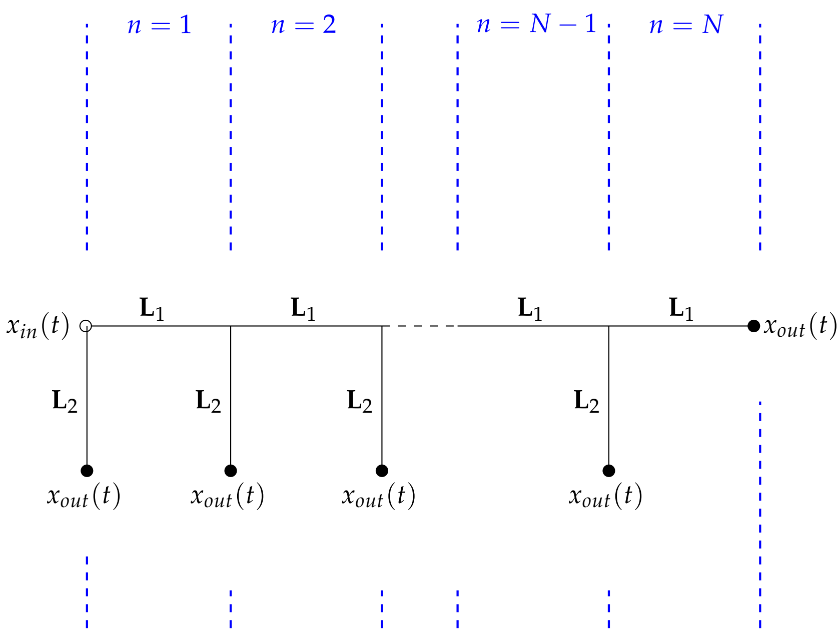

Figure 2.2: Ladder configuration; ∘ is input, • is fixed.

for the two nodes are

$$u_{1,1} = u_{2,1} + u_{2,2}, \tag{2.2}$$

and

$$u_{1,2} = u_{2,3} + u_{2,4}. \tag{2.3}$$

Finally, the total flow, u, through the simplified network is given by

$$u = u_{1,1} + u_{1,2}, \tag{2.4}$$

and $\mathbf{L}_2^*$ is the operator describing the behaviour of the simplified $2-\textit{generation}$ tree in

$$\mathbf{L}_2^* u = \Delta x. \tag{2.5}$$

By combining the transfer equations along the four unique paths from inlet to outlet, the interior potentials, $u_{1,1}$ and $u_{1,2}$, are eliminated to yield four new equations

$$\begin{aligned}
\mathbf{L}_1 u_{1,1} + \mathbf{L}_1 u_{2,1} &= x_{in} - x_{out} = \Delta x, \\
\mathbf{L}_1 u_{1,1} + \mathbf{L}_2 u_{2,2} &= x_{in} - x_{out} = \Delta x, \\
\mathbf{L}_2 u_{1,2} + \mathbf{L}_1 u_{2,3} &= x_{in} - x_{out} = \Delta x, \\
\mathbf{L}_2 u_{1,2} + \mathbf{L}_2 u_{2,4} &= x_{in} - x_{out} = \Delta x.
\end{aligned}$$

now, we find the $u_{2,j}$ as

$$\begin{aligned}
u_{2,1} &= \mathbf{L}_1^{-1}\left[\Delta x - \mathbf{L}_1 u_{1,1}\right], \\
u_{2,2} &= \mathbf{L}_2^{-1}\left[\Delta x - \mathbf{L}_1 u_{1,1}\right], \\
u_{2,3} &= \mathbf{L}_1^{-1}\left[\Delta x - \mathbf{L}_2 u_{1,2}\right], \\
u_{2,4} &= \mathbf{L}_2^{-1}\left[\Delta x - \mathbf{L}_2 u_{1,2}\right].
\end{aligned}$$

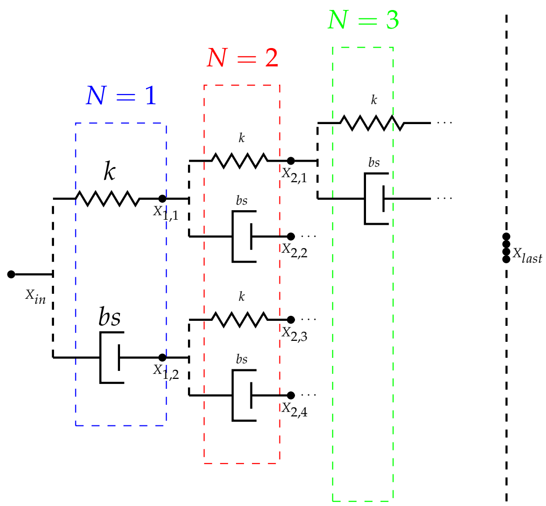

Figure 2.3: Network of interconnected simple mechanical elements.

Using equations (2.2) and (2.3)

$$u_{1,1} = \left\{\mathbf{L}_1^{-1} + \mathbf{L}_2^{-1}\right\}[\Delta x - \mathbf{L}_1 u_{1,1}], \tag{2.6}$$

$$u_{1,2} = \left\{\mathbf{L}_1^{-1} + \mathbf{L}_2^{-1}\right\}[\Delta x - \mathbf{L}_1 u_{1,2}]. \tag{2.7}$$

Now by expression (2.4) using (2.6) and (2.7) we obtain

$$u = \left\{\left\{\left\{\mathbf{L}_1^{-1} + \mathbf{L}_2^{-1}\right\}^{-1} + \mathbf{L}_1\right\}^{-1} + \left\{\left\{\mathbf{L}_1^{-1} + \mathbf{L}_2^{-1}\right\}^{-1} + \mathbf{L}_2\right\}^{-1}\right\}\Delta x. \tag{2.8}$$

Rewriting (2.8) in the form of (2.5) we see that the system operator for a bifurcating network with $N = 2$ generatios can be given as:

$$\mathbf{L}_2^* = \left\{\left\{\left\{\mathbf{L}_1^{-1} + \mathbf{L}_2^{-1}\right\}^{-1} + \mathbf{L}_1\right\}^{-1} + \left\{\left\{\mathbf{L}_1^{-1} + \mathbf{L}_2^{-1}\right\}^{-1} + \mathbf{L}_2\right\}^{-1}\right\}^{-1}. \tag{2.9}$$

The last expression has the form of a *Continued Fraction Expantion* (see, for further details (Wall, 1967)). This was proved in (Mayes and Sen, 2011) by adding more generations to the tree to finally conclude that for a large N, $\mathbf{L}_N^*$ can either be calculated in the same way or approximated as $\mathbf{L}_\infty = \lim_{N\to\infty} \mathbf{L}_N^*$. For our example the total operator $\mathbf{L}_N^*$ in the form of a continued fraction is given by

$$\mathbf{L}_N^* = \frac{1}{\frac{1}{\mathbf{L}_1 + \frac{1}{\frac{1}{\mathbf{L}_1+\cdots} + \frac{1}{\mathbf{L}_2+\cdots}}} + \frac{1}{\mathbf{L}_2 + \frac{1}{\frac{1}{\mathbf{L}_1+\cdots} + \frac{1}{\mathbf{L}_2+\cdots}}}}, \tag{2.10}$$

We can rewrite (2.10) as

$$\mathbf{L}_\infty = \frac{1}{\frac{1}{\mathbf{L}_1 + L_\infty} + \frac{1}{\mathbf{L}_2 + L_\infty}}. \tag{2.11}$$

Remark 2.0.1. *Taking advantage of the self-similarity property presented in a continued expantion (actually given by the nature of the operators in each generation of the binary tree) we can prove that a continued fraction converges in the following form:*

$$x_{eq} = \frac{1}{1 + \boxed{\frac{1}{1 + \frac{1}{1+\ldots}}}}, \quad = \frac{1}{1 + x_{eq}}.$$

Hence, if we consider the *Laplace*-transformed operators $\mathcal{L}_1 = \frac{1}{k}$, $\mathcal{L}_2 = \frac{1}{bs}$ and $\mathcal{L}_\infty$ of $\mathbf{L}_1, \mathbf{L}_2$ and $\mathbf{L}_\infty$ with initial conditions equals to zero, respectively. The total transfer function $\mathbf{L}_\infty$ can be found by solving

$$\mathbf{L}_\infty^2 - \mathbf{L}_1\mathbf{L}_2 = 0, \tag{2.12}$$

which is given by

$$\mathcal{L}_\infty = \sqrt{\mathcal{L}_1\mathcal{L}_2} = \frac{1}{\sqrt{kbs}}, \tag{2.13}$$

as presented in (Goodwine, 2016).

For the case of the infinity ladder shown in Fig. 2.2 we can use a similar analysis to obtain the total operator (see, for further details (Sen et al., 2018a)) which can be proved to have an equivalent implicitly-defined operator $\mathcal{L}_{eq}$ describing the dynamic response to the components equal to the solution of

$$\mathcal{L}_{eq} = \frac{1}{\frac{1}{\mathcal{L}_2} + \frac{1}{\mathcal{L}_1 + \mathcal{L}_{eq}}}, \tag{2.14}$$

which is given by

$$\mathcal{L}_{eq} = \frac{1}{2}\left[-\mathcal{L}_1 \pm \sqrt{\mathcal{L}_1^2 + 4\mathcal{L}_1\mathcal{L}_2}\right]. \tag{2.15}$$

As we can see by (2.13) the total operator relating x_{out} with x_{in} is of fractional nature. And it was given by a solution of a *operator-defining equation* $F(\mathcal{L}) = 0$.

For simplicity we have used *Laplace*-transformed the operators. In the case of avoiding such transformation, the total operator would be a special case of the solution of a *operator-defining equation* like

$$\mathbf{L}^m = \mathcal{D}^n, \tag{2.16}$$

where $\mathcal{D} = \frac{d}{dt}$.

A research question arises here: **What if the total operator is solution of a given *operator-defining equation* $F(\mathbf{L}) = 0$ such as:**

- $\mathbf{L}^2 + \mathbf{L} = \mathcal{D}$,
- $\sin(\mathbf{L}) = \mathcal{D}$,

etc.?

Such type of operators $\mathbf{L}$ are known as *implicitly-defined* operators (see, (Sen et al., 2018b)). The problem comes when trying to use a time-domain operator defined by means of such *operator-defining equations*. Take for example, the solution of the equation $\mathbf{L}^2 + \mathbf{L} = \mathcal{D}$, which is given by $\mathbf{L} = \sqrt{\mathcal{D} + \mathbf{I}}$ and $\mathbf{L} = 0$ where $\mathbf{I}$ would be the identity operator. The first solution defines $\mathbf{L}$ as $\sqrt{\frac{d}{dt} + 1}$, which is no longer in the theory fractional calculus where $\mathbf{L}$ is always a solution of (2.16).

Nontheless, if we *Laplace*-transform the operators used, before computing the *operator-defining equation* we obtain something meaninful in the *complex-domain*.

With these briefly discussed ideas, we present the following sections as part of some of the main results in the present work.

Infinite networks convergence and paradoxes

To obtain the flow dynamics of a infinite network as we have shown before, we base our analysis in the idea of convergence of *Continued Fractions* which are a type of *Series*. Hence, to study the convergence of *Continued Fractions* is of high importance. To understand this idea, consider scheme in Fig. 2.4.

Figure 2.4: Series configuration; ∘ is input, • is fixed.

In this scheme we aim at finding the relation $\mathcal{L}_N^* q = \Delta p = p_{in} - p_{out}$, which may be in the form of a *Continued Fraction* or not. Based on ideas in (Mayes and Sen, 2011) we know q is the total transfer through the complete branch, Δp is the total potential difference across the complete branch and $\mathcal{L}$ is the operator relating the two. In this scheme no bifurcation exists between each generation. Then, the conservation equation of the complete system would be written as

$$q = q_i \quad \forall \quad i \in \mathbb{N} \bigcup (\infty). \tag{2.17}$$

Then, if the following set of equations hold

$$\begin{aligned} \mathcal{L}_1 q_1 &= p_{in} - p_1, \\ \mathcal{L}_2 q_2 &= p_1 - p_2, \\ \mathcal{L}_3 q_3 &= p_2 - p_3, \\ \vdots &= \vdots \\ \mathcal{L}_n q_n &= p_n - p_{out}, \end{aligned}$$

we have that

$$\sum_{k=1}^{n} \mathcal{L}_k q_k = \Delta p, \tag{2.18}$$

and if $\forall k \in 1, 2, \ldots, n$ $\mathcal{L}_k = \mathcal{L}$, we conclude that

$$\frac{\Delta p}{q} = N\mathcal{L}. \tag{2.19}$$

where, such a relation converges when $N < \infty$.

As we could see (2.18) is in the form of a infinity series, which is natural due to the geometry of scheme 2.4. Therefore, we can apply convergence criterions for *Series* in this case.

Nontheless, for the infinite ladder and tree networks shown in Fig. 2.1 and 2.2 our criterions change. The expression shown in Remark 2.0.1 does actually converge to x_{eq}, but such a x_{eq} is a linear operator that when being *Laplace*-transformed has a frequency domain attached to it. Some analysis concerning to infinite networks convergence can be found at (Zemanian, 1988), (Singal, 2013) and (van Enk, 2000). Because we consider that such convergence considerations would act as design limitations in our models, the sutudy of convergence will not be considered in this work.

Inverse Laplace Transform (ILT) of Implicitly defined operators

In this section we will consider *Laplace*-transformed special cases of the *operator-defining equation* in the form of

$$A\mathbf{L}^2 + B\mathbf{L} + \mathbf{I} = \mathcal{D}, \tag{2.20}$$

where A, B are real constants, $\mathcal{D} = \frac{d}{dt}$, $\mathbf{I}$ is the identity operator and $\mathbf{L}$ is the implicitly-defined operator that as we have seen above can represent the total transfer function of a infinite tree or ladder network and its solution of (2.20) can be found using the quadratic equation formula.

As a sketch, the solution when considering (2.20) coming from a Laplace transformed series of operators would be in the form:

$$\mathcal{L}(s) = \frac{-B \pm \sqrt{B^2 - 4A(1+s)}}{2A}. \tag{2.21}$$

(2.21) is clearly a multivalued-function with BPs and a BC. Hence, we must analyze how to ILT multivalued functions. As a first example of the ILT technique used in this section for multivalued-functions, consider $\mathcal{L}_i$ to be the transformed operator defined as

$$\mathcal{L}_i := \frac{1}{s^\alpha}. \tag{2.22}$$

From (Valério and da Costa, 2013), we know that the ILT of (2.22) is given by

$$\mathscr{L}^{-1}\left[\frac{1}{s^\alpha}\right] = \frac{t^{\alpha-1}}{\Gamma(\alpha)}. \tag{2.23}$$

By remembering that such a operator $\mathcal{L}_i$ is a multivalued-function. To proof (2.23) we may use the ILT definition, and hence by solving the following integral

$$L_i(t) = \frac{1}{j2\pi}\int_{Br} \mathcal{L}_i(s)e^{st}ds. \tag{2.24}$$

By Figure 2.5, and from the residue theorem we know that

$$\oint_\Gamma \mathcal{L}_i(s)e^{st}ds = \int_{C_1+C_2+C_3+C_4+C_5} = 0, \tag{2.25}$$

besides,

$$\int_{C_1} = \int_{C_5} = 0, \tag{2.26}$$

because they vanish when $R \to \infty$, and

$$\int_{C_3} = 0, \tag{2.27}$$

it can be easily proof that $\int_{C_3} = 0$ when $\rho \to 0$. In order to do the integration along C_2 and C_4, let us do the parameterization $s = -r \pm \delta$ where positive and negative signs correspond to C_2 and C_4, respectively, $r \in (\rho, \infty)$ and δ, ρ are small positive numbers which tend to zero. Some algebra yields

$$\int_{C_2+C_4} = e^{j\pi}\int_\infty^\rho \frac{e^{-rt}}{e^{j\pi\alpha}r^\alpha}dr + e^{-j\pi}\int_\rho^\infty \frac{e^{-rt}}{e^{-j\pi\alpha}r^\alpha}dr = -2j\sin(\pi\alpha)\int_0^\infty \frac{e^{-rt}}{r^\alpha}dr = -2j\sin(\pi\alpha)t^{\alpha-1}\Gamma(1-\alpha). \tag{2.28}$$

Now, because

$$\Gamma(\alpha)\Gamma(1-\alpha) = \frac{\pi}{sin(\pi\alpha)}, \tag{2.29}$$

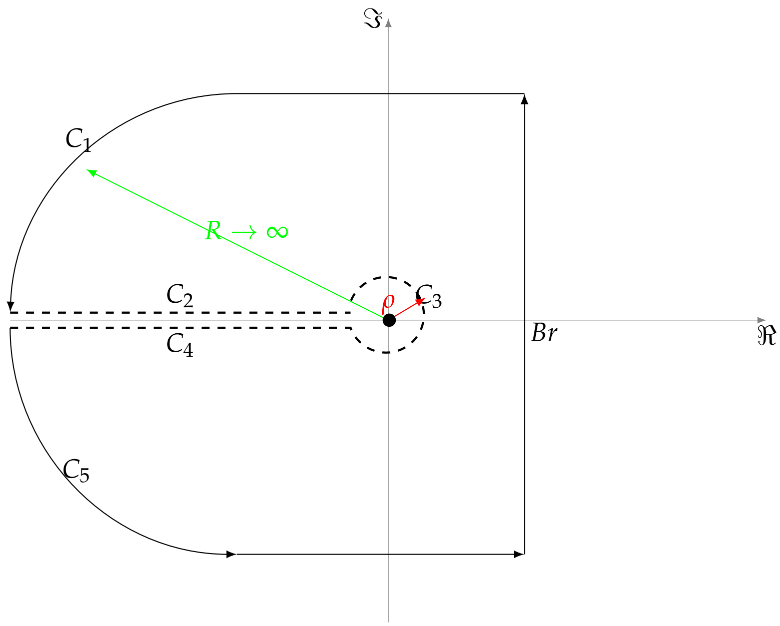

Figure 2.5: Integration path of function (2.22).

for $0 < \alpha < 1$. We have that

$$L_i(t) = \frac{t^{\alpha-1}}{\Gamma(\alpha)}. \tag{2.30}$$

Now consider the following interesting cases, which will be helpful in future results:

Poles under Branch Cuts

The following example allow us to understand how to deal with the integration contour in the ILT definition when poles of the transfer function are under its Branch cut.

Consider the transfer function given by

$$H(s) = \frac{1}{\sqrt{s}(s+1)}, \tag{2.31}$$

whose integration contour is depicted in Figure 2.6-B. From the Residue theroem we have

$$\int_{\Gamma} H(s)e^{st}ds = \int_{Br+C_1+C_2+\cdots+C_9} = 0 \tag{2.32}$$

and hence

$$\int_{c-j\infty}^{c+j\infty} \frac{e^{st}ds}{\sqrt{s}(s+1)} + \int_{\infty}^{1+\epsilon} \frac{e^{-xt}(-dx)}{j\sqrt{x}(1-x)} + \int_{\pi}^{0} \frac{e^{(-1+\epsilon e^{j\phi})j\epsilon e^{j\phi}d\phi}}{\sqrt{\epsilon e^{j\phi}-1}\epsilon e^{j\phi}} + \int_{1-\epsilon}^{\epsilon} \frac{e^{-xt}(-dx)}{j\sqrt{x}(1-x)} + \int_{\pi}^{-\pi} \frac{e^{t\epsilon e^{j\phi}}j\epsilon e^{j\phi}d\phi}{\sqrt{\epsilon e^{j\phi}}(1+\epsilon e^{j\phi})}$$
$$+ \int_{\epsilon}^{1-\epsilon} \frac{e^{-xt}(-dx)}{j\sqrt{x}(1-x)} + \int_{2\pi}^{\pi} \frac{e^{(-1+\epsilon e^{j\phi})t}j\epsilon e^{j\phi}d\phi}{\sqrt{\epsilon e^{j\phi}-1}\epsilon e^{j\phi}} + \int_{1+\epsilon}^{\infty} \frac{e^{-xt}(-dx)}{-j\sqrt{x}(1-x)} = 0$$

By making $\epsilon \to 0$ the above expression leads to

$$\int_{c-j\infty}^{c+j\infty} \frac{e^{st}ds}{\sqrt{s}(s+1)} + \int_{\infty}^{1+\epsilon} \frac{e^{-xt}(-dx)}{j\sqrt{x}(1-x)} + \int_{1-\epsilon}^{\epsilon} \frac{e^{-xt}(-dx)}{j\sqrt{x}(1-x)} + \int_{\epsilon}^{1-\epsilon} \frac{e^{-xt}(-dx)}{j\sqrt{x}(1-x)} + \int_{1+\epsilon}^{\infty} \frac{e^{-xt}(-dx)}{-j\sqrt{x}(1-x)} = 0, \tag{2.33}$$

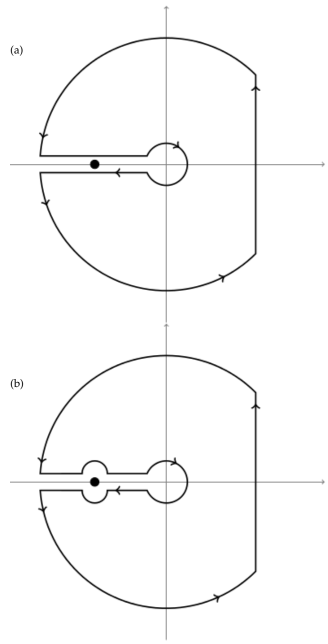

Figure 2.6: Integration contours for system (2.31), (a) Integration contour without considering the pole $s = -1$, (b) Integration contour considering the pole $s = 1$.

using the Cauchy principal value of the integral, this is specifically designed to deal with the pole at $x = 1$ we can combine the following integrals

$$PV \int_0^\infty \frac{e^{-xt}dx}{\sqrt{x}(1-x)} = \lim_{\epsilon \to 0} \left[\int_\epsilon^{1-\epsilon} \frac{e^{-xt}dx}{\sqrt{x}(1-x)} + \int_{1+\epsilon}^\infty \frac{e^{-xt}dx}{\sqrt{1-x}} \right], \tag{2.34}$$

$$PV \int_\infty^0 \frac{e^{-xt}dx}{\sqrt{x}(1-x)} = \lim_{\epsilon \to 0} \left[\int_\infty^{1+\epsilon} \frac{e^{-xt}dx}{\sqrt{x}(1-x)} + \int_{1-\epsilon}^\epsilon \frac{e^{-xt}dx}{\sqrt{1-x}} \right], \tag{2.35}$$

then,

$$\frac{1}{i2\pi} \int_{c-i\infty}^{c+i\infty} \frac{e^{st}}{\sqrt{s}(1+s)} ds + \frac{1}{2\pi} PVx \int_\infty^0 \frac{e^{-tx}}{\sqrt{x}(1-x)} dx - \frac{1}{2\pi} PV \int_0^\infty \frac{e^{-tx}}{\sqrt{x}(1-x)} dx = 0. \tag{2.36}$$

$$\frac{1}{2j\pi} \int_{c-j\infty}^{c+j\infty} \frac{e^{st}ds}{\sqrt{s}(s+1)} = \frac{1}{\pi} PV \int_0^\infty \frac{e^{-xt}dx}{\sqrt{x}(1-x)}. \tag{2.37}$$

To solve the above integral we use the change of variable $x = u^2$. Because in this case we are integrating a even function using the propety $\int_{-a}^{a} f(x)\, \mathrm{d}x = 2\int_0^a f(x)\, \mathrm{d}x$

$$\frac{1}{i2\pi} \int_{c-i\infty}^{c+i\infty} \frac{e^{st}}{\sqrt{s}(1+s)} ds = \frac{1}{\pi} PV \int_{-\infty}^\infty \frac{e^{-tu^2}}{1-u^2} du. \tag{2.38}$$

To evaluate the integral, we rewrite as

$$e^{-t} PV \int_{-\infty}^\infty \frac{e^{t(1-u^2)}}{1-u^2} du = e^{-t} I(t), \tag{2.39}$$

where

$$I'(t) = e^t PV \int_{-\infty}^\infty e^{-tu^2} du = \sqrt{\pi} t^{-1/2} e^t \tag{2.40}$$

and $I(0) = 0$. Thus,

$$\frac{1}{i2\pi}\int_{c-i\infty}^{c+i\infty}\frac{e^{st}}{\sqrt{s}(1+s)}ds = e^{-t}\frac{1}{\pi}\sqrt{\pi}\int_0^t t'^{-1/2}e^{t'}dt' = e^{-t}\frac{2}{\sqrt{\pi}}\int_0^{\sqrt{t}} e^{v^2}dv, \tag{2.41}$$

or, finally

$$\frac{1}{i2\pi}\int_{c-i\infty}^{c+i\infty}\frac{e^{st}}{\sqrt{s}(1+s)}ds = e^{-t}\,\mathrm{erfi}\left(\sqrt{t}\right) \tag{2.42}$$

Conjugate Branch Points

The following is a very useful result that allows us to deal with conjugate branch points (i.e. with multivalued functions with expressions like $\sqrt{s^2+a^2}$).

Theorem 2.0.1: ILT of functions with conjugate BPs. (Moslehi and Ansari, 2016)

Let $F(s)$ be an analytic function for $\Re(s) > c$, also it has two conjugate branch points $\pm aj$ and $F(re^{-j\pi}) = F(re^{j\pi})$, where $a > 0$ and $r > 0$. Furthermore, $F(s)$ satisfy the conditions

$$\begin{aligned} F(s) &= O(1), \quad |s| \to \infty \\ F(s) &= O(\frac{1}{|s|}) \quad |s| \to 0, \end{aligned}$$

for any sector $|\arg(s)| < \pi - \eta$, where $0 < \eta < \pi$. Then the inverse Laplace transfrom $f(t)$ can be written as two integral representations

$$f(t) = \mathscr{L}^{-1}\{F(s);t\} = -\frac{2}{\pi}\int_a^\infty \sin(rt)\Im\left[F(re^{j\frac{\pi}{2}})\right]dr, \tag{2.43}$$

$$f(t) = \mathscr{L}^{-1}\{F(s);t\} = \frac{2}{\pi}\int_a^\infty \cos(rt)\Re\left[F(re^{j\frac{\pi}{2}})\right]dr. \tag{2.44}$$

Theorem 2.0.1 shows that it is possible to find the ILT of a function with conjugate BPs, using any of the following deformations of the Bromwich integral.

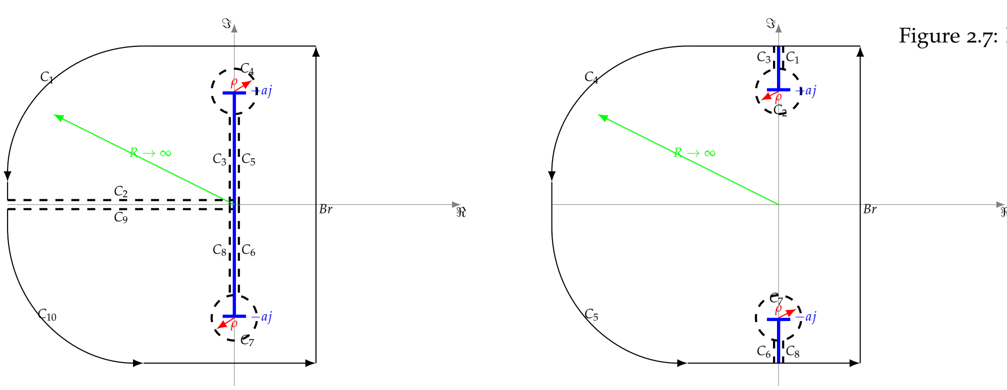

Figure 2.7: Integration path in Example.

Remark 2.0.2. *If we have other singularities inside the Bromwich contours (poles and essential singularities) or branch points, then, the sum of residues of the function $F(s)e^{st}$ at these singularities is added to the relations (2.43) and (2.44) in Theorem 2.0.1.*

Non-conventional fractional order systems

Before presenting physical systems described by multivalued-functions or as we may call them *Non-conventional fractional order transfer functions*. Consider the following results:

Proposition 2.0.1

Let $\mathcal{L}_o$ be the multivalued operator function defined as

$$\mathcal{L}_o(s) := \frac{1}{\sqrt{s^2 - k^2}}, \tag{2.45}$$

where $k > 0$. Then, its ILT is given by

$$L_o(t) := \frac{1}{\pi}\int_{-k}^{k} \frac{e^{rt}}{\sqrt{k^2 - r^2}} dr = J_0(jkt). \tag{2.46}$$

where, $J_0(\cdot)$ is the Bessel function of the first kind of zeroth order.

Proof. From figure 2.9, we may create a path that satisfies

$$\int_{\Gamma} \mathcal{L}_o(s) e^{st} ds = \int_{Br+C_1+C_2+C_3+C_4} = 0, \tag{2.47}$$

by making $\rho \to 0$ we have that

$$\int_{C_1+C_2} = 0. \tag{2.48}$$

Now, the paths C_3 and C_4, on which we shall write $s = r$, where r varies from $k - \rho$ to $-k + \rho$. We have that

$$\int_{C_3+C_4} \frac{e^{st}}{\sqrt{s^2 - k^2}} ds = -j\int_{-k+\rho}^{k-\rho} \frac{e^{rt}}{\sqrt{k^2 - r^2}} dr + j\int_{k-\rho}^{-k+\rho} \frac{e^{rt}}{\sqrt{k^2 - r^2}} dr = -2j\int_{-k+\rho}^{k-\rho} \frac{e^{rt}}{\sqrt{k^2 - r^2}} dr, \tag{2.49}$$

then,

$$L_o(t) = \frac{1}{j2\pi}\int_{Br} \mathscr{L}_o(s) e^{st} ds = \frac{1}{\pi}\int_{-k+\rho}^{k-\rho} \frac{e^{rt}}{\sqrt{k^2 - r^2}} dr \overset{\rho \to 0}{=} \frac{1}{\pi}\int_{-k}^{k} \frac{e^{rt}}{\sqrt{k^2 - r^2}} dr. \tag{2.50}$$

We may evaluate the integral on the right hand side as follows. Substitute $r = a\cos u$, then the integral is equal to

$$\frac{1}{\pi}\int_0^{\pi} e^{kt\cos u} du = I_0(kt) \tag{2.51}$$

We can express the modified first Bessel function in terms of the first Bessel function (this is valid if $-\pi < \arg(kt) \leq \frac{\pi}{2}$)

$$J_\alpha(jkt) = e^{\frac{\alpha\pi}{2}} I_\alpha(kt), \tag{2.52}$$

Hence we can write

$$I_0(kt) = J_0(jkt). \tag{2.53}$$

This ends the proof ■ □

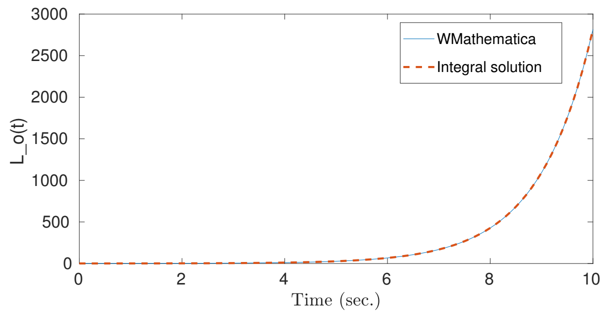

Figure 2.8: ILT of system (2.45) using Proposition 2.0.1 and the result given by Wolfram Mathematica $L_o(t) = J_0(j\sqrt{k}t)$ where J is the Bessel function (see, for further details (Arfken, 2005)) using $k = 1$.

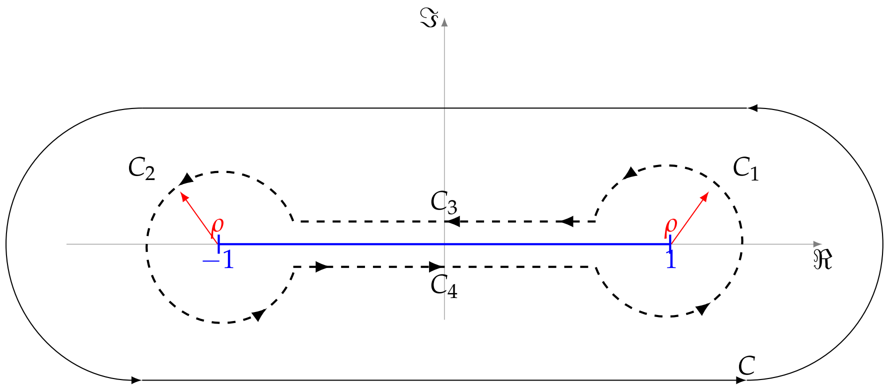

Figure 2.9: s-plane for integration around branch points of the function $(s^2 - k^2)^{1/2}$ with $k > 0$.

Consider the case when $k = 1$, the comparison of the ILT plot using Proposition 2.0.1 and the function **InverseLaplaceTransform** of the software Wolfram Alpha Mathematica is given in the following picture.

Proposition 2.0.2

Let $\mathcal{L}_o$ be the operator transfer function defined as

$$\mathcal{L}_o(s) := \frac{1}{\sqrt{s^2 + k^2}}, \tag{2.54}$$

where $k > 0$. Then, its ILT is given by

$$L_o(t) := J_0(kt). \tag{2.55}$$

where, $J_0(\cdot)$ is the Bessel function of the first kind of zeroth order.

Proof. To proof the Proposition 2.0.2 we use Theorem 2.0.1 to obtain the two relations

$$L_o(t) = \frac{2}{\pi}\int_k^\infty \sin(rt)\frac{1}{\sqrt{r^2 - k^2}}dr, \tag{2.56}$$

$$L_o(t) = \frac{2}{\pi}\int_0^k \cos(rt)\frac{1}{\sqrt{k^2 - r^2}}dr. \tag{2.57}$$

We know that the first Bessel function is defined as

$$J_n(x) = \frac{1}{\pi}\int_0^\pi \cos(n\tau - x\sin\tau)d\tau. \tag{2.58}$$

Taking (2.57) and substituting $r = k\sin(\theta)$ where $\theta \in (0, \frac{\pi}{2})$ we have

$$L_o(t) = \frac{2}{\pi}\int_0^{\pi/2} \cos(kt\sin(x))\frac{k\cos(x)dx}{k\cos(x)} = \frac{2}{\pi}\int_0^{\pi/2}\cos(kt\sin(x))dx = \frac{2}{\pi}\frac{\pi}{2}J_0(kt). \tag{2.59}$$

We can conclude the same for relation (2.56) ■ □

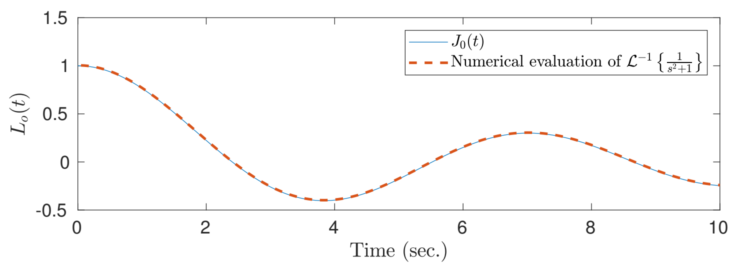

Figure 2.10: ILT of system (2.54) using Proposition 2.0.2 and the result given by using a numerical evaluation of the ILT using Matlab for $k = 1$.

Proposition 2.0.3

Let $\mathcal{L}_x$ be the multivalued operator function defined as

$$\mathcal{L}_x(s) := \sqrt{s^2 + k^2}, \tag{2.60}$$

where $k > 0$. Then, its ILT is given by

$$L_x(t) := \frac{2k^2}{\pi}\int_0^{\pi/2}\cos(kt\sin(u))\cos^2(u)du = \frac{k^2 J_1(t)}{t}. \tag{2.61}$$

Proof. By using Theorem 2.0.1, expression (2.44) ■ □

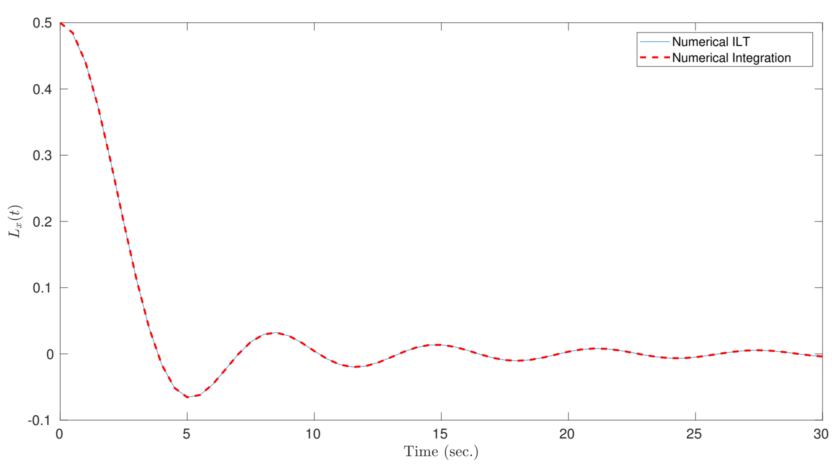

Figure 2.11: ILT of system (2.60) using Proposition 2.0.3 and the result given by using a numerical evaluation of the ILT and the numerical evaluation of the integral (2.61) in Matlab for $k = 1$.

Modeling an inverted flexible pendulum

According to (Singla, 2013) we may model a flexible inverted pendulum as a series of rigid rods connected by torsional springs as shown in Figure 2.12. The model of the system will imply a high number of non-linear differential equations.

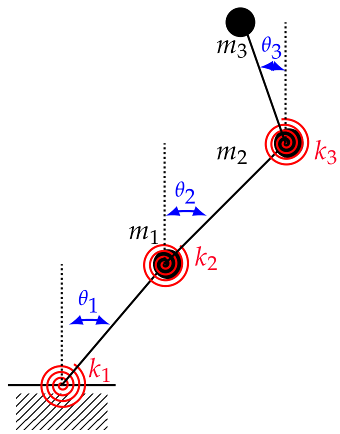

Figure 2.12: Flexible pole diagram.

If we obtain the non-linear model of the system considering just the first inverted pendulum of length ℓ_1 we have that

$$m_1\ell_1\ddot{\theta_1} + m_1 g\ell_1 \sin\theta_1 + k_1\theta_1 = 0, \tag{2.62}$$

which could be linearized using the small angle criterion as

$$m_1\ell_1\ddot{\theta_1} + (m_1 g\ell_1 + k_1)\theta_1 = 0, \tag{2.63}$$

by making $k_{g_1} = m_1 g\ell_1 + k_1$ we can easily conclude that the linearized model for the series of rigid rods can be schematized as in the following picture.

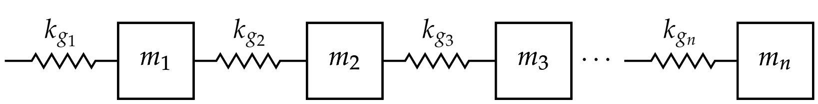

Figure 2.13: Linearized configuration for flexible inverted pendulum.

The last escheme is a particular case of scheme in Figure 2.4. Then, by Equations (2.17) and (2.19) when $m_1 = m_2 = \cdots = m_n$ and $k_{g_1} = k_{g_2} = \cdots = k_{g_n}$ we have

$$\frac{X_{in} - X_{out}}{F_{tot}} = N\frac{1}{ms^2 + k}, \tag{2.64}$$

where, $N \leq \infty$. Then, this arquitecture may converge only when $N < \infty$. Thus, this example is not convinient for our analysis. Consider now the case when we add a disipating factor to the system using the scheme in Fig.2.14.

The Rayleigh function for the disipating factor in the first inverted rod is given by

$$D = \frac{1}{2}b_1\dot{x}^2 = \frac{1}{2}b_1\left(\frac{d(\ell_1\sin\theta_1)}{dt}\right)^2 = \frac{1}{2}b_1\ell_1^2\cos^2\theta_1\dot{\theta_1}^2, \tag{2.65}$$

where ℓ_1 is the length of the first rod. Then, using the Euler-Lagrange formulation we have that the non-linear dynamical model for the first rod is given by

$$m_1\ell_1\ddot{\theta_1} + m_1 g\ell_1\sin\theta_1 + k_1\theta_1 + b_1\ell_1^2\cos^2\theta_1\dot{\theta_1} = 0, \tag{2.66}$$

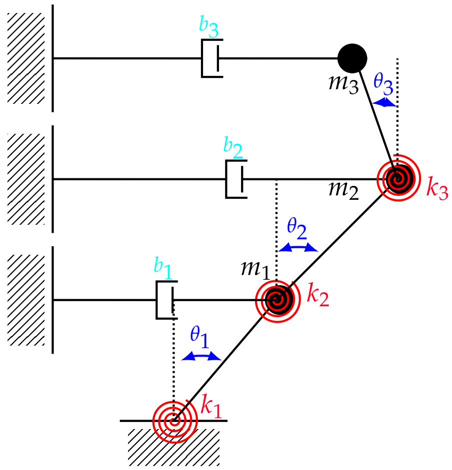

Figure 2.14: Flexible pole diagram adding damping to the system.

whose linear model is equal to

$$m_1\ell_1\ddot{\theta}_1 + b_1\ell_1^2\dot{\theta}_1 + (m_1 g\ell_1 + k_1)\theta_1 = 0, \tag{2.67}$$

and can be described by the following diagram, taking $k_{g_i} = m_i g\ell_i + k_i$ and $b_{g_i} = b_i\ell_i^2\ \forall i = 1, 2, 3, \ldots, n$

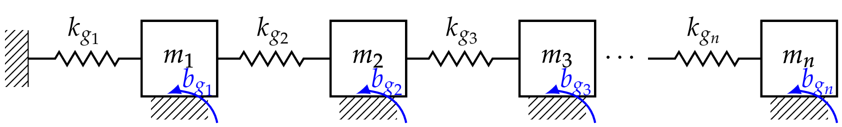

Figure 2.15: Linearized configuration for flexible inverted pendulum with damping.

Is obvious that this scheme is similar to the infinite ladder in Figure 2.2. Here, $\mathcal{L}_1 = \frac{1}{ms^2+k}$ and $\mathcal{L}_2 = \frac{1}{bs}$ considering $m = m_i$, $k = k_{g_i}$ and $b = b_{g_i}\ \forall i \in \mathbb{N} \bigcup \infty$. Then the relation between the ΔX and F is given by

$$\frac{\Delta X(s)}{F(s)} = \frac{1}{2}\left(-\frac{1}{k+ms^2} \pm \sqrt{\frac{4}{bs\,(k+ms^2)} + \frac{1}{(k+ms^2)^2}}\right), \tag{2.68}$$

$$= \frac{-\sqrt{bs} \pm \sqrt{4(k+ms^2)+bs}}{\sqrt{bs}(k+ms^2)}. \tag{2.69}$$

Proposition 2.0.4: Flexible inverted pendulum impulse response

Consider now, the already detailed transfer function for the linearized flexible inverted pendulum shown in Figure 2.14 given by Equation (2.69). Then, its impulse response is given by

$$\begin{aligned} \Delta x(t) &= -\frac{k_1 \sin\left(\sqrt{k_2}t\right)}{\sqrt{k_2}} \pm \frac{k_3\sqrt{\lambda}}{\sqrt[4]{k_2^3}} \cos(\sqrt{k_2}t + \tfrac{\delta}{2} - \tfrac{3}{4}\pi) + \frac{k_3}{\pi}\int_0^\infty \frac{\sqrt{x^2-2xr\cos\phi+r^2}}{\sqrt{x}(x^2+k_2)} e^{-xt}dx + \cdots \\ &+ \frac{2k_3\sqrt{\kappa(x)}}{\pi v(x)} \int_r^\infty \frac{e^{xt\cos\phi}\sin(\sin\phi + \frac{\phi}{2} + \frac{\sigma(x)}{2} - \varphi(x))}{\sqrt{x}} dx. \end{aligned} \tag{2.70}$$

Where,

$$\begin{aligned} \lambda &= \sqrt{(r^2-k_2)^2 + (2\sqrt{k_2}r\cos\phi)^2}, \\ \delta &= \arctan(\tfrac{2r\sqrt{k_2}\cos\phi}{r^2-k_2}), \\ \kappa(x) &:= \sqrt{(x^2\cos 2\phi + xr\cos 2\phi + xr + r^2)^2 + (x^2\sin 2\phi + xr\sin 2\phi)^2}, \\ \sigma(x) &:= \arctan(\tfrac{x^2\sin 2\phi + xr\sin 2\phi}{x^2\cos 2\phi + xr\cos 2\phi + xr + r^2}), \\ v(x) &:= \sqrt{(x^2\cos 2\phi + k_2)^2 + (x^2\sin 2\phi)^2}, \\ \varphi(x) &:= \arctan(\tfrac{x^2\sin 2\phi}{x^2\cos 2\phi + k_2}), \end{aligned}$$

Proof. System (2.69) can be rewritten as

$$\begin{aligned} \frac{\Delta X(s)}{F(s)} &= \frac{-\sqrt{bs} \pm \sqrt{4(k+ms^2)+bs}}{\sqrt{bs}(k+ms^2)}, \\ &= -\frac{1}{m(\frac{k}{m}+s^2)} \pm \frac{\sqrt{(s+z_1)(s+z_2)}}{m\sqrt{b}\sqrt{s}(\frac{k}{m}+s^2)}, \\ &= -\frac{k_1}{s^2+k_2} \pm k_3 \frac{\sqrt{(s+z_1)(s+z_2)}}{\sqrt{s}(s^2+k_2)}, \end{aligned} \tag{2.71}$$

where $k_1 = \frac{1}{m}, k_2 = \frac{k}{m}, k_3 = \frac{1}{m\sqrt{b}}$, $z_1 = \frac{b+\sqrt{b^2-64km}}{8m} = \sigma + j\omega$ and $z_2 = \frac{b-\sqrt{b^2-64km}}{8m} = \sigma - j\omega$. We know that the ILT of the term $-\frac{k_1}{s^2+k_2}$ is equal to $-\frac{k_1\sin\left(\sqrt{k_2}t\right)}{\sqrt{k_2}}$. The rightmost expression in (2.71) shows a multivalued function with four BPs $(z_1, z_2, 0, \infty)$ and two BCs, we write $z_{1,2} = re^{\pm j\phi}$ where $\phi = \arg(z_1), -\phi = \arg(z_2)$ and $|z_1| = |z_2| = r$. This leads to the following integration contour Γ By the Residue theorem we know that

$$\int_\Gamma k_3 \frac{\sqrt{(s+z_1)(s+z_2)}}{\sqrt{s}(s^2+k_2)} e^{st} ds = \int_{Br+C_1+C_2+\cdots+C_{13}} = 2j\pi \left[\frac{k_3\sqrt{\lambda}}{\sqrt[4]{k_2^3}} \cos(\sqrt{k_2}t + \tfrac{\delta}{2} - \tfrac{3}{4}\pi)\right], \tag{2.72}$$

with $\lambda = \sqrt{(r^2-k_2)^2 + (2\sqrt{k_2}r\cos\phi)^2}$ and $\delta = \arctan(\frac{2r\sqrt{k_2}\cos\phi}{r^2-k_2})$.

Based on Figure 2.16 we have that

$$\int_{C_1+C_5+C_9+C_{13}} = 0 \tag{2.73}$$

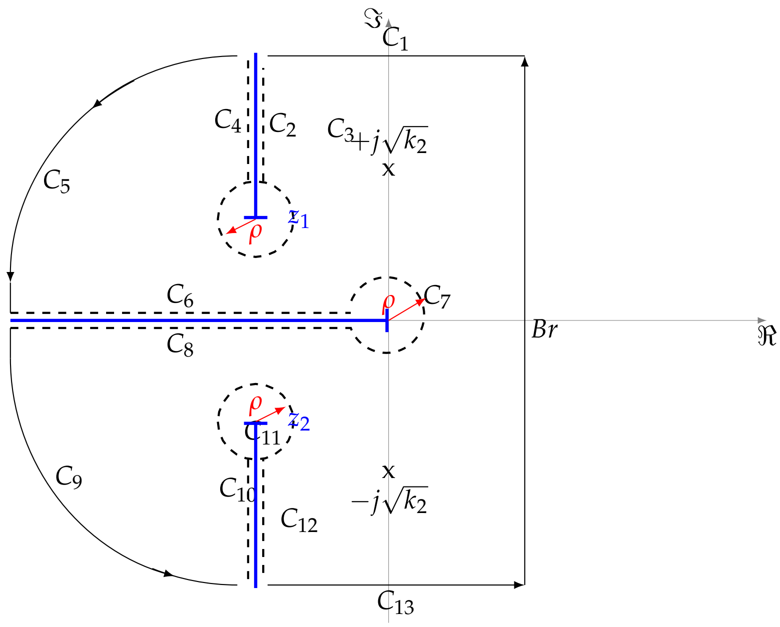

Figure 2.16: Integration path in Example.

and

$$\int_{C_2} k_3 \frac{\sqrt{(s+\sigma+j\omega)(s+\sigma-j\omega)}}{\sqrt{s}(s^2+k_2)} e^{st} ds \overset{s=-\sigma+xe^{j\frac{\pi}{2}}}{=} \int_{\infty}^{r} k_3 \frac{\sqrt{(xe^{j\phi}+re^{j\phi})(xe^{j\phi}+re^{-j\phi})}}{\sqrt{xe^{j\phi}}(x^2e^{j2\phi}+k_2)} e^{xe^{j\phi}t} e^{j\phi} dx,$$

$$\int_{C_4} k_3 \frac{\sqrt{(s+\sigma+j\omega)(s+\sigma-j\omega)}}{\sqrt{s}(s^2+k_2)} e^{st} ds \overset{s=-\sigma+xe^{-j\frac{3\pi}{2}}}{=} \int_{r}^{\infty} k_3 \frac{\sqrt{(xe^{j(\phi-2\pi)}+re^{j\phi})(xe^{j(\phi-2\pi)}+re^{-j\phi})}}{\sqrt{xe^{j(\phi-2\pi)}}(x^2e^{j2(\phi-2\pi)}+k_2)} e^{xe^{j(\phi-2\pi)}t} e^{j(\phi-2\pi)} dx,$$

$$\int_{C_3} k_3 \frac{\sqrt{(s+z_1)(s+z_2)}}{\sqrt{s}(s^2+k_2)} e^{st} ds \overset{s=\rho e^{j\theta}}{=} \int_{\phi}^{\phi-2\pi} k_3 \frac{\sqrt{(\rho e^{j\theta}+re^{j\phi})(\rho e^{j\theta}+re^{-j\phi})}}{\sqrt{\rho e^{j\theta}}(\rho^2e^{j2\theta}+k_2)} e^{\rho e^{j\theta}t} j\rho e^{j\theta} d\theta \overset{\rho\to 0}{=} 0,$$

$$\int_{C_{10}} k_3 \frac{\sqrt{(s+\sigma+j\omega)(s+\sigma-j\omega)}}{\sqrt{s}(s^2+k_2)} e^{st} ds \overset{s=-\sigma+xe^{j\frac{3\pi}{2}}}{=} \int_{\infty}^{r} k_3 \frac{\sqrt{(xe^{j(-\phi+2\pi)}+re^{j\phi})(xe^{j(-\phi+2\pi)}+re^{-j\phi})}}{\sqrt{xe^{j(-\phi+2\pi)}}(x^2e^{j2(-\phi+2\pi)}+k_2)} e^{xe^{j(-\phi+2\pi)}t} e^{j(-\phi+2\pi)} dx,$$

$$\int_{C_{12}} k_3 \frac{\sqrt{(s+\sigma+j\omega)(s+\sigma-j\omega)}}{\sqrt{s}(s^2+k_2)} e^{st} ds \overset{s=-\sigma+xe^{-j\frac{\pi}{2}}}{=} \int_{r}^{\infty} k_3 \frac{\sqrt{(xe^{-j\phi}+re^{j\phi})(xe^{-j\phi}+re^{-j\phi})}}{\sqrt{xe^{-j\phi}}(x^2e^{-j2\phi}+k_2)} e^{xe^{-j\phi}t} e^{-j\phi} dx,$$

$$\int_{C_{11}} k_3 \frac{\sqrt{(s+z_1)(s+z_2)}}{\sqrt{s}(s^2+k_2)} e^{st} ds \overset{s=\rho e^{j\theta}}{=} \int_{-\phi}^{-\phi+2\pi} k_3 \frac{\sqrt{(\rho e^{j\theta}+re^{j\phi})(\rho e^{j\theta}+re^{-j\phi})}}{\sqrt{\rho e^{j\theta}}(\rho^2e^{j2\theta}+k_2)} e^{\rho e^{j\theta}t} j\rho e^{j\theta} d\theta \overset{\rho\to 0}{=} 0,$$

$$\int_{C_7} k_3 \frac{\sqrt{(s+z_1)(s+z_2)}}{\sqrt{s}(s^2+k_2)} e^{st} ds \overset{s=\rho e^{j\theta}}{=} \int_{\pi}^{-\pi} k_3 \frac{\sqrt{(\rho e^{j\theta}+re^{j\phi})(\rho e^{j\theta}+re^{-j\phi})}}{\sqrt{\rho e^{j\theta}}(\rho^2e^{j2\theta}+k_2)} e^{\rho e^{j\theta}t} j\rho e^{j\theta} d\theta \overset{\rho\to 0}{=} 0,$$

$$\int_{C_6} k_3 \frac{\sqrt{(s+z_1)(s+z_2)}}{\sqrt{s}(s^2+k_2)} e^{st} ds \overset{s=xe^{j\pi}}{=} \int_{\infty}^{\rho} k_3 \frac{\sqrt{(xe^{j\pi}+re^{j\phi})(xe^{j\pi}+re^{-j\phi})}}{\sqrt{xe^{j\pi}}(x^2e^{j2\pi}+k_2)} e^{xe^{j\pi}t} e^{j\pi} dx,$$

$$\int_{C_8} k_3 \frac{\sqrt{(s+z_1)(s+z_2)}}{\sqrt{s}(s^2+k_2)} e^{st} ds \overset{s=xe^{-j\pi}}{=} \int_{\rho}^{\infty} k_3 \frac{\sqrt{(xe^{-j\pi}+re^{j\phi})(xe^{-j\pi}+re^{-j\phi})}}{\sqrt{xe^{-j\pi}}(x^2e^{-j2\pi}+k_2)} e^{xe^{-j\pi}t} e^{-j\pi} dx.$$

Now,

$$\begin{aligned}\int_{C_6+C_8} &= -\int_{\rho}^{\infty} k_3 \frac{\sqrt{x^2-2xr\cos\phi+r^2}}{j\sqrt{x}(x^2+k_2)} e^{-xt} e^{j\pi} dx + \int_{\rho}^{\infty} k_3 \frac{\sqrt{x^2-2xr\cos\phi+r^2}}{-j\sqrt{x}(x^2+k_2)} e^{-xt} e^{-j\pi} dx, \\ &\overset{\rho\to 0}{=} -2jk_3 \int_{0}^{\infty} \frac{\sqrt{x^2-2xr\cos\phi+r^2}}{\sqrt{x}(x^2+k_2)} e^{-xt} dx.\end{aligned}$$

Besides, taking $\kappa(x) := \sqrt{(x^2\cos 2\phi + xr\cos 2\phi + xr + r^2)^2 + (x^2\sin 2\phi + xr\sin 2\phi)^2}$, $\sigma(x) := \arctan(\frac{x^2\sin 2\phi + xr\sin 2\phi}{x^2\cos 2\phi + xr\cos 2\phi + xr + r^2})$, $v(x) := \sqrt{(x^2\cos 2\phi + k_2)^2 + (x^2\sin 2\phi)^2}$ and $\varphi(x) := \arctan(\frac{x^2\sin 2\phi}{x^2\cos 2\phi + k_2})$

$$\begin{aligned}
\int_{C_1+C_4+C_{10}+C_{12}} &= -2k_3 e^{j\phi}\int_r^\infty \frac{\sqrt{\kappa(x)e^{j\sigma(x)}}}{\sqrt{xe^{j\phi}}(v(x)e^{j\varphi(x)})}e^{xe^{j\phi}t}dx + 2k_3 e^{-j\phi}\int_r^\infty \frac{\sqrt{\kappa(x)e^{-j\sigma(x)}}}{\sqrt{xe^{-j\phi}}(v(x)e^{-j\varphi(x)})}e^{xe^{-j\phi}}dx \\
&= -2k_3 e^{j\frac{\phi}{2}}\int_r^\infty \frac{\sqrt{\kappa(x)e^{j\sigma(x)}}e^{-j\varphi(x)}}{v(x)\sqrt{x}}e^{xe^{j\phi}t}dx + 2k_3 e^{-j\frac{\phi}{2}}\int_r^\infty \frac{\sqrt{\kappa(x)e^{-j\sigma(x)}}e^{j\varphi(x)}}{v(x)\sqrt{x}}e^{xe^{-j\phi}}dx \\
&= -\frac{2k_3\sqrt{\kappa(x)}}{v(x)}\int_r^\infty \frac{e^{xt\cos\phi}e^{j(\sin\phi+\frac{\phi}{2}+\frac{\sigma(x)}{2}-\varphi(x))}}{\sqrt{x}}dx + \frac{2k_3\sqrt{\kappa(x)}}{v(x)}\int_r^\infty \frac{e^{xt\cos\phi}e^{-j(\sin\phi+\frac{\phi}{2}+\frac{\sigma(x)}{2}-\varphi(x))}}{\sqrt{x}}dx \\
&= -\frac{j4k_3\sqrt{\kappa(x)}}{v(x)}\int_r^\infty \frac{e^{xt\cos\phi}\sin(\sin\phi+\frac{\phi}{2}+\frac{\sigma(x)}{2}-\varphi(x))}{\sqrt{x}}dx
\end{aligned}$$

Finally

$$\frac{1}{j2\pi}\int_{Br} = \frac{k_3\sqrt{\lambda}}{\sqrt[4]{k_2^3}}\cos(\sqrt{k_2}t + \frac{\delta}{2} - \frac{3}{4}\pi) + \frac{k_3}{\pi}\int_0^\infty \frac{\sqrt{x^2-2xr\cos\phi+r^2}}{\sqrt{x}(x^2+k_2)}e^{-xt}dx + \frac{2k_3\sqrt{\kappa(x)}}{\pi v(x)}\int_r^\infty \frac{e^{xt\cos\phi}\sin(\sin\phi+\frac{\phi}{2}+\frac{\sigma(x)}{2}-\varphi(x))}{\sqrt{x}}dx \tag{2.74}$$

$\square$

ISSUE: The following simulation made on Matlab is avoiding the last integral in Eq. (2.70), because it does not converge numerically and no closed solution of the integration has been found using Wolfram Mathematica by now. Nonetheless, the result is pretty similar to the ILT of (2.71) obtained numerically in Matlab, showing that the last integral has a convergent solution in the time domain.

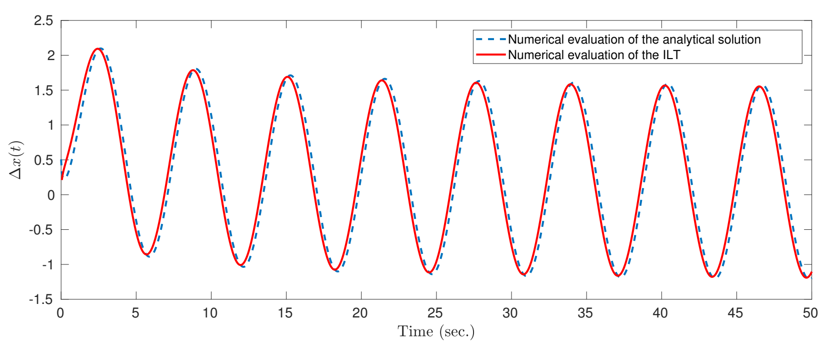

Figure 2.17: Numerical ILT of system (2.71) and the numerical evaluation of (2.70) in Matlab for $k_1 = 1, k_2 = 1, k_3 = 1$, $z_1 = 1 + j2$ and $z_2 = 1 - j2$.

Modeling a flexible beam

Consider the scheme describing a flexible beam of length ℓ in Fig. 2.18. From Figure 2.18, we can see that such a scheme is similar to the ladder network in Figure 2.2. Consider the Laplace-transformed operators $\mathcal{L}_1 = \frac{1}{ms^2}$ and $\mathcal{L}_2 = \frac{1}{k}$, where $m = m_i, i = 1,2,3,\ldots,n$ and $k = k_i, i = 1,2,3,\ldots,n$. Then, $\mathcal{L}_{eq}$ is equal to

$$\mathcal{L}_{eq} = \frac{1}{2}\left[-\mathcal{L}_1 \pm \sqrt{\mathcal{L}_1^2 + 4\mathcal{L}_1\mathcal{L}_2}\right] = \frac{1}{2}\left[-\frac{1}{ms^2} \pm \sqrt{\left(\frac{1}{ms^2}\right)^2 + 4\frac{1}{mks^2}}\right] = \frac{-\sqrt{k} \pm \sqrt{k + 4ms^2}}{2m\sqrt{ks^2}}. \tag{2.75}$$

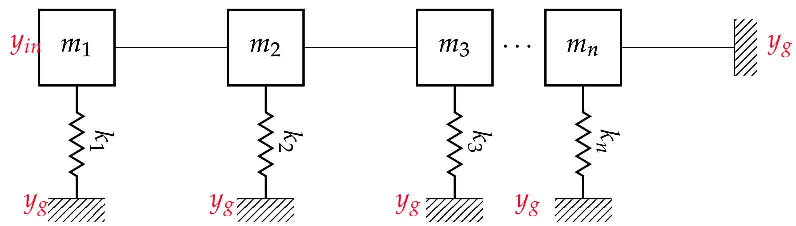

Figure 2.18: Linearized configuration for flexible inverted pendulum.

This leads to the relation between the input and output system as follows

$$\mathcal{L}_{eq}(s) = \frac{\Delta Y(s)}{F(s)} = \frac{Y_{in}(s) - Y_g(s)}{F(s)} = \frac{Y_{in}(s)}{F(s)} = \frac{-\sqrt{k} \pm \sqrt{k + 4ms^2}}{2m\sqrt{k}s^2}, \tag{2.76}$$

which holds because $y_g(t) = 0$.

Proposition 2.0.5: Flexible beam impulse response

Consider now, the already detailed transfer function for the flexible beam shown in Figure 2.18 given by Equation (2.76). Then, its impulse response is given by

$$y_{in}(t) = -\frac{t}{k_3} \pm \left[\frac{\sqrt{k_1}}{k_2}t + \frac{2}{\pi}\int_{\sqrt{k_1}}^{\infty} \frac{\sin(xt)}{k_2 x^2}\sqrt{x^2 - k_1}dx\right]. \tag{2.77}$$

Where,

$$k_1 = \frac{k}{4m}, \tag{2.78}$$
$$k_2 = \sqrt{km}, \tag{2.79}$$
$$k_3 = 2m. \tag{2.80}$$

Proof. Applying the ILT to (2.76) Equation follows from the solution of

$$y_{in}(t) = \frac{1}{2j\pi}\int_{Br} \mathcal{L}_{eq}(s)F(s)e^{st}ds, \tag{2.81}$$

where

$$\mathcal{L}_{eq}(s) = \frac{y_{in}(s)}{F(s)} = \frac{-\sqrt{k} \pm \sqrt{k + 4ms^2}}{2m\sqrt{k}s^2} = -\frac{1}{k_3 s^2} \pm \frac{\sqrt{k_1 + s^2}}{k_2 s^2}, \tag{2.82}$$

$k_1 = \frac{k}{4m}$, $k_2 = \sqrt{km}$, $k_3 = 2m$ and $F(s) = 1$. The ILT of the term $-\frac{1}{k_3 s^2}$ is known to be $-\frac{t}{k_3}$, then

$$y_{in}(t) = -\frac{t}{k_3} \pm \frac{1}{2j\pi}\int_{Br} \frac{\sqrt{k_1 + s^2}}{k_2 s^2}e^{st}ds. \tag{2.83}$$

The Bromwich contour of the lacking integrations can be depicted as in Fig. 2.19.

From Figure 2.19 we have that

$$\int_{\Gamma} \mathcal{L}_{eq}(s)e^{st}ds = \int_{Br+C_1+C_2+\cdots+C_8} = 2\pi j\frac{\sqrt{k_1}}{k_2}t, \tag{2.84}$$

due to the residue theorem. Besides, it can easily be proven that

$$\int_{C_4+C_5} = 0. \tag{2.85}$$

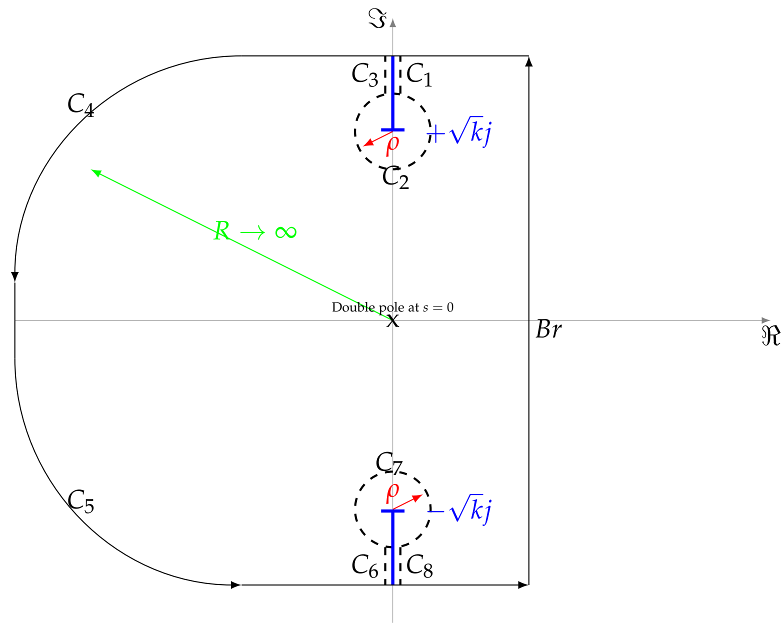

Figure 2.19: Integration path in Example.

Now for C_2 and C_7 we can introduce the notation $s = \rho e^{j\phi} \pm j\sqrt{k_1}$, $ds = j\rho e^{j\phi} d\phi$. We consider that C_2 and C_7 is in the first sheet, it follows that $\frac{\pi}{2} \leq \phi < -\frac{3\pi}{2}$ and

$$\int_{C_2} \frac{\sqrt{s^2+k_1}}{k_2 s^2} e^{st} ds = \int_{C_2} \frac{\sqrt{\rho^2 e^{2j\phi} + 2j\rho e^{j\phi}\sqrt{k_1}} e^{\rho e^{j\phi} + j\sqrt{k_1}}}{k_2 \rho^2 e^{2j\phi} + 2k_2 j\rho e^{j\phi}\sqrt{k_1} - k_1 k_2} j\rho e^{j\phi} d\phi, \tag{2.86}$$

$$\int_{C_7} \frac{\sqrt{s^2+k_1}}{k_2 s^2} e^{st} ds = \int_{C_7} \frac{\sqrt{2k_1 + \rho^2 e^{2j\phi} + 2j\rho e^{j\phi}\sqrt{k_1}} e^{\rho e^{j\phi} + j\sqrt{k_1}}}{k_2 \rho^2 e^{2j\phi} + 2k_2 j\rho e^{j\phi}\sqrt{k_1} - k_1 k_2} j\rho e^{j\phi} d\phi. \tag{2.87}$$

by making $\rho \to 0$ we can conclude that

$$\left| \int_{C_2+C_7} \right| = 0. \tag{2.88}$$

Now we need to find

$$\int_{Br+C_1+C_3+C_6+C_8}. \tag{2.89}$$

To solve (2.89) we know that

$$\int_{C_1} \frac{\sqrt{k_1+s^2}}{k_2 s^2} e^{st} ds \overset{s=xe^{j\pi/2}}{=} \int_{\infty}^{\sqrt{k_1}} \frac{\sqrt{k_1 + x^2 e^{j\pi}}}{k_2 x^2 e^{j\pi}} e^{jxt} e^{j\pi/2} dx, \tag{2.90}$$

$$\int_{C_3} \frac{\sqrt{k_1+s^2}}{k_2 s^2} e^{st} ds \overset{s=xe^{j\pi/2}}{=} \int_{\sqrt{k_1}}^{\infty} \frac{-\sqrt{k_1 + x^2 e^{j\pi}}}{k_2 x^2 e^{j\pi}} e^{jxt} e^{j\pi/2} dx, \tag{2.91}$$

$$\int_{C_6} \frac{\sqrt{k_1+s^2}}{k_2 s^2} e^{st} ds \overset{s=xe^{-j\pi/2}}{=} \int_{\infty}^{\sqrt{k_1}} \frac{-\sqrt{k_1 + x^2 e^{-j\pi}}}{k_2 x^2 e^{-j\pi}} e^{-jxt} e^{-j\pi/2} dx, \tag{2.92}$$

$$\int_{C_8} \frac{\sqrt{k_1+s^2}}{k_2 s^2} e^{st} ds \overset{s=xe^{-j\pi/2}}{=} \int_{\sqrt{k_1}}^{\infty} \frac{\sqrt{k_1 + x^2 e^{-j\pi}}}{k_2 x^2 e^{-j\pi}} e^{-jxt} e^{-j\pi/2} dx, \tag{2.93}$$

hence,

$$\int_{C_1+C_6} = \int_{\infty}^{\sqrt{k_1}} 2\sin(xt)\frac{\sqrt{k_1 - x^2 e^{j\pi}}}{k_2 x^2}dx, \tag{2.94}$$

$$\int_{C_3+C_8} = \int_{\sqrt{k_1}}^{\infty} 2\sin(xt)\frac{\sqrt{k_1 - x^2 e^{-j\pi}}}{k_2 x^2}dx. \tag{2.95}$$

Finally because

$$\int_{C_1+C_3+C_6+C_8} = -2j\int_{\sqrt{k_1}}^{\infty}\frac{\sin(xt)}{k_2x^2}\sqrt{x^2-k_1}dx - 2j\int_{\sqrt{k_1}}^{\infty}\frac{\sin(xt)}{k_2x^2}\sqrt{x^2-k_1}dx = -4j\int_{\sqrt{k_1}}^{\infty}\frac{\sin(xt)}{k_2x^2}\sqrt{x^2-k_1}dx, \tag{2.96}$$

we have that

$$L_{eq}(t) = \int_{Br}\mathcal{L}_{eq}(s)e^{st}ds = -\frac{t}{k_3} \pm \left[\frac{\sqrt{k_1}}{k_2}t + \frac{2}{\pi}\int_{\sqrt{k_1}}^{\infty}\frac{\sin(xt)}{k_2x^2}\sqrt{x^2-k_1}dx\right] \tag{2.97}$$

$\square$

COMMENT: When solving the rightmost integral in expression (2.97) with Wolfram Mathematica we obtain

$$\frac{2}{\pi}\int_{\sqrt{k_1}}^{\infty}\frac{\sin(xt)}{k_2x^2}\sqrt{x^2-k_1}dx = \frac{t\left(\pi k_1 t^2 \boldsymbol{H}_0\left(\sqrt{k_1}|t|\right)J_1\left(\sqrt{k_1}|t|\right) + \left(-\pi k_1 t^2 \boldsymbol{H}_1\left(\sqrt{k_1}|t|\right) + 2k_1t^2 + 2\right)J_0\left(\sqrt{k_1}|t|\right) - 2\sqrt{k_1}|t|\left(J_1\left(\sqrt{k_1}|t|\right)+1\right)\right)}{2k_2|t|}, \tag{2.98}$$

where $\boldsymbol{H}_0, \boldsymbol{H}_1$ are the StruveH functions of order $0, 1$ respectively. Such a solution needs to be proven by hand.

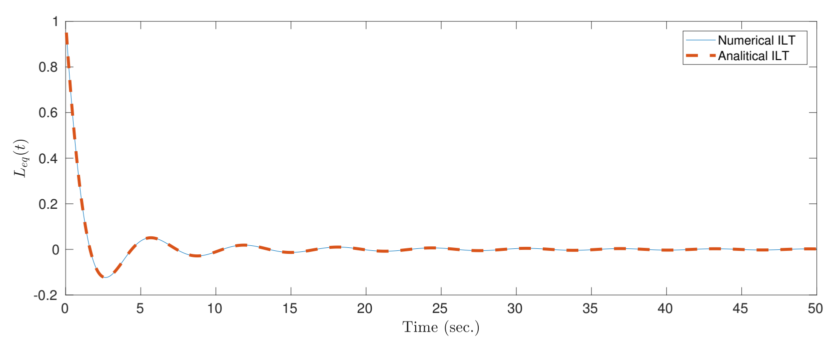

Figure 2.20: ILT of system (2.76) using the result given by a numerical evaluation of the ILT in Matlab and the analytical result of the ILT of (2.76) in Mathematica (2.98) for $k_1 = 1, k_2 = 1$ and $k_3 = 1$.

Modeling an infinite tree of simple mechanical components

As we have seen, we can conclude that the Laplace transformed operators $\mathcal{L}$ are essentially transfer functions $G(s)$ when considering the initial conditions equals zero. Then, consider now the network of dampers and springs interconnected as in the following picture:

We have the next results

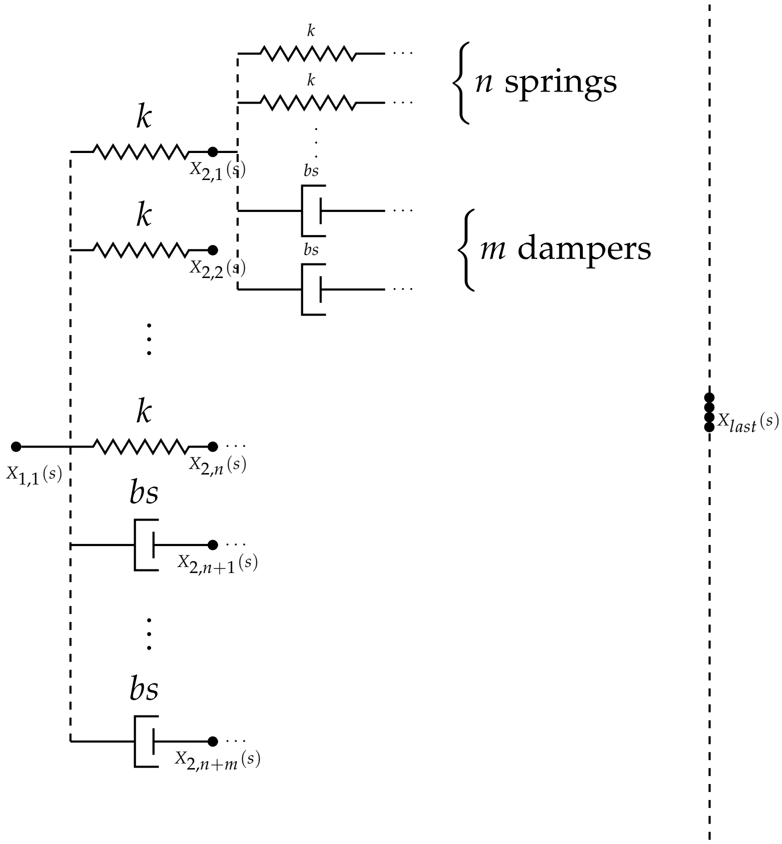

Figure 2.21: Networked mechanical system.

Proposition 2.0.6: (Goodwine, 2018)

The operator or transfer function $G_\infty(s)$ satisfying the relation $F(s) = G_\infty(s)\Delta X(s)$ where $\Delta X(s)$ is the difference of position between the first node $x_{1,1}$ and the last node x_{last} of a network of springs and dampers interconnected as in Fig. 2.21 is given by

$$G_\infty(s) = \frac{1}{2}\left[(n-1)k + (m-1)bs \pm \sqrt{[(n-1)k + (m-1)bs]^2 + 4(n+m-1)kbs}\right], \tag{2.99}$$

for $n > 1$ and $m \geq 1$.

From Proposition 2.0.6, we have the following useful trasfer functions of the system

$$G_f(s) = \frac{\Delta X(s)}{F(s)} = \frac{1}{G_\infty(s)}, \tag{2.100}$$

$$G_x(s) = \frac{X_{last}(s)}{X_{1,1}(s)} = \frac{G_\infty(s)}{m_{last}s^2 + G_\infty(s)}. \tag{2.101}$$

Before computing the ILT (ILT) to expressions (2.100) and (2.101) we first analyze the characterisc polynomial of both transfer functions and the expression $G_\infty(s)$ itself to see what kind of singularities we deal with in the systems.

Proposition 2.0.7

Let $G_f(s)$ be a transfer function given by (2.100). Then, it has a pole in $s = 0$ when finding the negative solution of $G_\infty(s)$ and two real branch points (BP) in

$$s_1 = -\frac{2k\sqrt{mn(m+n-1)} + k(mn+m+n-1)}{b(m-1)^2} \tag{2.102}$$

$$s_2 = \frac{2k\sqrt{mn(m+n-1)} - k(mn+m+n-1)}{b(m-1)^2} \tag{2.103}$$

for $m > 1$, when $m = 1$ we have two real BPs at

$$s_1 = -\tfrac{k(n-1)^2}{4bn}, s_2 = \infty. \tag{2.104}$$

Proof. We have that the characteristic polynomial of the system $G_f(s)$ is equal to $G_\infty(s)$. Then by finding the solution of $G_\infty(s) = 0$ when $m \geq 1$ we have

$$(n-1)k + (m-1)bs \pm \sqrt{[(n-1)k + (m-1)bs]^2 + 4(n+m-1)kbs} = 0, \tag{2.105}$$

$$(n-1)k + (m-1)bs = \mp\sqrt{[(n-1)k + (m-1)bs]^2 + 4(n+m-1)kbs}, \tag{2.106}$$

$$[(n-1)k + (m-1)bs]^2 = [(n-1)k + (m-1)bs]^2 + 4(n+m-1)kbs, \tag{2.107}$$

$$0 = 4(n+m-1)kbs, \tag{2.108}$$

$$0 = s. \tag{2.109}$$

When substituting $s = 0$ in $G_\infty(s)$ we find that it is a solution in the case of choosing the negative sign of the square root in G_∞.

The BPs are found by computing the square root argument equal to zero and solving for s

$$[(n-1)k + (m-1)bs]^2 + 4(n+m-1)kbs = 0, \tag{2.110}$$

this gives equations (2.102) and (2.103) when $m > 1$ and (2.104) when $m = 1$. Becuse $k > 0$ and $b > 0$, we conclude that s_1 and s_2 are always real numbers. This completes the proof. □

Proposition 2.0.8

Let $G_x(s)$ be a transfer function given by (2.101). Then, it has two BPs given by (2.102) and (2.103) when $m > 1$ and two given by (2.104) when $m = 1$. Besides, it has two poles solution of the characteristic equation

$$P(s) = m_{last}s^2 + G_\infty(s) = 0, \tag{2.111}$$

which depend of the sign of the square root in $G_\infty(s)$.

Proof. The BPs in system $G_x(s)$ are found like in Proposition 2.0.7. Besides, the solution of the characteristic equation of $G_x(s)$ is found as follows

$$m_{last}s^2 + \tfrac{1}{2}\left[(n-1)k + (m-1)bs \pm \sqrt{[(n-1)k + (m-1)bs]^2 + 4(n+m-1)kbs}\right] = 0, \tag{2.112}$$

$$\begin{aligned}(2m_{last}s^2 + (n-1)k + (m-1)bs)^2 &= [(n-1)k + (m-1)bs]^2 + 4(n+m-1)kbs,\\ 4m_{last}^2 s^4 + 4m_{last}s^2\left[(n-1)k + (m-1)bs\right] &= 4(n+m-1)kbs,\\ m_{last}^2 s^4 + m_{last}s^2\left[(n-1)k + (m-1)bs\right] - (n+m-1)kbs &= 0. \end{aligned}\tag{2.113}$$

(2.113) shows a 4th order equation implying 4 solutions when Eq. (2.111) is a second order polynomial. For example $s = 0$ is a solution of (2.113) but it is a solution of (2.111) when $G_\infty(s)$ has a minus sign in the square root. □

Proposition 2.0.9: Network with multiple springs and one damper

Let $n > 1$ and $m = 1$ in $G_f(s)$. Then the impulse response of $G_f(s)$ when using its positive solution is given by

$$\Delta x(t) = \tfrac{1}{\sqrt{c\pi t}}e^{-\frac{a^2}{c}t} - \tfrac{a}{c}\text{Erfc}\left(a\sqrt{\tfrac{t}{c}}\right), \tag{2.114}$$

where $c = 4nkb$ and $a = (n-1)k$.

Proof. Let us express $G_f(s)$ as

$$G_f(s) = \frac{1}{(n-1)k \pm \sqrt{(n-1)^2k^2 + 4nkbs}} = \frac{1}{a \pm \sqrt{a^2 + cs}} = \frac{1}{\sqrt{c}}\frac{1}{\frac{a}{\sqrt{c}} \pm \sqrt{\frac{a^2}{c} + s}}, \tag{2.115}$$

by using the Frequency shifting property we have

$$\mathscr{L}^{-1}\left[\frac{1}{\frac{a}{\sqrt{c}} \pm \sqrt{\frac{a^2}{c} + s}}\right] \overset{\text{sgn}=+}{=} e^{-\frac{a^2}{c}t}\mathscr{L}^{-1}\left[\frac{1}{\frac{a}{\sqrt{c}} + \sqrt{s}}\right] = e^{-\frac{a^2}{c}t}\mathscr{L}^{-1}\left[\frac{\sqrt{s}}{s - \frac{a^2}{c}} - \frac{\frac{a}{\sqrt{c}}}{s - \frac{a^2}{c}}\right]. \tag{2.116}$$

Then, we see that in the last expression $\frac{\sqrt{s}}{s - \frac{a^2}{c}}$ needs a deeper analysis. In this vein, we have

$$\int_{Br + C_2 + C_3 + C_4} \frac{\sqrt{s}e^{st}}{s - \frac{a^2}{c}}ds = j2\pi\tfrac{a}{\sqrt{c}}e^{\frac{a^2}{c}t}, \tag{2.117}$$

thus

$$\tfrac{1}{j2\pi}\int_{Br} \frac{\sqrt{s}e^{st}}{s - \frac{a^2}{c}}ds = \tfrac{a}{\sqrt{c}}e^{\frac{a^2}{c}t} + \tfrac{1}{\pi}\int_0^\infty \frac{\sqrt{x}e^{-xt}}{x + \frac{a^2}{c}}dx. \tag{2.118}$$

The last integral in (2.118) is solved as follows

$$\begin{aligned} \frac{1}{\pi}\int_0^\infty \frac{\sqrt{x}e^{-xt}}{x+\frac{a^2}{c}}dx &\overset{u=\sqrt{x}}{=} \frac{2}{\pi}\int_0^\infty \frac{u^2e^{-u^2t}}{u^2+\frac{a^2}{c}}du, \\ &= \frac{1}{\pi}\int_{-\infty}^\infty \frac{u^2}{u^2+\frac{a^2}{c}}e^{-u^2t}du, \\ &= \frac{1}{\pi}\int_{-\infty}^\infty e^{-u^2t}du - \frac{1}{\pi}\int_{-\infty}^\infty \frac{\frac{a^2}{c}}{\frac{a^2}{c}+u^2}e^{-u^2t}du, \\ &= \frac{1}{\sqrt{\pi t}} - \frac{a}{\sqrt{c}}e^{\frac{a^2}{c}t}\mathrm{Erfc}\left(\frac{\sqrt{t}}{\frac{\sqrt{c}}{a}}\right). \end{aligned}$$

Hence,

$$\mathscr{L}^{-1}\left[\frac{\sqrt{s}}{s-\frac{a^2}{c}}\right] = \frac{a}{\sqrt{c}}e^{\frac{a^2}{c}t} + \frac{1}{\sqrt{\pi t}} - \frac{a}{\sqrt{c}}e^{\frac{a^2}{c}t}\left(1-\mathrm{Erf}\left(a\sqrt{\frac{t}{c}}\right)\right), \tag{2.119}$$

$$= \frac{1}{\sqrt{\pi t}} + \frac{a}{\sqrt{c}}e^{\frac{a^2}{c}t}\mathrm{Erf}\left(a\sqrt{\frac{t}{c}}\right). \tag{2.120}$$

Then, the final result is given by

$$\Delta x(t) = \mathscr{L}^{-1}\left[G_f(s)\right] = \left[\frac{1}{\sqrt{c\pi t}}e^{-\frac{a^2}{c}t} + \frac{a}{c}\mathrm{Erf}\left(a\sqrt{\frac{t}{c}}\right)\right] - \frac{a}{c} = \frac{1}{\sqrt{c\pi t}}e^{-\frac{a^2}{c}t} - \frac{a}{c}\mathrm{Erfc}\left(a\sqrt{\frac{t}{c}}\right) \tag{2.121}$$

□

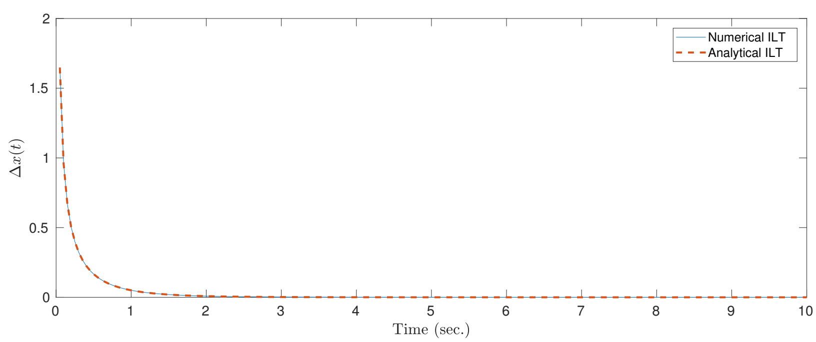

Figure 2.22: Numerical and Analytical Impulse response of system (2.100) for $a = 1$ and $c = 1$.

Consider now (2.101). Then, we can write it as follows

$$G_x(s) = \frac{X_{last}(s)}{X_{1,1}(s)} = \frac{G_\infty}{m_{last}s^2+G_\infty} = \frac{\varrho+\sigma s\pm\sqrt{(\varrho+\sigma s)^2+\varsigma s}}{ms^2+\varrho+\sigma s\pm\sqrt{(\varrho+\sigma s)^2+\varsigma s}}, \tag{2.122}$$

where $\varrho = (n-1)k$, $\sigma = (m-1)b$, $\varsigma = 4(n+m-1)kb$ and $m' = 2m_{last}$.

Simple binary tree network with one spring and one damper

When $n = 1$ and $m = 1$ in (2.122) this gives us the basiest case:

$$G_x(s) = \frac{X_{last}(s)}{X_{1,1}(s)} = \frac{G_\infty(s)}{m_{last}s^2 + G_\infty(s)} = \frac{\pm\sqrt{\varsigma s}}{m's^2 \pm \sqrt{\varsigma s}}. \tag{2.123}$$

Proposition 2.0.10: One spring and one damper infinite tree respose

Given system (2.123), its impulse response is described by

$$x_{last}(t) = \frac{\sqrt[3]{\varsigma}e^{-\frac{\sqrt[3]{\varsigma}t}{2m'^{2/3}}}\left(-e^{\frac{3\sqrt[3]{\varsigma}t}{2m'^{2/3}}} + \sqrt{3}\sin\left(\frac{\sqrt{3}\sqrt[3]{\varsigma}t}{2m'^{2/3}}\right) + \cos\left(\frac{\sqrt{3}\sqrt[3]{\varsigma}t}{2m'^{2/3}}\right)\right)}{3m'^{2/3}}$$
$$\pm \sum_{\ell=1}^{3} z_\ell \left[\sqrt{\varsigma}\left(\sqrt{r_\ell}e^{r_\ell t}\operatorname{erf}\left(\sqrt{r_\ell t}\right) + \frac{1}{\sqrt{\pi}\sqrt{t}}\right)\right], \tag{2.124}$$

where,

$$r_1 = \frac{\sqrt[3]{\varsigma}}{m'^{2/3}} \tag{2.125}$$

$$r_2 = -\frac{\sqrt[3]{-1}\sqrt[3]{\varsigma}}{m'^{2/3}} \tag{2.126}$$

$$r_3 = \frac{(-1)^{2/3}\sqrt[3]{c}}{m'^{2/3}} \tag{2.127}$$

$$z_1 = \frac{m'^{7/3}}{\left(1+\sqrt[3]{-1}\right)\left(1+(-1)^{2/3}\right)\sqrt[3]{\varsigma}} \tag{2.128}$$

$$z_2 = \frac{m'^{7/3}}{\left(\sqrt[3]{-1}-1\right)\left(1+\sqrt[3]{-1}\right)\sqrt[3]{\varsigma}} \tag{2.129}$$

$$z_3 = \frac{\sqrt[3]{-1}m'^{7/3}}{\left(\sqrt[3]{-1}-1\right)\left(1+(-1)^{2/3}\right)\sqrt[3]{\varsigma}} \tag{2.130}$$

Proof. This statement can easily be proved by computing the ILT of (2.123) by rationalizing it, i.e.

$$x_{last}(t) = \mathscr{L}^{-1}\left[H_1(s) + H_2(s)\right] \tag{2.131}$$

where $H_1(s) = \pm\frac{ms\sqrt{\varsigma s}}{m'^2s^3 - \varsigma}$ and $H_2(s) = -\frac{\varsigma}{m'^2s^3 - \varsigma}$.

$H_2(s)$ is clearly easy to ILT and its inversion result corresponds to the first fraction in (2.124), meanwhile for $H_1(s)$ we can use the Laplace transform inversion formula considering that $H_1(s)$ has BPs at the origin and at infinity of the complex plane. We commonly choose The negative real numbers of the complex plane as a BC. Then, r_1, r_2 and r_3 are the roots of the characteristic polynomial $m'^2s^3 - \varsigma$ and z_1, z_2 and z_3 are the partial fraction expantion of $\frac{m's}{m'^2s^3 - \varsigma}$. So that, each element in the summation corresponds to the ILT of expressions of the type $\frac{z_\ell\sqrt{\varsigma s}}{s - r_\ell}$ $\forall\ \ell = 1, 2, 3$ corresponding to each pole of $H_1(s)$. This completes the proof. □

One of our objectives is to proof the efficiency of our results when trying to model tree-networks of finite generations. This could be uselful for avoiding long computations due to the high number of differential equations needed when adding more levels to the tree. In the next figures we show some simulations which compare our analytical expressions with the time response of a FGS. The FGS solution $x_{last_j}(t)$ $\forall$ $j = 1, 2, \cdots, N$ is computed in Octave by using *lsode()* routine with a code made by Bill Goodwine presented in (Goodwine, 2018).

For such a purpose we considered an impulse like input $x_{1,1}(t) = \delta_\alpha(t-1) \approx \frac{1}{|\alpha|\sqrt{\pi}} e^{-\left(\frac{t-1}{\alpha}\right)^2}$. This input is time shifted one second in order to obtain better numerical results when solving the differential equations of the FGSs. So, every $x_{last}(t)$ expressed analytically from Propositions 2.0.10 were also time shifted by 1 second, in order to make the comparison of the impulse responses. Furthermore, we add bar plots with error-index values, the error measured used is the common *Integral Square Error* (ISE), defined as: $\mathbf{E}_I = \int_0^{30} \epsilon(t)^2 dt$, where $\epsilon(t) = x_{last}(t-1)H(t-1) - x_{last_j}(t)$, $H(t)$ stands for the Heaviside step function.

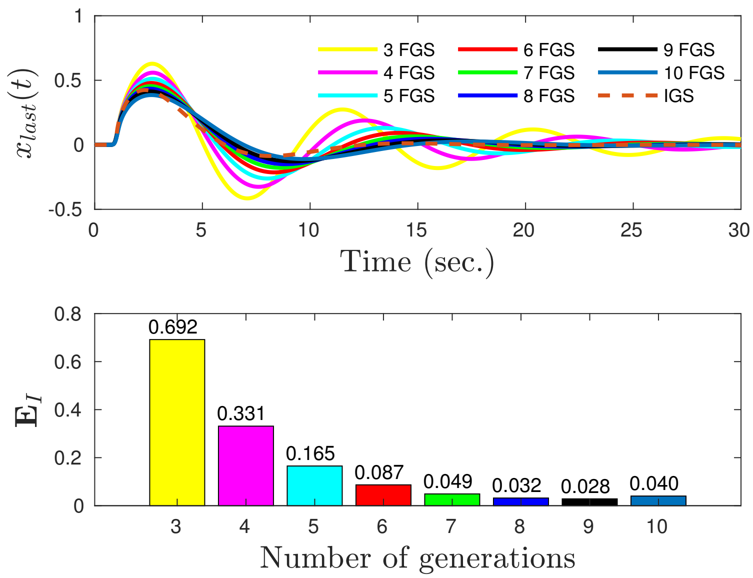

Figure 2.23: Impulse response comparison for the case $n = 1$ and $m = 1$. The legend *IGS* stands for *Infinite Generations System* and uses x_{last} as in Proposition 2.0.10 but time-shifted 1 second, *i-FGS.* uses finite generations response time domain solution using Octave with $x_{1,1} = \delta_{\frac{1}{8}}(t-1)$.

Matlab methods

The numerical ILT used can be found at `https://la.mathworks.com/matlabcentral/fileexchange/39035-numerical-i`

The numerical integration method used can be found at `https://la.mathworks.com/help/matlab/ref/integral.html`.

3
Stability of fractional order systems

Stability of fractional LTI Systems

Consider the fractional system described by

$$G(s) = \frac{P(s)}{Q(s)}, \tag{3.1}$$

where $P(s)$ and $Q(s)$ are defined as

$$Q(s) \quad := \quad \sum_{k=0}^{n} a_k s^{\alpha_k}, \tag{3.2}$$

$$P(s) \quad := \quad \sum_{k=0}^{m} b_k s^{\delta_k}, \tag{3.3}$$

where α_k and δ_k are real non-negative numbers and $a_0 \neq 0$, $b_0 \neq 0$. Without lost of generality we will assume that $\alpha_n > \alpha_{n-1} > \cdots > \alpha_0 = 0$ and $\delta_m > \delta_{m-1} > \cdots > \delta_1 > \delta_0 \geq 0$.

The fractional order system described by the transfer function (3.1) is:

- of commensurate order if

$$\alpha_k = k\alpha \quad (k = 0, 1, \ldots, n) \quad \text{and} \quad \delta_k = k\alpha \quad (k = 0, 1, \ldots, m), \tag{3.4}$$

  where $\alpha > 0$ is a real number,
- of a rational order if it is of commensurate order and $\alpha = \frac{1}{v}$, where v is a positive integer (in such a cae $0 < \alpha \leq 1$),
- of non-commensurate order if (3.4) does not hold.

Because, α_k and δ_k are real non-negative numbers a way to choose α is $\mathrm{lcm}(\mathrm{den}(\alpha_k, \delta_k))$, where $lcm(\cdot)$ and $den(\cdot)$ lie for the least common multiple and denominator, respectively. In this section we will consider only fractional systems of commensurate order.

In section we saw how using the ILT we conclude that the time response of a fractional simple system like

$$G(s) = \frac{1}{s^\alpha \mp a}, \tag{3.5}$$

is expressed in an anomalous decay given by the Mittag Leffler function $E_{\alpha,\alpha}(\cdot)$. With these ideas the stability study of commensurate order systems was first done by D. Matignon in (Matignon, 1996) by considering similar asymptotic expansions of the Mittag Leffler fuction to the following ones reviewed by I. Podlubny:

Mittag Leffler function asymptotic expansions

Theorem 3.0.1: (Podlubny, 1999)

If $0 < \alpha < 2$, β is an arbitrary complex number and μ is an arbitrary real number such that

$$\frac{\pi\alpha}{2} < \mu < \min\{\pi, \alpha\pi\}, \tag{3.6}$$

then fo an arbitrary integer $p \geq 1$ the following expansion holds:

$$E_{\alpha,\beta}(z) = \frac{1}{\alpha} z^{\frac{1-\beta}{\alpha}} e^{z^{1/\alpha}} - \sum_{k=1}^{p} \frac{z^{-k}}{\Gamma(\beta - \alpha k)} + O(|z|^{-1-p}), \quad |z| \to \infty, \quad |\arg(z)| \leq \mu. \tag{3.7}$$

Theorem 3.0.2: (Podlubny, 1999)

If $0 < \alpha < 2$, β is an arbitrary complex number and μ is an arbitrary real number such that

$$\frac{\pi\alpha}{2} < \mu < \min\{\pi, \alpha\pi\}, \tag{3.8}$$

then for an arbitrary integer $p \geq 1$ the following expansion holds:

$$E_{\alpha,\beta}(z) = -\sum_{k=1}^{p} \frac{z^{-k}}{\Gamma(\beta - \alpha k)} + O(|z|^{-1-p}), \quad |z| \to \infty, \quad \mu \leq |\arg(z)| \leq \pi. \tag{3.9}$$

Theorem 3.0.3: (Podlubny, 1999)

If $\alpha \geq 2$ and β is arbitrary, then for an arbitrary integer number $p \geq 1$ the following asyptotic formula holds:

$$E_{\alpha,\beta}(z) = \frac{1}{\alpha} \sum_{n} \left(z^{1\alpha} e^{\frac{j2\pi n}{\alpha}} \right)^{1-\beta} e^{e^{\frac{j2\pi n}{\alpha}} z^{\frac{1}{\alpha}}} - \sum_{k=1}^{p} \frac{z^{-k}}{\Gamma(\beta-\alpha k)} + O\left(|z|^{-1-p} \right), \tag{3.10}$$

where the sum is taken for integer n satisfying the condition

$$|\arg(z) + 2\pi n| \leq \frac{\alpha\pi}{2}.$$

The proof of the last statements can be found in (Podlubny, 1999) and (Valério and da Costa, 2013). Besides, they clearly express that the stability of a fractional commensurate order systems is dependent of the poles argument and the value of the fractional order α.

Therefore, the stability must obviously be different from that of the integer case (see, for integer order systems stability criterions (Stojic and Siljak, 1965)). An interesting reason for it is that a stable fractional system may have roots in right half of the complex w-plane. Since the principal sheet of the Riemann surface is defined $-\pi < \arg(s) < \pi$, by using the mapping $w = s^{\alpha}$, the corresponding domain is defined by $-\alpha\pi < \arg(w) < \alpha\pi$, and the ω plane region corresponding to the right half plane of this sheet is defined by $-\alpha\pi/2 < \arg(w) < \alpha\pi/2$.

Hence in the case of a fractional order linear time invariant (FOLTI) system with commensurate order where the system poles are in general complex conjugate, the stability condition can also be expressed as follows

Theorem 3.0.4: (Matignon, 1996), (Matignon, 1998)

A commensurate order system described by a rational transfer function

$$G(w) = \frac{Q(w)}{P(w)},$$

where $w = s^\alpha$, $\alpha \in \mathbb{R}^+$, $(0 < \alpha < 2)$, is stable if only if

$$|\arg(\lambda)| > \alpha\frac{\pi}{2},$$

with $\forall\lambda_i \in \mathbb{C}$ the i-th root of $P(w) = 0$.

Proof. The proof of this theorem is based on the asymptotic approximations shown in section , where (Matignon, 1996) uses the following similar result

Theorem 3.0.5

We have the following asymptotic equivalents for $E^j_\alpha(\lambda, t)$ as t reaches infinity:

- for $|\text{Arg}(\lambda)| \leq \alpha\pi/2$,

$$E^j_\alpha(\lambda, t) \sim \frac{1}{\alpha(j-1)!}\left\{\left(\frac{d}{d\sigma}\right)^{j-1} e^{\sigma^{1/\alpha}t}\right\}\Bigg|_{\sigma=\lambda}, \tag{3.11}$$

  it has the structure of a polynomial of degree $j-1$ in t, multiplied by $e^{\lambda^{1/\alpha}t}$.

- for $|\text{Arg}(\lambda)| > \alpha\pi/2$,

$$E^j_\alpha(\lambda, t) \sim \frac{1}{\Gamma(1-\alpha)}(-\lambda)^{-j}t^{-\alpha}, \tag{3.12}$$

  which decays slowly towards 0.

Here, λ is a fractional pole of for example a transfer fuction like $s^{\alpha-1}(s^\alpha - \lambda)^{-j}$

by inspection of Theorem 3.0.5, we can conclude easily that the system will have a bounded response if and only if $|\text{Arg}(\lambda)| > \alpha\frac{\pi}{2}$, in such a case the components of the state decay towards 0 like $t^{-\alpha}$ ■ □

When $w = 0$ is a single root (singularity at the origin) of P, the system cannot be stable. For $\alpha = 1$, this is the classical theorem of pole location in the complex plane: it has no pole in the closed right half plane of the first Riemann sheet. The stability region suggested by this theorem tends to the whole s-plane when α tends to 0, corresponds to the Routh-Hurwitz stability when $\alpha = 1$, and tends to the negative real axis when α tends to 2.

The stability analysis criteria for a general FOLTI system can be sumarized as follow (Radwan et al., 2009):

- The characteristic equation of a generat LTI fractional order system

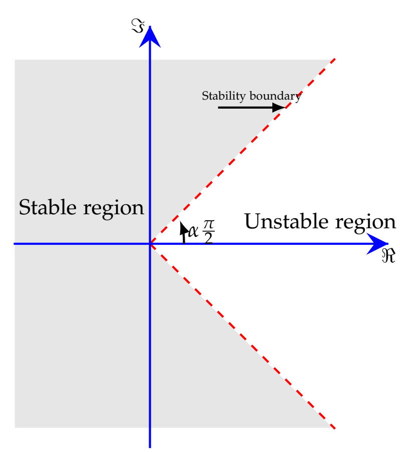

Figure 3.1: $0 < \alpha < 1$.

of the form:

$$a_n s^{\alpha_n} + \cdots + a_1 s^{\alpha_1} + a_0 s^{\alpha_0} \equiv \sum_{i=0}^{n} a_i s^{\alpha_i} = 0, \tag{3.13}$$

may be rewritten as:

$$\sum_{i=0}^{n} a_i s^{\frac{u_i}{v_i}} = 0,$$

and transformed into w-plane

$$\sum_{i=0}^{n} a_i w^i = 0, \tag{3.14}$$

with $w = s^{\frac{k}{m}}$, where m is the LCM of v_i. The procedure of stability analysis is:

1. For a given a_i compute the roots of equation (3.14) and find the absolute phase of all roots $|\phi_\omega|$.
2. Roots in the primary sheet of the ω-plane which have corresponding roots in the s-plane can be obtained by finding all roots which lie in the region $\phi_\omega < \frac{\pi}{m}$ then applying the inverse transformation $s = \omega^m$. The region where $|\phi_\omega| > \frac{\pi}{m}$ is not physical.
3. The condition for stability is $\frac{\pi}{2m} < |\phi_\omega| < \frac{\pi}{m}$. The condition for oscillation is $|\phi| = \frac{\pi}{2m}$ otherwise the system is unstable. If there is no root in the physical s-plane, the system will always be stable.

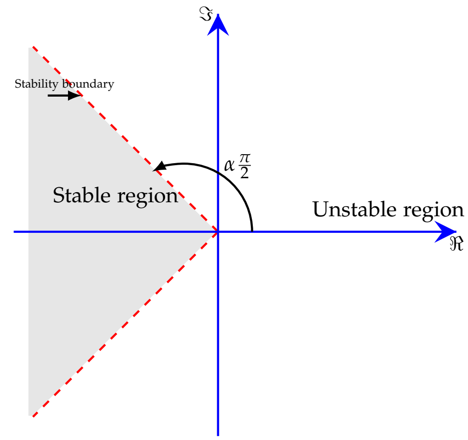

Figure 3.2: $1 < \alpha < 2$.

Further reading: For further reading about the stability analysis in fractional order systems see (Tavazoei and Haeri, 2009; Petráš, 2011b; Zhang and Li, 2011; Abu-Saris and Al-Mdallal, 2013; Lenka and Banerjee, 2018), for another proof on the stability of commensurate fractional order systems see (Sabatier and farges, 2012). Finally, for a modification of the Mikhailov stability criterion for fractional commensurate order systems see (Mendiola-Fuentes and Melchor-Aguilar, 2018).

Example-stability analysis (Caponetto, 2010)

Consider the closed loop system with the controlled system (electrical heater)

$$G(s) = \frac{1}{39.96 s^{1.25} + 0.598},$$

and PD controller

$$C(s) = 64.47 + 12.46 s.$$

The resulting closed loop transfer function $G_c(s)$ becomes

$$G_c(s) = \frac{Y(s)}{W(s)} = \frac{12.46s + 64.47}{36.69 s^{1.25} + 12.46 s + 65.068}. \tag{3.15}$$

The characteristic equation of this system is

$$36.69 s^{1.25} + 12.46 s + 65.068 = 0 \Rightarrow 36.69 s^{\frac{5}{4}} + 12.46 s^{\frac{4}{4}} + 65.068 = 0.$$

Using the notation $\omega = s^{\frac{1}{m}}$, where LCM is $m = 4$, we obtain a polynomial of the complex variable ω in form

$$36.69\omega^5 + 12.46\omega^4 + 65.068 = 0. \tag{3.16}$$

Solving the polynomial (3.16), we get the following roots and their arguments:

$$\begin{aligned}\omega_1 &= -1.17474, |\arg(\omega_1)| = \pi,\\ \omega_{2,3} &= -0.40540 \pm 1.0426j, |\arg(\omega_{2,3})| = 1.9416,\\ \omega_{4,5} &= 0.83580 \pm 0.64536j, |\arg(\omega_{4,5})| = 0.6575.\end{aligned}$$

This first Riemann sheet is defined as a sector in the w-plane within interval $-\pi/4 < \arg(\omega) < \pi/4$. Complex conjugate roots $\omega_{4,5}$ lie in this interval and satisfies the stability condition given as $|\arg(\omega)| > \frac{\pi}{8}$, therefore the system is stable. The region where $|\arg(\omega)| > \frac{\pi}{4}$ is not physical. See Fig. 3.3

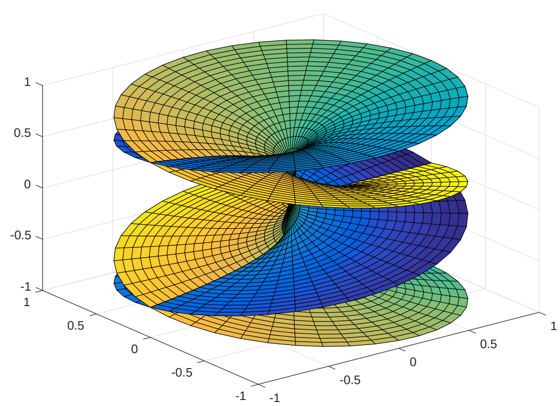

Figure 3.3: $\omega = s^{1/4}$ Riemann surface.

Time response analysis of fractional-order LTI systems

Now that we understand the concept of stability for commensurate fractional-order LTI systems. It is useful to understand and analyze its time response.

For control purposes we consider to analyze the unit step $(H(s))$ response of the fractional commensurate order system given by

$$T(s) = \bar{T}(s^\alpha) = \frac{B(s^\alpha)}{A(s^\alpha)} = \frac{b_{n-1}s^{(n-1)\alpha} + \cdots + b_1 s^\alpha + b_0}{s^{n\alpha} + a_{n-1}s^{(n-1)\alpha} + \cdots + a_1 s^\alpha + a_0} \tag{3.17}$$

If $A(s)$ does not have any multiple roots, the partial fraction expansion of the transfer function $\bar{T}(s^\alpha)$ can be written as

$$\bar{T}(s^\alpha) = \sum_{k=1}^{n} \frac{r_k}{s^\alpha - \lambda_k}. \tag{3.18}$$

Proposition 3.0.1

The transfer function (3.18) impulse response is given by

$$h(t) = t^{\alpha-1} \sum_{k=1}^{n} r_k E_{\alpha,\alpha}(\lambda_k t^\alpha). \tag{3.19}$$

Proof. The proof follows straightforwardly by using (1.42) in (3.18) ■ □

Proposition 3.0.2: (Tavazoei, 2010)

The step response of system (3.18) is given by

$$y(t) = \sum_{k=1}^{n} r_k \frac{E_{\alpha,1}(\lambda_k t^{\alpha}) - 1}{\lambda_k} \tag{3.20}$$

Proof. Integrating $h(t)$ brought in (3.19) we get

$$\begin{aligned}
\int_0^t h(\tau)d\tau &= \sum_{k=1}^{n}\sum_{r=0}^{\infty}\int_0^t \frac{r_k\lambda_k^r t^{\alpha(r+1)-1}}{\Gamma(\alpha(r+1))}d\tau \\
&= \sum_{k=1}^{n}\sum_{r=0}^{\infty}\frac{r_k\lambda_k^r}{\Gamma(\alpha(r+1))}\frac{t^{\alpha(r+1)}}{(\alpha(r+1))}, \\
&= t^{\alpha}\sum_{k=1}^{n} r_k E_{\alpha,\alpha+1}(\lambda_k t^{\alpha}). \qquad (3.21)
\end{aligned}$$

which corresponds to the equation already expressed in (1.43) as the step response of one of the partial fractions. We now want to prove that (3.21) and (3.20) are equivalent.

Taking (3.20) we get

$$\begin{aligned}
\sum_{k=1}^{n} r_k \frac{E_{\alpha,1}(\lambda_k t^{\alpha}) - 1}{\lambda_k} &= \sum_{k=1}^{n}\sum_{r=0}^{\infty}\frac{r_k\lambda_k^{r-1}t^{\alpha r}}{\Gamma(\alpha r+1)} - \sum_{k=1}^{n}\frac{r_k}{\lambda_k} \\
&= \sum_{k=1}^{n}\frac{r_k}{\lambda_k} + \sum_{k=1}^{n}\sum_{r=1}^{\infty}\frac{r_k\lambda^{r-1}t^{\alpha r}}{\Gamma(\alpha r+1)} - \sum_{k=1}^{n}\frac{r_k}{\lambda_k} \\
&= t^{\alpha}\sum_{k=1}^{n}\sum_{r=0}^{\infty}\frac{\lambda_k^r t^{\alpha r}}{\Gamma(\alpha(r+1)+1)} \blacksquare \qquad (3.22)
\end{aligned}$$

□

Proposition 3.0.3

Let $A(s)$ in representation (3.17) does not have any multiple roots. Also, each root of this polynomial is settled outside of sector $|\mathrm{Arg}(s)| \leq \frac{\alpha\pi}{2}$. Then, the step response of (3.17) is given by

$$y(t) = -\sum_{r=1}^{p}\frac{t^{-\alpha r}}{\Gamma(1-\alpha r)}\left(\sum_{k=1}^{n}\frac{r_k}{\lambda_k^{r+1}}\right) + O\left(|t|^{-\alpha(p+1)}\right) - \sum_{k=1}^{n}\frac{r_k}{\lambda_k} \tag{3.23}$$

Proof. By substituting (3.9) in (3.20) ■ □

Proposition 3.0.3 will allow us to analyze how the values of α and λ change the time response characteristics of the system. Before that let us present the following examples:

Example-time response analysis (a one pole system)

Consider the LTI system given by the following transfer function

$$G(s) = \frac{3}{s^{1/2}+2}. \tag{3.24}$$

Then, we know its step response is given by

$$\mathcal{L}^{-1}\left[\frac{3}{s^{1/2}+2}\mathcal{L}\left[H(t)\right]\right] = 3t^{1/2}E_{1/2,3/2}(-2t^{1/2}). \tag{3.25}$$

Because, in this case $\mathrm{Arg}(-2) = \pi > \frac{\alpha\pi}{2}$ we can write

$$3t^{1/2}E_{1/2,1}(-2t^{1/2}) = 3t^{1/2}\left[-\sum_{k=1}^{p}\frac{(-2)^{-k}t^{-k/2}}{\Gamma(\frac{3}{2}-\frac{k}{2})} + O(|t|^{-(1+p)/2})\right], \tag{3.26}$$

then, when $t \to \infty$ we have

$$3t^{1/2}E_{1/2,1}(-2t^{1/2}) = \frac{3}{2}. \tag{3.27}$$

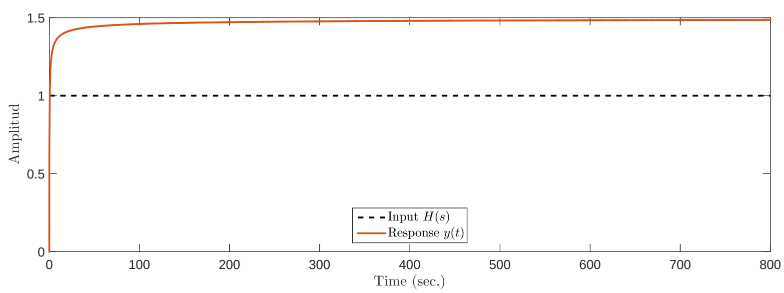

Figure 3.4: Step response simulation of system (3.24)

Note 3.0.1

A more genral example of a transfer function like (3.24) is given by

$$G(s) = \frac{k}{s^{\alpha}-\lambda}. \tag{3.28}$$

Whose step response taking λ outside of the region $|\mathrm{Arg}(s)| \leq \frac{\alpha\pi}{2}$ is

$$\mathcal{L}^{-1}\left[\frac{k}{s^{\alpha}-\lambda}\mathcal{L}\left[H(t)\right]\right] = kt^{\alpha}\left[-\sum_{r=1}^{p}\frac{(\lambda)^{-r}t^{-r\alpha}}{\Gamma(\alpha+1-\alpha r)} + O(|t|^{-\alpha(1+p)})\right]. \tag{3.29}$$

From (3.29) we see that the $t^{-\alpha r}$ will reach towards zero faster when α is bigger.

Example-time response analysis (two pole system)

Consider a transfer function $D(s)$ to be written in the following partial fraction expansion

$$D(s) = \frac{Ae^{j\theta}}{s^{\alpha} + Be^{j\phi}} + \frac{Ae^{-j\theta}}{s^{\alpha} + Be^{-j\phi}}. \tag{3.30}$$

By some computations we find that $D(s)$ is equal to

$$D(s) = \frac{2A\cos(\theta)s^{\alpha} + 2AB\cos(\theta - \phi)}{s^{2\alpha} + 2AB\cos(\phi)s^{\alpha} + B^2}. \tag{3.31}$$

Expression (3.31) is useful to start understanding the time response of fractional order systems with complex conjugate poles.

From (3.20) we know that the step response of (3.30) is given by

$$y(t) = \sum_{k=1}^{2} \frac{r_k}{\lambda_k} E_{\alpha,1}(\lambda_k t^{\alpha}) + C, \tag{3.32}$$

where

$$\begin{aligned} r_k &= Ae^{j\theta(-1)^{k+1}}, \\ \lambda_k &= B'e^{j\phi'}, \end{aligned}$$

where

$$\begin{aligned} B' &= \mathrm{Abs}(-Be^{j\phi(-1)^{k+1}}) \\ \phi' &= (-1)^{k+1}\phi + (-1)^{k}\pi \end{aligned}$$

and the function $E(\cdot)$ is defined depending of the $\mathrm{Arg}(\lambda_k)$ using Teorems 3.0.1 and 3.0.2. Besides, C is defined as

$$C = \begin{cases} D(0), & \mathrm{Arg}(\lambda_k) \geq \frac{\alpha\pi}{2} \\ -\sum_{k=1}^{2} \frac{r_k}{\lambda_k}, & \mathrm{Arg}(\lambda_k) < \frac{\alpha\pi}{2} \end{cases}. \tag{3.33}$$

Using Teorem 3.0.1 we get

$$\begin{aligned} y(t) &= \sum_{k=1}^{2} \frac{r_k}{\lambda_k} \left\{ \frac{1}{\alpha}(\lambda_k t^{\alpha})^{\frac{1-\beta}{\alpha}} e^{(\lambda_k t^{\alpha})^{1/\alpha}} - \sum_{r=1}^{p} \frac{(\lambda_k t^{\alpha})^{-r}}{\Gamma(\beta - \alpha r)} + O(|t|^{-\alpha(1+p)}) \right\} + C, \\ &= \sum_{k=1}^{2} \frac{r_k}{\lambda_k} \left\{ \frac{1}{\alpha} e^{(\lambda_k)^{1/\alpha} t} - \sum_{r=1}^{p} \frac{(\lambda_k t^{\alpha})^{-r}}{\Gamma(1 - \alpha r)} + O(|t|^{-\alpha(1+p)}) \right\} + C. \end{aligned} \tag{3.34}$$

Because expression (3.7) in Theorem 3.0.1 holds for an arbitrary integer $p \geq 1$, choosing $p = 1$ in (3.34) for simplicity we get

$$y(t) = \sum_{k=1}^{2} \frac{r_k}{\lambda_k} \left\{ \frac{1}{\alpha} e^{(\lambda_k)^{1/\alpha} t} - \frac{t^{-\alpha}}{\lambda_k \Gamma(1-\alpha)} + O(|t|^{-2\alpha}) \right\} + C. \tag{3.35}$$

Consider now the following three cases

$*$ Case 1: $|\mathrm{Arg}(\lambda_k)| = \phi' = \frac{\alpha\pi}{2}$. In such a case we expect an oscillatory response given by

$$\begin{aligned} y(t) &= \sum_{k=1}^{2} \frac{r_k}{\lambda_k}\left\{\frac{1}{\alpha}e^{(\lambda_k)^{1/\alpha}t} - \frac{t^{-\alpha}}{\lambda_k\Gamma(1-\alpha)} + O(|t|^{-2\alpha})\right\} + D(0) \\ &= \frac{Ae^{j\theta}}{\alpha B' e^{j(\phi-\pi)}}e^{(B'e^{j(\phi-\pi)})^{1/\alpha}t} + \frac{Ae^{-j\theta}}{\alpha B' e^{j(-\phi+\pi)}}e^{(B'e^{j(-\phi+\pi)})^{1/\alpha}t} - \frac{Ae^{j\theta}t^{-\alpha}}{B'^2 e^{j2(\phi-\pi)}\Gamma(1-\alpha)} - \frac{Ae^{-j\theta}t^{-\alpha}}{B'^2 e^{j2(-\phi+\pi)}\Gamma(1-\alpha)} + O(|t|^{-2\alpha}) + D(0) \\ &= \frac{Ae^{j\theta}}{\alpha B' e^{-j\phi'}}e^{-j(B')^{1/\alpha}t} + \frac{Ae^{-j\theta}}{\alpha B' e^{j\phi'}}e^{j(B')^{1/\alpha}t} - \frac{2At^{-\alpha}}{B'^2\Gamma(1-\alpha)}\cos(\theta + 2(-\phi+\pi)) + O(|t|^{-2\alpha}) + D(0) \\ &= \frac{2A}{\alpha B'}\cos((B')^{1/\alpha}t - \theta - (-\phi+\pi)) - \frac{2At^{-\alpha}}{B'^2\Gamma(1-\alpha)}\cos(\theta + 2\phi') + O(|t|^{-2\alpha}) + D(0) \end{aligned} \tag{3.36}$$

$*$ Case 2: $|\mathrm{Arg}(\lambda_k)| = \phi' > \frac{\alpha\pi}{2}$. In this case the stable response would be

$$y(t) = -\frac{2At^{-\alpha}}{B'^2\Gamma(1-\alpha)}\cos(\theta + 2\phi') + O(|t|^{-2\alpha}) + D(0) \tag{3.37}$$

$*$ Case 3: $|\mathrm{Arg}(\lambda_k)| = \phi' < \frac{\alpha\pi}{2}$. The unstable response its given by

$$y(t) = \sum_{k=1}^{2} \frac{r_k}{\lambda_k}\left\{\frac{1}{\alpha}e^{(\lambda_k)^{1/\alpha}t} - \frac{t^{-\alpha}}{\lambda_k\Gamma(1-\alpha)} + O(|t|^{-2\alpha})\right\} - \sum_{k=1}^{2}\frac{r_k}{\lambda_k} \tag{3.38}$$

A specific example could be the transfer function

$$D(s) = \frac{\frac{16}{3}}{s^{2\alpha} + 2s^{\alpha} + 5} = \frac{\frac{4}{3}j}{s^{\alpha} + 1 + 2j} + \frac{-\frac{4}{3}j}{s^{\alpha} + 1 - 2j}, \tag{3.39}$$

whose poles $\lambda_1 = -1 - 2j$ and $\lambda_2 = -1 + 2j$ are complex conjugate of order α. We can easily find that the step response of system (3.39) is

$$\begin{aligned} d(t) &= \frac{\frac{4}{3}j}{(-1-2j)}E_{\alpha,1}((-1-2j)t^{\alpha}) + \frac{-\frac{4}{3}j}{(-1+2j)}E_{\alpha,1}((-1+2j)t^{\alpha}) - \left[\frac{\frac{4}{3}j}{-1-2j} + \frac{-\frac{4}{3}j}{-1+2j}\right], \\ &= \frac{\frac{4}{3}j}{(-1-2j)}E_{\alpha,1}((-1-2j)t^{\alpha}) + \frac{-\frac{4}{3}j}{(-1+2j)}E_{\alpha,1}((-1+2j)t^{\alpha}) + \frac{\frac{16}{3}}{5}. \end{aligned} \tag{3.40}$$

Now, expression (3.40) will behave differently depending on the value of α. The three posible behaviours are given by

$\star$ Case 1: $|\mathrm{Arg}(\lambda_k)| = \phi' = \frac{\alpha\pi}{2}$. In this case $\alpha = \frac{2\phi}{\pi} = 1.2952$

$$d(t) = 0.9208\cos(1.8614t + 2.6779) + 0.0915t^{-1.2952} + O(|t|^{-2(1.2952)}) + \frac{\frac{16}{3}}{5}. \tag{3.41}$$

$\star$ Case 2: $|\mathrm{Arg}(\lambda_k)| = \phi' > \frac{\alpha\pi}{2}$. In this case $\alpha = 0.8$

$$d(t) = 0.0915t^{-1.2952} + O(|t|^{-2(1.2952)}) + \frac{\frac{16}{3}}{5}. \tag{3.42}$$

Once we understand how to obtain the time response of two and one pole systems. We can deduce the following results:

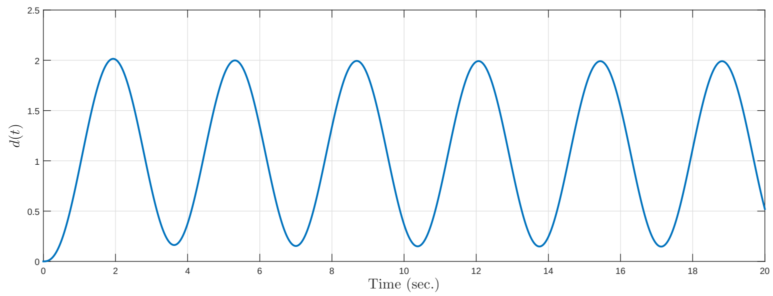

Figure 3.5: Step response simulation of system (3.39) with $\alpha = 1.2952$.

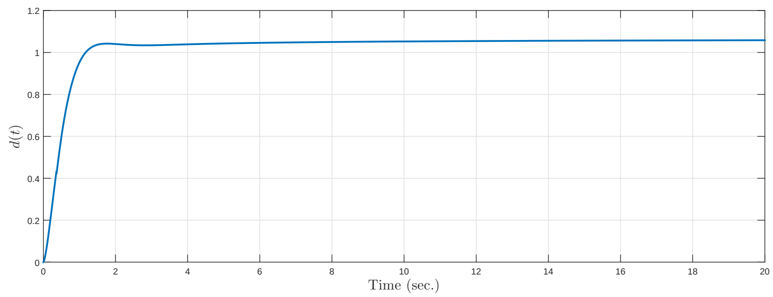

Figure 3.6: Step response simulation of system (3.39) with $\alpha = 0.8$.

Theorem 3.0.6: One pole system. How real poles value change the step response

Let $\alpha_1 > \alpha_2$ where $\alpha_1, \alpha_2 \in (0, 1)$, to be the commensurate order fractional degrees of $H_1(s)$ and $H_2(s)$ which are defined as

$$H_1(s) = \frac{1}{s^{\alpha_1} - \xi} \tag{3.43}$$

$$H_2(s) = \frac{1}{s^{\alpha_2} - \xi} \tag{3.44}$$

and $\xi \in \mathbb{R}^-$. Then, the time $H_1(s)$ takes to arrive the steady gain $H_1(0) = H_2(0)$ is smaller than the time for $H_2(s)$ in the step response.

Proof. By using Proposition 3.0.3, we find that the step response of $H_1(s)$ and $H_2(s)$ are given by

$$y_1(t) = \frac{1}{\xi}\left(-\sum_{r=1}^{p} \frac{t^{-r\alpha_1}}{\xi^r \Gamma(1-\alpha_1 r)} + O\left(|t|^{-\alpha_1(1+p)}\right) - 1\right), \tag{3.45}$$

$$y_2(t) = \frac{1}{\xi}\left(-\sum_{r=1}^{p} \frac{t^{-r\alpha_2}}{\xi^r \Gamma(1-\alpha_2 r)} + O\left(|t|^{-\alpha_2(1+p)}\right) - 1\right), \tag{3.46}$$

by inspection we notice that $y_1(t) = y_2(t) = -\frac{1}{\xi}$ as $t \to \infty$, but because $\alpha_1 > \alpha_2$ then $y_1(t)$ show a faster response due to the faster decay of the $t^{-r\alpha_1}$ and $t^{-\alpha_1(1+p)}$ terms. $\square$

Example: One pole system. How real poles value change the step response

Take $H(s)$ to be

$$H(s) = \frac{1}{s^{\alpha} - 1}. \tag{3.47}$$

where $\alpha \in (0, 1)$. Figure 3.7 shows the step response of $H(s)$ when changing α.

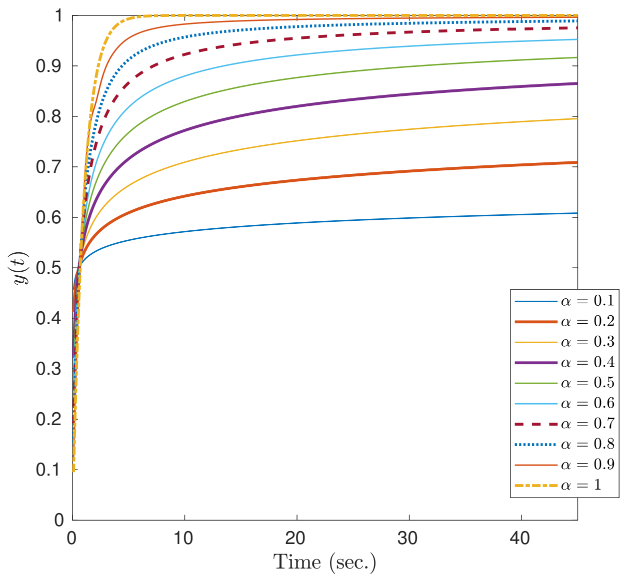

Figure 3.7: Step response $y(t)$ of $H(s)$ when varying α.

Theorem 3.0.7: One polse system. How fractional order value changes the step response

Let $\xi_1 < \xi_2$ such that $\xi_1, \xi_2 \in \mathbb{R}^{-}$, to be the poles of the w-transform transfer functions $H_1(s)$ and $H_2(s)$ given by

$$H_1(s) = \frac{1}{s^{\alpha} - \xi_1}, \tag{3.48}$$

$$H_2(s) = \frac{1}{s^{\alpha} - \xi_2}, \tag{3.49}$$

and $\alpha \in (0, 2)$. Then, the time response of $H_1(s)$ is faster than the $H_2(s)$ response in arriving its steady gain.

Proof. Taking a fixed α we see that the sumation terms at the step responses of $H_1(s)$ and $H_2(s)$ in the form

$$-\sum_{r=1}^{p} \frac{t^{-r\alpha_1}}{\xi^r \Gamma(1 - \alpha_1 r)} \tag{3.50}$$

have smaller impact when ξ is bigger. Then a more negative ξ will lead to a faster response. □

Remark 3.0.1. *Theorem 3.0.7 shows that a more negative ξ shows a faster response, but the steady gain will decrease, showing a smaller response.*

Example: One polse system. How fractional order value changes the step response

Take $H(s)$ to be

$$H(s) = \frac{1}{s^{\alpha} - \xi}. \tag{3.51}$$

where $\alpha \in (0, 2)$. Figure 3.8 shows the step response of $H(s)$ when changing ξ.

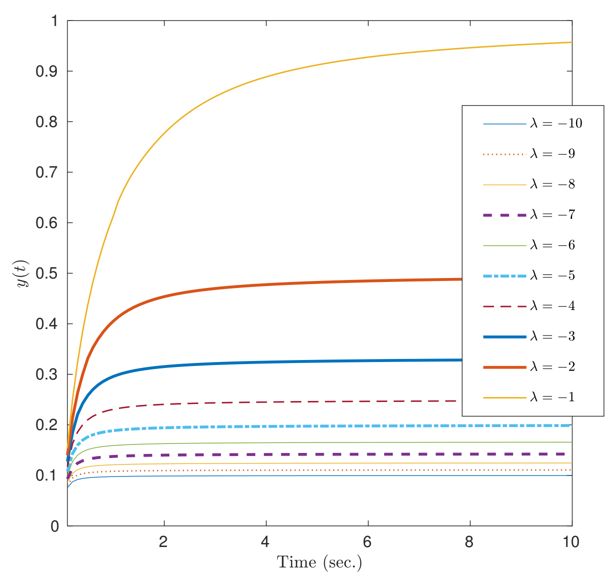

Figure 3.8: Step response $y(t)$ of $H(s)$ when varying ξ.

Theorem 3.0.8: Two pole system. How the magnitude value of its conjugate poles change the step response

Let the stable fractional order two pole systems $H_1(s)$ and $H_2(s)$ to be defined as

$$H_1(s) = \sum_{k=1}^{2} \frac{\chi_k}{s^{\alpha} - \psi_k'}, \tag{3.52}$$

$$H_2(s) = \sum_{k=1}^{2} \frac{\chi_k}{s^{\alpha} - \psi_k''}, \tag{3.53}$$

where ψ_k' and ψ_k'' are the complex conjugate poles of system $H_1(s)$ and $H_2(s)$ respectively, such that $|\psi_k'| > |\psi_k''|$. Then the step response of the system $H_1(s)$ will arise its steady gain $H_1(0)$ faster than system $H_2(s)$.

Theorem 3.0.9: Two pole system. How the fractional order value of its conjugate poles change the step response

Let $\alpha_1 > \alpha_2$ where $\alpha_1, \alpha_2 \in (0,1)$, to be the commensurate order fractional degrees of $H_1(s)$ and $H_2(s)$ which are defined as

$$H_1(s) = \sum_{k=1}^{2} \frac{\chi_k}{s^{\alpha_1} - \psi_k}, \quad (3.54)$$

$$H_2(s) = \sum_{k=1}^{2} \frac{\chi_k}{s^{\alpha_2} - \psi_k}, \quad (3.55)$$

and $\psi_k \in \mathbb{C}$ for $k = 1,2$ are complex conjugated poles. Then, the time $H_1(s)$ takes to arrive the steady gain $H_1(0) = H_2(0)$ is smaller than the time for $H_2(s)$ in the step response. Furthermore if $\mathrm{Arg}(\psi_k) \approxeq \frac{\alpha_i \pi}{2}, k = 1,2$. Then, we start having oscilations in the system $H_i(s), i = 1,2$ response.

Example: Two pole system. How the magnitude and fractional order values of its conjugate poles change the step response

Consider the two pole fractional order system given by

$$H(s) = \frac{\omega_n^2}{s^{2\alpha} + 2\xi\omega_n s^{\alpha} + \omega_n^2} = \sum_{k=1}^{2} \frac{r_k}{s^{\alpha} - \psi_k}, \quad (3.56)$$

then, according to Theorem 3.0.8 if we increase the magnitud of the complex conjugate poles ψ_k of $H(s)$ we will obtain a rapid response. The following figures show the simulation results

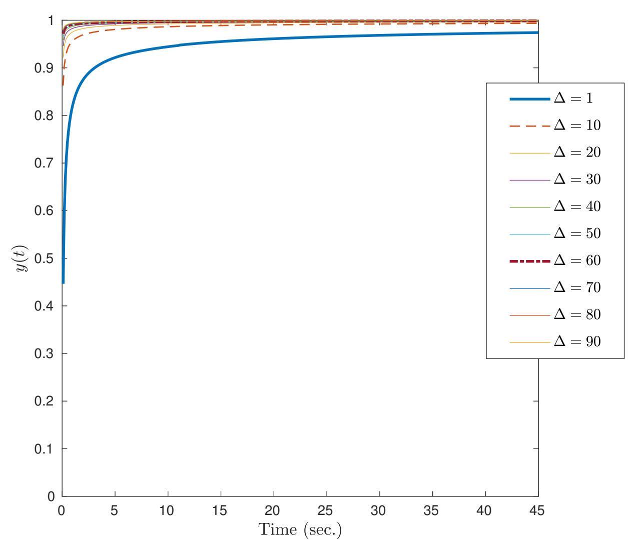

Figure 3.9: Step response simulation of system (3.56) with using the complex conjugate poles $\psi = -1 - \Delta \pm j(2 + \Delta)$ and $\alpha = 0.5$.

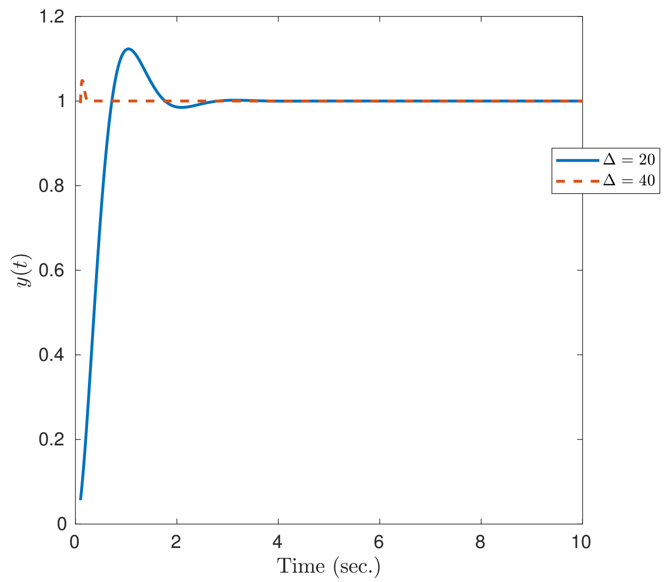

Figure 3.10: Step response simulation of system (3.56) with using the complex conjugate poles $\psi = -1 - \Delta \pm j(2+\Delta)$ and $\alpha = 1$.

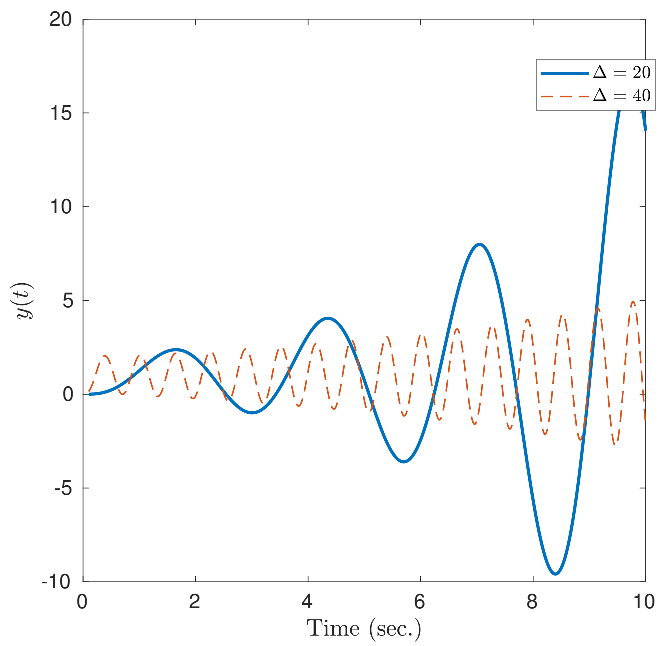

Figure 3.11: Step response simulation of system (3.56) with using the complex conjugate poles $\psi = -1 - \Delta \pm j(2+\Delta)$ and $\alpha = 1.5$.

Overshoot in the step response

One of the important characteritics in the time response of a system is the *overshoot*. In this vein, if we do a *Matlab* simulation for the step

Further reading: A common way to analyze the time response of integer order systems is by means of the *Root-Locus* method. This method for fractional order systems is discussed in (Merrikh-Bayat and Afshar, 2008).

response of (3.28) we obtain something similar to the result of Fig. 3.12 for various α values and taking $\lambda = -2$ and $k = 3$. This shows that the settling time is smaller when α is bigger but if $\alpha > 1$ the step response shows the existence of an overshoot.

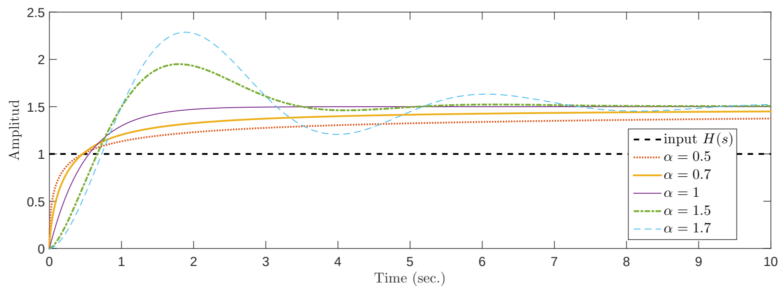

Figure 3.12: Step response simulation of system (3.24)

If we aim to find the reasons of existence of an overshoot we can apply the idea of using weighting functions (see, for further details (Sigdell, 1967) and (Genin and Calvez, 1970)).

First, we define the response $f(t)$ to have an overshoot if, for any $t > 0$, we have $f(t) > \lim_{t\to\infty} f(t) = A$. Another case (besides the oscillatory one), where it is simple to say that an overshoot exists, is when $f(+0) > A$ or in the Laplace domain,

$$\exists \lim_{s\to\infty} sF(s) > \lim_{s\to+0} sF(s) = A, \tag{3.57}$$

where $F(s) = \mathcal{L}[f(t)]$. If none of the elementary criteria above is applicable, we may still have an overshoot. One approach to determining wheter this is the case is to investigate the integral :

$$\int_0^\infty \varsigma(t)\,\{f(t) - A\}\,dt, \tag{3.58}$$

where $\varsigma(t) \geq 0$ in $(0, \infty)$. If this integral is positive or zero for ay such (nontrivial) $\varsigma(t)$, an overshoot must exist. (For appropiate $\varsigma(t) : s$, this approach includes the cases where the elementary criteria above apply.) We can determine the values of this integral for $\varsigma(t) = t^n$ quite easily by expanding the Laplace transform in a Maclaurin series, whithin the neighbourhood of the origin of the complex plane

$$\begin{aligned} F(s) = \int_0^\infty e^{-st} f(t)dt &= \frac{A}{s} + \int_0^\infty e^{-st}\,\{f(t) - A\}\,dt, \\ &= \frac{A}{s} + \int_0^\infty \{f(t) - A\} \sum_{n=0}^{\infty} \frac{(-1)^n (st)^n}{n!} dt. \end{aligned} \tag{3.59}$$

In engineering applications , the function $f(t)$ is such that we may integrate each term in the sum individually:

$$F(s) = \frac{A}{s} + \sum_{n=0}^{\infty} \frac{(-1)^n a_n s^n}{n!} \tag{3.60}$$

where

$$a_n = \int_0^\infty t^n\,\{f(t) - A\}\,dt. \tag{3.61}$$

Lemma 3.0.2. *Let $F(s)$ being expanded in series as in (3.60). If for any n we have $a_n \geq 0$, then , there must be an overshoot. If not, there may be still one.*

Lemma 3.0.2 requires to determine the value of a_n. We can determine a_n from the derivatives of $F(s)$, as is clear from the serial development. an alternative way is to use the Laplace formula

$$\mathcal{L}\left[t^n f(t)\right] = (-1)^n f^{(n)}(s) \tag{3.62}$$

which gives

$$a_n = \int_0^\infty t^n \{f(t) - A\}\, dt = \lim_{s\to+0} \left\{(-1)^n f^{(n)}(s) - \frac{An!}{s^{n+1}}\right\}. \tag{3.63}$$

Remark 3.0.3. *Equation (3.60) requires, that $F(s)$ has not more than one pole at the origin (due to the step-function input), but if it had a multiple pole there, then $f(t)$ would show a unstable behaviour.*

There are other alternative criteria for weighting functions $\varsigma(t)$, such as $e^{\beta t}$ or $1 + \sin(\omega t + \phi)$, may also be used:

$$\int_0^\infty e^{-\beta t} \{f(t) - A\}\, dt = F(s) - \frac{A}{\beta}, \tag{3.64}$$

if $\beta > 0$; for $\beta < 0$ the integral may not exists (in fact, β must lie to the right of all poles) or

$$\int_0^\infty \{1 + \sin(\omega t + \phi)\} \{f(t) - A\}\, dt = \lim_{s\to+0} \left\{F(s) - \frac{A}{s}\right\} + \frac{1}{2j}\left\{e^{j\phi} F(-j\omega) - e^{-j\phi} F(j\omega)\right\} - \frac{A}{w}\cos(\phi) \tag{3.65}$$

Another approach would be to inspect from which direction $f(t)$ approaches its limit for large t. If $\lim_{t\to\infty} f(t) = A + 0$, the function $f(t)$ must clearly have an overshoot. But we would like to judge this from $F(s)$ and its behaviour as $s \to 0$.

Based on the above ideas we get the following result

Theorem 3.0.10: (Tavazoei, 2011)

The strictly proper and BIBO stable transfer function $G(s)$ in the form

$$G(s) = \frac{Q(s)}{P(s)} = \frac{q_m s^{\beta} + q_{m-1} s^{\beta_{m2-1}} + \cdots + q_1 s^{\beta_1} + q_0}{s^{\alpha_r} + p_{r-1} s^{\alpha_{r-1}} + \cdots + p_1 s^{\alpha_1} + p_0} \tag{3.66}$$

with the steady state gain $G(0) \neq 0$ has always an overshoot in its step response if

$$\lim_{s\to 0} \frac{G(s) - G(0)}{s} = 0 \tag{3.67}$$

Proof. Without loss of generality, assume that $G(0) > 0$. Also, let $y(t)$ be the step response of $G(s)$, i.e. $y(t) = \mathcal{L}^{-1}\left\{\frac{G(s)}{s}\right\}$. It can be easily verified that

$$\int_0^\infty (1 \pm \cos(\omega_0 t)) \{y(t) - G(0)\}\, dt = \int_0^\infty \{y(t) - G(0)\}\, dt \pm \int_0^\infty \cos(\omega_0 t) \{y(t) - G(0)\} \tag{3.68}$$

$$\overset{(3.67)}{=}$$

$$= \lim_{s\to 0}\left(\frac{G(s) - G(0)}{s}\right) \pm \Im\left[\frac{G(j\omega_0)}{\omega_0}\right], \tag{3.69}$$

where $\omega_0 \in (0, \pi)$. If condition (3.67) is hold, we have

$$\int_0^\infty (1 \pm \cos(\omega_0 t)) \{y(t) - G(0)\}\, dt = \pm \Im\left[\frac{G(j\omega_0)}{\omega_0}\right]. \tag{3.70}$$

Hence, at least one of the integrals $\int_0^\infty (1+\cos(\omega_0 t))\{y(t)-G(0)\}\,dt$ and $\int_0^\infty (1-\cos(\omega_0 t))\{y(t)-G(0)\}\,dt$ should be nonnegative. According to this point and considering the inequality $1 \pm \cos(\omega_0 t) \geq 0$ for all $t \in (0,\infty)$, it is concluded that there existis an interval time (t_1, t_2) such that $y(t) > G(0) = y(\infty)$ for all $t \in (t_1, t_2)$. This means that the step response $y(t)$ has an overshoot. The proof for the case $G(0) < 0$ is similar as that presented for the case $G(0) > 0$, and consequently ommited here ■ □

Corollary 3.0.1: Existence of an overshoot in the step response (Tavazoei, 2011)

The step response of a stable fractional-order transfer function in the form (3.66) has an overshoot if $\alpha_1 > 1$ and $\beta_1 > 1$.

Corollary 3.0.2: Existence of an overshoot in the step response (Tavazoei, 2011)

The step response of each stable fractional-order system with commensurate order α, where $1 < \alpha < 2$, has an overshoot.

Corollary 3.0.3: One pole system

The step response of the transfer function $H(s)$ given by

$$H(s) = \frac{1}{s^\alpha - 1} \tag{3.71}$$

with commensurate order α has an overshoot if $1 < \alpha < 2$.

Proof. Taking $H(s)$ as in Eq. (3.71) and its steady gain $H(0) \neq 0$ we have always an overshoot in its step response if

$$\lim_{s \to 0} \frac{H(s) - H(0)}{s} = 0, \tag{3.72}$$

then,

$$\lim_{s \to 0} \frac{\frac{1}{s^\alpha - \xi} + \frac{1}{\xi}}{s} = \lim_{s \to 0} \frac{s^\alpha}{\xi s (s^\alpha - \xi)} \tag{3.73}$$

which is equal to zero when $\alpha > 1$ □

Example: Overshoot in a one pole system

Take $H(s)$ to be (3.71) where $\alpha \in (1,2)$. The following figure shows the step response of $H(s)$ when changing α.

Further reading: A survey paper about time response analysis of fractional order systems recommended is (Tavazoei, 2014).

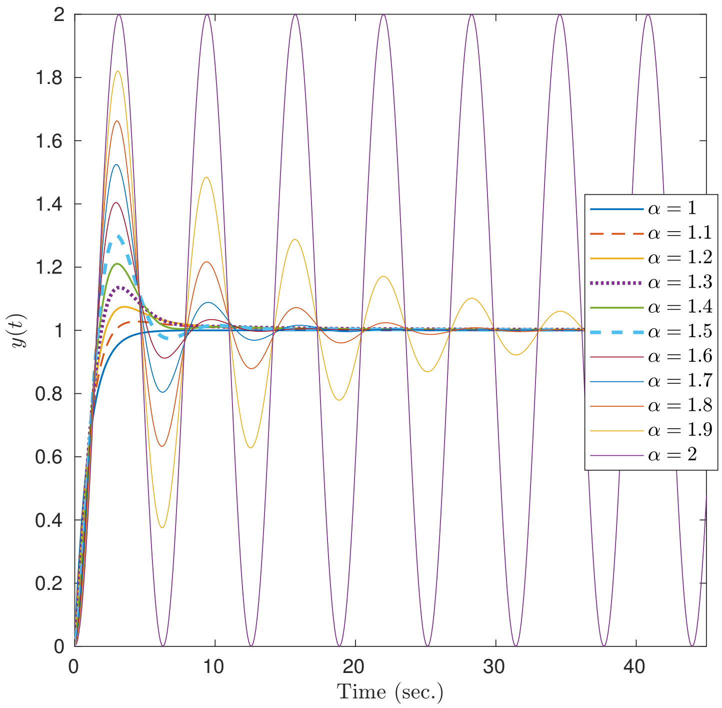

Figure 3.13: Step response $y(t)$ of $H(s)$ when varying α.

Stability for fractional LTI systems with time delay

Time-delay systems are of great interest in this work, there are many practical systems and problems in engineering that involve time lags: Bioreactors, Rolling mills, Ship stabilization, turbojet engine, Microwave oscillator, etcetera (see, (Kolmanovskii and Nosov, 1986)).

It is known, that the classical stability analysis for non time-delay systems is made by criterions like: *Routh-Hurwitz*, *Nyquist*, *Mikhailov* and *Hermite-Biehler* (see, for further details (Stojic and Siljak, 1965),(Ho et al., 1999) and (Ho et al., 2000)). But, when talk about linear time-delay systems, such criterions change. The characteristic polynomials of time-delay systems are known as *Quasi-polynomials*, which are functions of the following type:

$$F(s) = \sum_{k=0}^{n} f_k(s)e^{\lambda_k s}, \tag{3.74}$$

where $f_k(s)$ are polynomials in s with constant coefficients, and λ_k, $k = 0, \ldots, n$, are real (or complex) numbers. By other words, (3.74) is a sum, where the terms are the product of an exponential and a polynomial function with constant coefficients. In control theory, such exponentials corresponds to delays which can be commensurable real numbers, that is $\lambda_k = k\lambda$ $k = 0, \ldots, n$, and $\lambda > 0$. One of the most used criterions for stability analysis of quasi-polynomials is the generalization of the *Hermite-Biehler* theorem by Pontryagin in (Pontryagin, 1955). Successively in (Bhattacharyya et al., 1995) and (Bellman and Cooke, 1963), based on

Pontryagin's results, and extension of the *Hermite-Biehler* theorem was developed to study the stability of a certain class of quasipolynomials.

Now for Linear-Time-Invariant (LTI) fractional commensurate order systems with time-delay, consider a system of such a nature described by the transfer function

$$P(s) = \frac{\sum_{i=0}^{n_2} q_i(s)e^{-\beta_i s}}{\sum_{i=0}^{n_1} p_i(s)e^{-\gamma_i s}} = \frac{N(s)}{D(s)} \tag{3.75}$$

where $0 = \gamma_0 < \gamma_1 < \cdots < \gamma_{n_1}$, $0 \leq \beta_0 < \cdots < \beta_{n_2}$, the p_i and q_i being polynomials of the form

$$p_i(s) = \sum_{k=0}^{l_i} a_k s^{\alpha_k}, \tag{3.76}$$

$$q_i(s) = \sum_{k=0}^{m_i} b_k s^{\delta_k}, \tag{3.77}$$

where α_k and δ_k are real non-negative numbers. We shall assume that throughout that $N(s)$ and $D(s)$ have no common zeroes in $\{\Re[s] \geq 0\} \setminus \{0\}$.

Note that, for $s \neq 0$ and $\delta \in \mathbb{R}$, we define s^δ to be $e^{\delta(\log|s|+j\arg(s))}$, and a continuous choise of $\arg(s)$ in a domain leads to an analytic branch of s^δ. In this work we shall normally make the choice $-\pi < \arg(s) < \pi$, for $s \in \mathbb{C} \setminus \mathbb{R}^-$.

As for the classical delay systems, we shall consider the class of retarded and neutral systems, that is systems which satisfy, respectively, condition 1 or 2 below:

Further reading: For further reading about the stability criterions for time-delay systems (Gu et al., 2003) and (Michiels and Niculescu, 2007).

Further reading: In (Buslowicz, 2008) the stability of fractional order systems of retarded type is also discussed. The sufficient and neccesary conditions for stability of fractional time-delay systems of neutral type is discussed in (Moornani and Haeri, 2011). Besides (Nguyen and Bonnet, 2012; Bonnet et al., 2009) and (Fioravanti et al., 2010) present some results in stability analysis for fractional time-delay of neutral type.

Conditions 3.0.4 (Retarded and neutral type systems)**.** *Condition 1:* $\deg p_0 > \deg p_i$ *for* $i = 1, \ldots, n_1$ *and* $\deg p_0 > \deg q_i$ *for* $i = 0, \ldots, n_2$.

Condition 2: $\deg p_0 \geq p_i$ *for* $i = 1, \ldots, n_1$ *(with equality for at least one polynomial* p_i*) and* $\deg p_0 > \deg q_i$ *for* $i = 0, \ldots, n_2$.

Note that these conditions imply that we deal here with strictly proper systems. Besides, these conditions are similar to those used to classify integer order time-delay systems.

In this work we will consider only the case of retarded systems. to investigate the properties of the class of retarded systems of type (3.75) satisfying *Condition 1*. the necessary and sufficient condition of stability turns out to be the same as for the classical class of retarded systems.

Theorem 3.0.11: (Bonnet and Partington, 2000, 2002)

Let $P(s)$ of the form (3.75) be the strictly proper transfer function, where $N(s)$ and $D(s)$ have no common zeros. Then the fractional order system described by the transfer function (3.75) is bounded-input bounded-output (BIBO) stable (shortly stable) if and only if $P(s)$ has no poles with non-negative real parts, i.e.

$$D(s) \neq 0 \quad \text{for} \quad \Re(s) \geq 0. \tag{3.78}$$

The fractional degree characteristic quasi-polynomial of the system of retarded type form of (3.75) has the form

$$D(s) = p_0(s) + \sum_{i=1}^{n_1} p_i(s)e^{-\gamma_i s}. \tag{3.79}$$

Then, the following *Lemmas* are of great interest to analyze the stability of (3.79):

Lemma 3.0.5 ((Buslowicz, 2008)). *The fractional quasi-polinomial of* (3.79) *satisfy the condition* (3.78) *if and only if all its zeros satisfy the condition*

$$|Arg(w)| > \alpha\frac{\pi}{2}, \tag{3.80}$$

where $w = s^{\alpha}$ *and* $-\pi < Arg(w) \leq \pi$.

Proof. From Theorem 3.0.11, we concluded that the boundary of the satbility region of the fractional quasi-polynomial (3.79) is the imaginary axis of the complex s-plane with the parametric description $s = j\omega$ $\omega \in (-\infty, \infty)$. Zeros of fractional quasi-polynomial $D(s)$ of the form (3.79) satisfy the relationship $\lambda = s^{\alpha}$. Hence, the boundary of stability region in the complex $\lambda-$plane has the parametric description

$$\lambda = (j\omega)^{\alpha} = |\omega|^{\alpha}e^{j\alpha\pi/2}, \quad \omega \in (-\infty, \infty). \tag{3.81}$$

All zeros of quasi-polynomial (3.79) lie in the stability region with the boundary (3.81) if and only if (3.80) holds ■ □

Lemma 3.0.6 ((Buslowicz, 2008)). *The fractional quasi-polynomial* (3.79) *is not stable for any* $\alpha > 1$.

Proof. From (3.80) and Fig. 3.2 it follows that if $1 < \alpha < 2$ then the stability region is a cone in the open left half-plane. The fundamental properties of distribution of zeros of quasi-polinomials show that a quasi-polynomial like (3.79) of retarded type always has at least one chain of asymptotic zeros satisfying the conditions

$$\lim_{|\lambda|\to\infty} \Re(\lambda) = -\infty, \quad \lim_{|\lambda|\to\infty} \Im(\lambda) = \pm\infty. \tag{3.82}$$

Therefore, the condition (3.80) with $\alpha > 1$ does not hold for the asymptotic zeros of quasi-polinomial (3.79) ■ □

Further reading: For time domain analysis of linear fractional differential system with time delays see (Deng et al., 2007) and (Xiao et al., 2017).

Overshoot in the step response for delayed systems

The following analysis is a generalization of the overshoot in the step response of fractional order systems without time delat discussed in Section by using weighting functions.

Let $y(t-\tau)u(t-\tau)$ with $u(t-\tau) = 0$ for $0 \leq t < \tau$, be the step response of the fractional LTI system with time delay $G(s)$ in the form

$$G(s) = \frac{Q(s^{\alpha})}{P(s^{\alpha})}e^{-\tau s}, \tag{3.83}$$

where

$$P(s^{\alpha}) = \sum_{k=0}^{m} p_k s^{\alpha_k}, \ \alpha_k = k\alpha \ (k = 0, 1, \ldots, m), \tag{3.84}$$

$$Q(s^{\alpha}) = \sum_{k=0}^{n} q_k s^{\alpha_k}, \ \alpha_k = k\alpha \ (k = 0, 1, \ldots, n), \tag{3.85}$$

$\tau > 0$, $P(s^\alpha)$, $\alpha \in (0,1]$ and $\deg P < \deg Q$. Besides, $G(s)$ is considered to be BIBO-stable.

Using the weighting functions introduced in (Genin and Calvez, 1970), let A to be equal to

$$\lim_{s\to+0} sF(s) = A \tag{3.86}$$

where $F(s) = \mathcal{L}\left[y(t-\tau)u(t-\tau)\right]$. From (Genin and Calvez, 1970) we see that an overshoot must exist if the integral (3.58) is positive or zero. Then, applying the same analysis we see that for $\varsigma = t^n$ and expanding the Laplace transform in a Maclauring series, within the neighbourhood of the origin of the complex plane we get

$$\begin{aligned} F(s) = \int_0^\infty e^{-st} f(t-\tau)u(t-\tau)dt &= = \frac{A}{s} + \int_0^\infty e^{-st}\left\{f(t-\tau)u(t-\tau) - A\right\}dt, \\ &= \frac{A}{s} + \int_0^\infty \left\{f(t-\tau)u(t-\tau) - A\right\}\sum_{n=0}^\infty \frac{(-1)^n(st)^n}{n!}dt, \\ &= \frac{A}{s} + \sum_0^\infty (-1)^n \vartheta_n \frac{s^n}{n!}, \end{aligned} \tag{3.87}$$

where

$$\vartheta_n = \int_0^\infty t^n \left\{f(t-\tau)u(t-\tau) - A\right\}dt \tag{3.88}$$

To determine the value of ϑ_n, we use the Laplace formula

$$\mathcal{L}\left[t^n f(t-\tau)u(t-\tau)\right] = (-1)^n \frac{d^n}{ds^n}\mathcal{L}\left[f(t-\tau)u(t-\tau)\right] = (-1)^n \frac{d^n}{ds^n}\left\{e^{-\tau s}\mathcal{L}\left[f(t)\right]\right\} \tag{3.89}$$

which gives

$$\begin{aligned} \vartheta_n = \int_0^\infty t^n\left\{f(t-\tau)u(t-\tau) - A\right\}dt &= \lim_{s\to+0}\left\{(-1)^n\frac{d^n}{ds^n}\left\{e^{-\tau s}\mathcal{L}\left[f(t)\right]\right\} - A\frac{n!}{s^{n+1}}\right\} \\ &= \lim_{s\to+0}\left\{(-1)^n\frac{d^n}{ds^n}\left\{e^{-\tau s}F(s)\right\} - A\frac{n!}{s^{n+1}}\right\} \end{aligned} \tag{3.90}$$

If for any n we have $\vartheta_n \geq 0$, there must be an overshoot. If not as in the case without time delay, there may be still be one. Lets take $(1 \pm \cos(\omega_0 t))$ as our weighting function with $\omega_0 \in (0,\pi)$. Then, we get the following

$$\begin{aligned} \int_0^\infty (1\pm\cos(\omega_0 t))\left\{f(t-\tau)u(t-\tau) - A\right\}dt &= \lim_{s\to 0}\mathcal{L}\left[(1\pm\cos(\omega_0 t))\left\{f(t-\tau)u(t-\tau) - A\right\}\right], \\ &= \lim_{s\to+0}\left\{e^{-\tau s}F(s) - \tfrac{A}{s}\right\} \pm \lim_{s\to 0}\mathcal{L}\left[\cos(\omega_0 t)f(t-\tau)u(t-\tau)\right], \\ &= \lim_{s\to+0}\left\{\tfrac{G(s)e^{-\tau s}-A}{s}\right\} \pm \lim_{s\to 0}\left[\tfrac{e^{-\tau s}G(s-j\omega_0)}{s-j\omega_0} + \tfrac{e^{-\tau s}G(s+j\omega_0)}{s+j\omega_0}\right], \\ &= \lim_{s\to+0}\left\{\tfrac{G(s)e^{-\tau s}-G(0)}{s}\right\} \pm \left[\tfrac{G(-j\omega_0)}{-j\omega_0} + \tfrac{G(j\omega_0)}{j\omega_0}\right], \\ &= \lim_{s\to+0}\left\{\tfrac{G(s)e^{-\tau s}-G(0)}{s}\right\} \pm \Im\left[\tfrac{G(-j\omega_0)-G(j\omega_0)}{\omega_0}\right]. \end{aligned} \tag{3.91}$$

A sufficient but not neccesary condition for the integral $\int_0^\infty (1\pm\cos(\omega_0 t))\left\{f(t-\tau)u(t-\tau) - A\right\}dt \geq 0$ is that in (3.91)

$$\lim_{s\to+0}\left\{\frac{G(s)e^{-\tau s} - G(0)}{s}\right\} = 0, \tag{3.92}$$

then the system will have an overshoot. Since, (3.92) holds such an integral should be nonnegative. According to this point, it is concluded that there exist an interval time (t_1, t_2) such that $y(t) > G(0) = y(\infty)$ for all

$t \in (t_1, t_2)$. This may happen when $G(0)$ is either positive or negative. We state this as the following result

Theorem 3.0.12: Overshoot existence in time-delay fractional order systems

The strictly proper and BIBO stable transfer function $G(s)$ in (3.83) with steady state gain $G(0) = A \neq 0$ has always an overshoot in its step response if

$$\lim_{s \to +0} \left\{ \frac{G(s)e^{-\tau s} - G(0)}{s} \right\} = 0. \tag{3.93}$$

The Mittag-Leffler stability of fractional order systems

The concept of exponential stability is very known in control theory of integer order systems. Nevertheless, fractional order systems time response is of anomalous decay (i.e. non-exponential). We saw in previous sections that fractional order systems time response uses the *Mittag-Leffler* funcion. Hence, we may talk about a *Mittag-Leffler* stability, which is defined as follows:

Further reading: The *Mittag-Leffler* stability is presented and discussed deeply in (Li et al., 2009),(Baleanu et al., 2010) and (Wyrwas and Mozyrska, 2015).

Definition 3.0.1: Definition of the Mittag-Leffler stability (Li et al., 2009)

The solution of

$$_{t_0}D_t^{\alpha} x(t) = f(t, x) \tag{3.94}$$

which is a considered fractional nonautonomous system with initial condition $x(t_0)$. where D denotes either the *Caputo* or *Riemann-Liouville* fractional operator, $\alpha \in (0, 1)$, $f : [t_0, \infty] \times \Omega \to \mathbb{R}^n$ is piecewise continuoues in t and locally *Lipschitz* in x on $[t_0, \infty] \times \Omega$, and $\Omega \in \mathbb{R}^n$ is a domain that contains the origin $x = 0$.
Is said to be *Mittag-Leffler* stable if

$$\parallel x(t) \parallel \leq \left\{ m \left[x(t_0) \right] E_{\alpha}(-\lambda(t - t_0)^{\alpha}) \right\}^{b}, \tag{3.95}$$

where $\lambda > 0, b > 0, m(0) = 0, m(x) \geq 0$, and $m(x)$ is locally lipschitz on $x \in \mathbb{B} \in \mathbb{R}^n$ with Lipschitz constant m_0.

Lyapunov direct method

Lyapunov direct method provides a way to analyze the stability of dynamical systems without solving their differential equations. It is especially advantageous when the solution is difficult or even impossible to find with classical methods. Therefore, it is interesting to investigate extension of the method for non-integer order systems. Such extension relies heavily on a notion of *Mittag-Leffler* stability.

Lyapunov direct method for fractional order systems is proposed in (Li et al., 2010) and is reviewed in (Zagórowska et al., 2015).

Complex order systems stability

Fractional order systems generalizes the idea of integer order systems by considering real order derivatives and integrals in their dynamics. Hence, it is natural to wonder about the case of *complex-order* systems which may consider derivatives and integrals of order q such that $q \in \mathbb{C}$.

Consider a linear complex-order system having the transfer function

$$G(s) = \frac{p}{s^q - k}, \tag{3.96}$$

where $p, q, k \in \mathbb{C}$. Then, the output of the system will be given by

$$Y(s) = \left[\frac{p}{s^q - k}\right] U(s). \tag{3.97}$$

For the unit impulse input $u(t) = \delta(t)$, the *Laplace* transform will be $U(s) = 1$. Therefore (3.97) becomes

$$\begin{aligned} Y(s) &= \frac{p}{s^q - k}, \\ \therefore y(t) &= \mathscr{L}^{-1}\left[Y(s)\right]. \end{aligned}$$

We know that the ILT in this case is given by

$$\mathscr{L}^{-1}\left[\frac{1}{s^q - k}\right] = t^{q-1} E_{q,q}(kt^q). \tag{3.98}$$

Hence,

$$y(t) = pt^{q-1} E_{q,q}(kt^q). \tag{3.99}$$

(3.99) is a series that is complex-valued. since complex time-reponse is meaningless, we use a combination of this system with its complex conjugate-order system to obtain a series that is real-valued. The conjugate-order system is defined by the transfer function

$$G(s) = \frac{p}{s^q - k} + \frac{\bar{p}}{s^{\bar{q}} - \bar{k}}, \tag{3.100}$$

that will have an output

$$Y(s) = \left[\frac{p}{s^q - k} + \frac{\bar{p}}{s^{\bar{q}} - \bar{k}}\right] U(s), \tag{3.101}$$

which is real-valued.

The stability for these type of systems is presented by Jay L. Adams et al. in (Adams et al., 2012) and a review of time and frequency domain stability analysis is presented in (Jacob et al., 2016).

Extension of the concept of stability

We mentioned in the Preliminaries section of this work that the concept of *Multivalued* functions would be used continuously. In this section we show a stability result that concludes how not only the poles but also the branch points (which are part of *Multivalued functions*) are crucial in determining the stability.

Almost all LTI systems can be represented by rational transfer functions (possibly with delay) but there are some important exceptions. In (Curtain and Zwart, 1995) some examples of infinite-dimentional systems that lead to fractional order transfer functions are shown. For example

$$H(s) = \frac{\tanh(\sqrt{s})}{\sqrt{s}}, \tag{3.102}$$

appears in a boundary controlled and observed diffusion process in a bounded domain. Besides, the transfer function

$$H(s) = \frac{\cosh(\sqrt{s}x_0)}{\sqrt{s}\sinh(\sqrt{s})}, \quad 0 < x_0 < 1, \tag{3.103}$$

corresponds to the heat equation with Neumann boundary control.

For these kind of tranfer functions we must consider the following result when talking about their stability:

Theorem 3.0.13: (Merrikh-Bayat and Karimi-Ghartemani, 2008)

A given multivalued transfer function is stable if and only if it has no pole in $\mathbb{C}_+$ and no BP in $\mathbb{C}_-$. Here, $\mathbb{C}_+$ and $\mathbb{C}_-$ stand for the closed right half plane (RHP) and the open RHP of the first Riemann sheet, respectively.

Proof. The proof needs the following definition

Definition 3.0.2: Region of Convergence (ROC)

Let $h(t)$ denote the impulse response of an LTI causal system. Then its Laplace transform $H(s)$ (the system transfer function) is defined as

$$\int_0^\infty h(t)e^{-st}dt. \tag{3.104}$$

Then, the set of all points on the first Riemann sheet for which the Laplace integral (3.104) is absolutely convergent is called the region of convergence (ROC), that is, $s = \sigma + j\omega$ belongs to ROC if

$$\int_0^\infty |h(t)e^{-st}|dt = \int_0^\infty |h(t)|e^{-\sigma t}dt < \infty. \tag{3.105}$$

It is obvious that the ROC of (3.104) is a half-plane to right of the abscissa of convergence σ_c. The left-hand boundary of ROC is a line parallel to the imaginary axis.

Assume the class of bounded input signals $u \in L_\infty$, that is , $\max_t\{|u(t)|\} < \infty$. The system is stable if for every input $u \in L_\infty$, the output $y(t) = u(t) * h(t) = \int_0^\infty h(\tau)u(t-\tau)d\tau$ is also bounded, that is, $y \in L_\infty$. It is easy to prove that for a causal LTI system with impulse response $h(t)$ to be BIBO stable (as defined above), the necessary and suficient condition is that $h \in L_1$, that is

$$\int_0^\infty |h(t)|dt < \infty. \tag{3.106}$$

Comparing to (3.105), $h(t)$ corresponds to a stable system if and only if the ROC of $H(s)$ includes the imaginary axis. It will be the case if and only if $H(s)$ has no pole in $\mathbb{C}_+$ and no BP in $\mathbb{C}_-$(because, else the Laplace integral will not be convergent). This completes the proof ■ □

Example: Stability effect by the location of Branch Points in a multivalued function

Consider the following multivalued transfer function

$$G(s) = \frac{1}{\sqrt{s^2+k}}, \tag{3.107}$$

where $k \in \mathbb{R}$. It can be proof that the impulse response of (3.107) is given by

$$y(t) = \mathscr{L}^{-1}\left[\frac{1}{\sqrt{s^2+k}}\right] = \begin{cases} J_0(\sqrt{k}t) & \text{if} \quad k > 0 \\ J_0(j\sqrt{k}t) & \text{if} \quad k < 0 \\ 1 & \text{if} \quad k = 0 \end{cases}, \tag{3.108}$$

where, $J_0(\cdot)$ is known as the *Bessel* function of the first kind of order zero. It is clear that the cases in (3.108) depend on the location of the BPs of (3.107), which can be found by solving $s^2 + k = 0$. If Theorem 3.0.13 is true when $k < 0$ the system must be unstable, this can be proof by plotting (3.108).

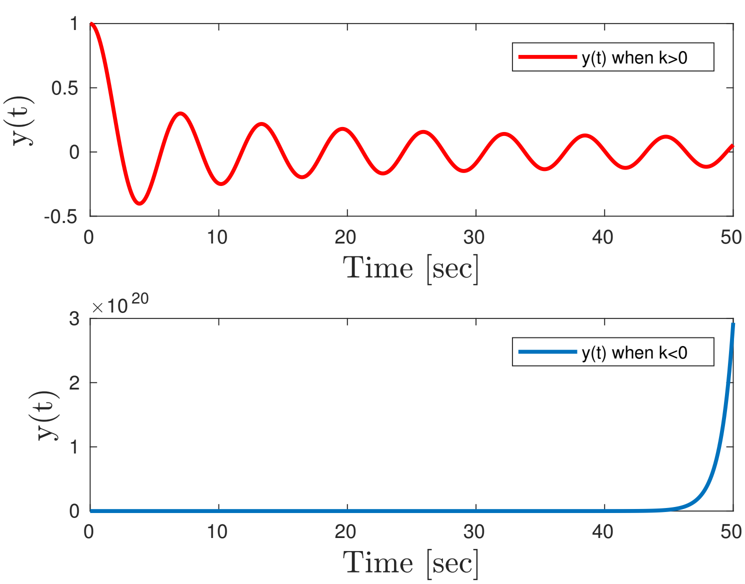

Figure 3.14: Step response of system (3.107).

Consider now the system

$$G(s) = \frac{1}{\sqrt{s+k}}, \tag{3.109}$$

where $k \in \mathbb{R}$. We can proof that the impulse response of system (3.109) is given by

$$y(t) = \mathscr{L}^{-1}\left[\frac{1}{\sqrt{s+k}}\right] = \begin{cases} \frac{e^{-kt}}{\sqrt{\pi t}} & \text{if} \quad k > 0 \\ \frac{e^{kt}}{\sqrt{\pi t}} & \text{if} \quad k < 0 \\ \frac{1}{\sqrt{\pi t}} & \text{if} \quad k = 0 \end{cases}. \tag{3.110}$$

In this case the position of the BP is found by solving $s + k = 0$ and its easy to conclude that according to Theorem 3.0.13, (3.109) must be unstable when $k < 0$ which is correct according to (3.110).

4
Design of fractional PD^{μ} and PI^{λ} controllers

In (Podlubny, 1994) Podlubny published the idea of creating a PID-type controller containig non-integer order derivate and integral terms, titled the fractional $PI^{\lambda}D^{\mu}$ controller. Therefore, fractional order controllers are a very recent idea. This type of algorithms are proved to provide better results when being applied to fractional-order systems (Podlubny, 1994, 1999). However, when they are applied to integer order systems we can used them as PID-type controller algorithms with more degrees of freedom which is helpful to obtain results that otherwise would be difficult or even impossible to characterize (Valério and da Costa, 2013).

As we have seen, it is said that fractional order operators present heredity, nonlocality, selfsimilarity and stochasticity properties(Uchaikin, 2013). Besides, some infinite dimensional order systems are presented as examples of fractional order systems(Curtain, 1992) and many recent results in system modeling using fractional calculus(Hollkamp et al., 2018; Leyden and Goodwine, 2016; Goodwine, 2014; Mayes and Sen, 2011; Galvao et al., 2013) justify the study of stability and control design for fractional order systems.

In this vein, we propose the study of the design of fractional PD^{μ} and PI^{λ} controllers for non-integer order systems. Meanwhile, we have shown in (Guel-Cortez et al., 2018) that for integer order systems the PD^{μ} controller improves the performance of the derivative term when using a classical PD controller in a robotic system based on the hypothesis concluded by visualizing a simulation (Fig. 4.1) comparing the result of deriving and half-deriving a sinusoidal noisy signal, where we see the almost null effect in the noise of the half derivative compared to the integer order one.

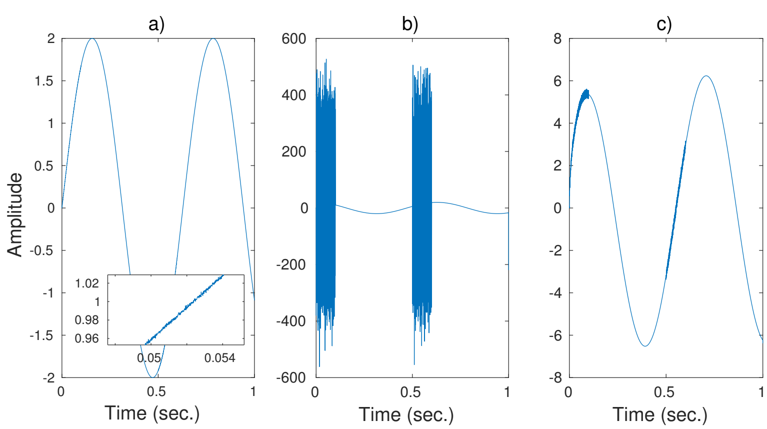

Figure 4.1: Fractional derivative compared with the integer derivative. (a) Sine wave signal with intermittent high-frequency noise. (b) Integer order derivative. (c) Fractional derivative with $\mu = 1/2$.

Various results in designing fractional order controllers have been published,(Hamamci, 2007, 2008; Caponetto, 2010; Monje et al., 2010) but there is a need for easier methodologies and applications to the methods in real experiments (Shah and Agashe, 2016; Caponetto, 2010).

One of the contributions of this work, is a geometrical method for finding the stabilizing PD^{μ} controllers for linear time invariant (LTI) fractional order systems with time delay. Which is based on the $\mathcal{D}$-partition curves (Neimark, 1949; Gryazina, 2004; Gryazina et al., 2008), allowing us to construct the stability crossing curves in the parameters space defined by the gains 'k_p' (proportional gain) and 'k_d' (fractional derivative gain of order μ) and the implicit function theorem that permit us to detect the cross direction (to stability or instability) of the roots of the characteristic polynomial of the closed loop system which enables the determination of the number of unstable roots in each region. Furthermore, we show the procedure in a general algorithm and discuss the performance of the closed-loop system in terms of the controller's fragility.

Further reading: To see more about fractional PID controllers see (Shah and Agashe, 2016). A comparison between fractional and integero order controllers can be found at (Dulău et al., 2017). Details about the fractional PD^{λ} algorithm are discussed in (Tavazoei, 2012). Besides, more fractional order $PI^{\lambda}D^{\mu}$ design algorithms can be found at (Oprzędkiewicz and Dziedzic, 2017; Boudjehem and Boudjehem, 2016).

Problem Formulation

Consider a LTI-fractional order system with time-delay described by the transfer function

$$G(s) = \tfrac{P(s)}{Q(s)} e^{-\tau s}, \tag{4.1}$$

where $\tau > 0$,

$$\begin{aligned} P(s) &:= b_m s^{\beta_m} + \cdots + b_1 s^{\beta_1} + b_0 s^{\beta_0}, && (4.2)\\ Q(s) &:= a_n s^{\alpha_n} + \cdots + a_1 s^{\alpha} + a_0 s^{\alpha_0} && (4.3)\end{aligned}$$

and a_k $(k = 0, \ldots, n)$, b_k $(k = 0, \ldots, m)$ are constant real numbers; and α_k $(k = 0, \ldots, n)$, β_k $(k = 0, \ldots, m)$ are arbitrary rational numbers which can be arranged as $\alpha_n > \alpha_{n-1} > \cdots > \alpha_0$ and $\beta_m > \beta_{m-1} > \cdots > \beta_0$ with $\deg P < \deg Q$. Hence, we can express (3.75) as an integer order system of the form

$$G(w) = \tfrac{b_m w^m + \cdots + b_1 w + b_0}{a_n w^n \cdots + a_1 w + a_0} e^{-\tau w^v} = \tfrac{P(w)}{Q(w)} e^{-\tau w^v}, \tag{4.4}$$

by using the transformation $w = s^{\alpha}$, $\alpha = \frac{1}{v}$ with $v > 1$ given by the $\mathrm{lcm}(\mathrm{den}(\alpha_k, \beta_k))$.

The closed-loop fractional characteristic quasi-polynomial of system (4.1) is defined by

$$\Delta_G(s) := Q(s) + P(s) e^{-\tau s}. \tag{4.5}$$

Let the w-transformed system (4.4) where P and Q are assumed to satisfy the following assumptions:
Assumption 1. *Polynomials P and Q satisfy the following conditions:*

(i) $\deg Q(w) > \deg P(w)$.

(ii) *$P(w)$ and $Q(w)$ are coprime polynomials.*

(iii) $|P((j\omega)^{\alpha})| > 0, \forall\, \omega \in \mathbb{R}$.

(iv) If $Q((j\omega^*)^\alpha) = 0$, then $|Q'((j\omega^*)^\alpha)| > 0$, $\omega^* \in \mathbb{R}$.

It is clear that assumption (i) states that we are looking at systems of *retarded type*. If assumption (ii) is not fulfilled, this implies that there exist a non constant common factor $c(w)$, such that $P(w) = c(w)\bar{P}(w)$ and $Q(w) = c(w)\bar{Q}(w)$. In such a case, choosing $c(w)$ to be of the highest possible degree, the analysis can be pursued if $c(w)$ is a stable polynomial satisfying Theorem 3.0.11, contrarily, the system will remain unstable independently of the control action. Finally, in order to simplify the presentation, assumptions (iii) and (iv) are imposed to avoid multiple roots on the imaginary axis in P and Q, respectively.

The problems considered in this paper can be sumarized as follows:

Problem 1. *To find precise conditions on the parameters (k_p, k_d) such that the Fractional-PD$^\mu$ controller*

$$C(s) = k_p + k_d s^\mu, \tag{4.6}$$

makes the closed-loop plant described by the transfer function (4.1) BIBO stable.

Problem 2. *To find precise conditions on the parameters (k_p, k_i) such that the Fractional-PI$^\lambda$ controller*

$$C(s) = k_p + k_i s^\lambda, \tag{4.7}$$

makes the closed-loop plant described by the transfer function (4.1) BIBO stable.

In the sucessive results we will focus in solving Problem 1. Subsequently, we will mention the considerations we must take to apply the same procedure to Problem 2.

Fractional PD$^\mu$ controller design

Let us solve Problem 1 as stated above and the following problem:

Problem 3. *To determine a Fractional-PD$^\mu$ controller $\mathbf{k}^* := [k_p, k_d]^T \in \mathbb{R}^2$ and a positive value d such that the controller (4.6) stabilizes system (3.75) for any k_p and k_d, satisfying*

$$\sqrt{(k_p - k_p^*)^2 + (k_d - k_d^*)^2} < d. \tag{4.8}$$

From a geometrical perspective, we can define the collection of all controller gains $\mathbf{k} \in \mathbb{R}^2$ as points in the k_p-k_d parameters plane. Thus, Problem 2 can be explained as the task of finding at least one region in the k_p-k_d parameters plane such that, for all $\mathbf{k}$-points inside this region, the characteristic equation of the closed-loop system has all of its roots in the LHP. A region of the k_p-k_d parameters plane with such a feature is defined as a stability region.

Remark 4.0.1. *In this work we take μ to be a fixed value defined as $\mu := u\alpha$ where $u \in \mathbb{N}$, such that $u \geq 0$. Besides, it is neccesary to have a closed loop system of the retarded type in order to use Theorem 3.0.11,(Bonnet and Partington, 2002) for this $\mu < \alpha_n - \beta_m$. Furthermore, we always consider the parameter $\tau \in \mathbb{R}_+$ as a fixed value.*

Remark 4.0.2. *In this paper we will use the term w-transformation when refering to the already used transformation using $w = s^\alpha$, $\alpha = \frac{1}{v}$ to some equation dependent of $s \in \mathbb{C}$.*

Stability Crossing Curves

We start by characterizing the stability crossing curves for fractional-PD^μ controllers applied to general LTI-fractional order systems, meanwhile we announce some useful definitions.

We are interested in finding stability regions in the (k_p, k_d)-parameter space of the closed-loop system described by its characteristic equation given by:

$$\Delta(s; k_p, k_d) := Q(s) + P(s)(k_p + k_d s^\mu)e^{-\tau s} = 0. \tag{4.9}$$

Definition 4.0.1: Frequency crossing set

The frequency crossing set $\Omega \subset \mathbb{R}$ is the set of all ω such that, there exists at least a duplet (k_p, k_d) for which

$$\Delta(j\omega; k_p, k_d) = Q(j\omega) + P(j\omega)(k_p + k_d(j\omega)^{\mu})e^{-j\tau\omega} = 0. \tag{4.10}$$

Remark 4.0.3. *It is clear that if we take the complex conjugate of (4.10), the following equality holds:*

$$\Delta(-j\omega; k_p, k_d) = \overline{\Delta(j\omega; k_p, k_d)}.$$

Therefore, in the rest of the paper we will consider only nonnegative frequencies. i.e. $\Omega := \Omega_+ \cup \{0\}$, *where* $\Omega_+ = \mathbb{R}^+$.

Definition 4.0.2: Stability crossing curves

The stability crossing curves $\mathcal{T}$ is the set of all parameters $(k_p, k_d) \in \mathbb{R}^2$ for which there exists at least one $\omega \in \Omega$ such that $\Delta(j\omega; k_p, k_d) = 0$. Additionally, any point $\mathbf{k} \in \mathcal{T}$ is known as a crossing point.

Stability crossing curves characterization

Imaginary crossing curves (ICC)

Proposition 4.0.1: Imaginary Crossing Curves

Let $\tau \in \mathbb{R}^+$ be a fixed value. Then, $\omega \in \Omega_+$ is a crossing frequency if and only if $\mathbf{k}(\omega) := \left[k_p(\omega),\, k_d(\omega)\right]^T$, where

$$k_p(\omega) = \frac{\cos\left(\frac{\mu\pi}{2} - \tau\omega\right)\Im\left\{\frac{Q(j\omega)}{P(j\omega)}\right\} - \sin\left(\frac{\mu\pi}{2} - \tau\omega\right)\Re\left\{\frac{Q(j\omega)}{P(j\omega)}\right\}}{\sin\left(\frac{\mu\pi}{2}\right)}, \tag{4.11a}$$

$$k_d(\omega) = -\frac{\cos(\tau\omega)\Im\left\{\frac{Q(j\omega)}{P(j\omega)}\right\} + \sin(\tau\omega)\Re\left\{\frac{Q(j\omega)}{P(j\omega)}\right\}}{\omega^{\mu}\sin\left(\frac{\mu\pi}{2}\right)}, \tag{4.11b}$$

defines a crossing point $\mathbf{k}(\omega) \in \mathcal{T}$.

Proof. Consider the characteristic equation (4.9). It is clear that all the crossing points $\mathbf{k} \in \mathcal{T}$ are given by the pairs $\mathbf{k} \in \mathbb{R}^2$ solving (4.9) for $s = j\omega$. Taking the real and imaginary part gives the following:

$$\Re\left[\Delta(j\omega; k_p, k_d)\right] = 0, \tag{4.12}$$

$$\Im\left[\Delta(j\omega; k_p, k_d)\right] = 0, \tag{4.13}$$

the solution of this system for k_p and k_d leads to (4.11a) and (4.11b) by using simple algebraic manipulations. Furthermore, from (4.11a) and (4.11b), it can be observed that $\mathbf{k}(\omega)$ is a real solution for $\omega \in \mathbb{R}_+$. Therefore, $\mathbf{k}(\omega)$ is a real solution for all $\omega \in \Omega_+$. $\square$

Proposition 4.0.2

Let $\mathbf{k}(\omega) \in \mathbb{R}^2$ be defined by (4.11). Then,

$$\lim_{\omega \to 0} \mathbf{k}(\omega) = \begin{bmatrix} -\frac{q_0}{p_0} \\ 0 \end{bmatrix}. \tag{4.14}$$

Proof. We have that

$$H(s) = \frac{Q(s)}{P(s)} = \frac{q_n s^n + q_{n-1} s^{n-1} + \cdots + q_1 s + q_0}{p_m s^m + p_{m-1} s^{m-1} + \cdots + p_1 s + p_0}, \tag{4.15}$$

evaluating in the boundary $s = j\omega$, we can write $Q(j\omega)$ and $P(j\omega)$ as follows

$$Q(j\omega) = Q^e(\omega) + j\omega Q^o(\omega), \tag{4.16}$$

$$P(j\omega) = P^e(\omega) + j\omega P^o(\omega), \tag{4.17}$$

where

$$\begin{aligned} Q^e(\omega) &= q_0 - q_2\omega^2 + q_4\omega^4 - \cdots, \\ Q^0(\omega) &= q_1 - q_3\omega^2 + q_5\omega^4 - \cdots, \\ P^e(\omega) &= p_0 - p_2\omega^2 + p_4\omega^4 - \cdots, \\ P^0(\omega) &= p_1 - p_3\omega^2 + p_5\omega^4 - \cdots. \end{aligned}$$

Hence

$$H(j\omega) = \frac{Q^e(\omega)P^e(\omega) + \omega^2 Q^o(\omega)P^o(\omega)}{P^e(\omega)^2 + \omega^2 P^o(\omega)^2} + j\frac{\omega\left(P^e(\omega)Q^o(\omega) - P^o(\omega)Q^e(\omega)\right)}{P^e(\omega)^2 + \omega^2 P^o(\omega)^2}, \tag{4.18}$$

the last equation describes how $\Im\left[H(j\omega)\right]$ and $\Re\left[H(j\omega)\right]$ are defined. Now, computing their limits as ω approaches 0 we obtain the following

$$\begin{aligned} \lim_{\omega \to 0} \Im\left[H(j\omega)\right] &= 0, \\ \lim_{\omega \to 0} \Re\left[H(j\omega)\right] &= \frac{q_0}{p_0}. \end{aligned}$$

Then, straightfordwardly we have that for $k_p(\omega)$

$$\lim_{\omega \to 0} k_p(\omega) = -\frac{q_0}{p_0}, \tag{4.19}$$

As mentioned. Now, for the case of $k_d(\omega)$ we start from the fact that for $\mu \in (0,1)$

$$\lim_{\omega \to 0} \omega^\mu = 0, \tag{4.20}$$

and here we have

$$\lim_{\omega \to 0} k_d(\omega) = \lim_{\omega \to 0} -\frac{1}{\omega^\mu}\frac{\cos\theta_1}{\sin\theta_2}\Im\left[H(j\omega)\right] + \lim_{\omega \to 0} -\frac{1}{\omega^\mu}\frac{\sin\theta_1}{\sin\theta_2}\Re\left[H(j\omega)\right], \tag{4.21}$$

here, we obtain limits in the indeterminated form $0/0$ which can be computed by means of the L'Hôpital's rule. An important observation tells us that

$$\frac{d\omega^\mu}{d\omega} = \mu\omega^{\mu-1} = \mu\frac{1}{\omega^{1-\mu}} \quad \forall \mu \in (0,1). \tag{4.22}$$

Therefore

$$\begin{aligned}
\lim_{\omega\to 0} -\frac{1}{\omega^{\mu}}\frac{\cos\theta_1}{\sin\theta_2}\Im\left[H(j\omega)\right] &= \lim_{\omega\to 0} -\frac{-\sin\theta_1\Im\left[H(j\omega)\right]+\cos\theta_1\frac{d}{d\omega}\Im\left[H(j\omega)\right]}{\mu\frac{1}{\omega^{1-\mu}}\sin\theta_2}\\
&= \lim_{\omega\to 0} -\frac{-\omega^{1-\mu}\sin\theta_1\Im\left[H(j\omega)\right]+\omega^{1-\mu}\cos\theta_1\frac{d}{d\omega}\Im\left[H(j\omega)\right]}{\mu\sin\theta_2}\\
&= 0+\lim_{\omega\to 0} -\frac{\omega^{1-\mu}\cos\theta_1\left(A\frac{dB}{d\omega}-B\frac{dA}{d\omega}\right)}{\mu\sin\theta_2 A^2}\\
&= 0.
\end{aligned}$$

Where

$$\begin{aligned}
A &= P^e(\omega)^2+\omega^2P^o(\omega)^2,\\
B &= \omega\left(P^e(\omega)Q^o(\omega)-P^o(\omega)Q^e(\omega)\right).
\end{aligned}$$

A similar analysis for the rightmost term in Eq. (4.21) give us that

$$\lim_{\omega\to 0} k_d(\omega)=0. \tag{4.23}$$

$\square$

Remark 4.0.4. *Proposition 4.0.2 grant us to conclude that the initial crossing point of* $\mathbf{k}(\omega)$ *is at a* $\mathbf{k}^* = \left[-\frac{q_0}{p_0}, 0\right]$*, which helps to build the stability region charts and to stablish restrictions in Algortihm 1.*

Real crossing curves (RCC)

Proposition 4.0.3: Real Crossing Curves

Let $\tau\in\mathbb{R}^+$ be a fixed value. Then, $\mathbf{k}_0$ belongs to the stability crossing curve, where $\mathbf{k}_0$ is the line with coordinates given by

$$\mathbf{k}_0 := \begin{bmatrix} -\frac{q_0}{p_0} \\ k_d \end{bmatrix}, \tag{4.24}$$

with $k_d\in\mathbb{R}$. Furthermore, this corresponds to a crossing through the origin of the complex plane.

Proof. By taking $s=0$ in (4.9), we have

$$\begin{aligned}
\Delta(0;k_p,k_d) &= 0,\\
\leftrightarrow \frac{q_0}{p_0}+k_p &= 0.
\end{aligned}$$

Then, $k_p=-\frac{q_0}{p_0}$ for every $k_d\in\mathbb{R}$ which gives (4.24). Finally, it can be observed that $\mathbf{k}_0$ is a real solution for $\omega=0$. Therefore, $\mathbf{k}_0$ is a crossing point $\mathbf{k}\in\mathcal{T}$. $\square$

Remark 4.0.5. *We can find equivalent stability crossing curves to Propositions 4.0.1 and 4.0.3, by substituting* $w=(j\omega)^{\alpha}$ *in the w-transformed characteristic equation of* (4.9).

Given all the crossing points $\mathbf{k}$ and the crossing-frequency set Ω, we can define each stability crossing curve through its continuity, as follows,

$$\mathcal{T}_0 := \left\{[-q_0/p_0, k_d]^T \in \mathbb{R}^2 | k_d \in \mathbb{R}\right\}, \tag{4.25}$$

$$\mathcal{T}_\omega := \left\{\mathbf{k}(\omega) \in \mathbb{R}^2 | \omega \in \Omega_+\right\}. \tag{4.26}$$

Then, it is evident that

$$\mathcal{T} = \mathcal{T}_\omega \bigcup \mathcal{T}_0. \tag{4.27}$$

Crossing Directions

The results presented in Propositions 4.0.1-4.0.3 enable us to determine the values of k_p and k_d for which a crossing root exists, but do not give any information on their crossing direction. Thus, in order to characterize regions according to their number of unstable roots, we must make a distinction between switches (crossing towards instability) and reversals (crossing towards stability), and carry out a careful accounting of the unstable roots in each region.

Proposition 4.0.4: Crossing Directions

Consider the w-transformed characteristic equation $\Delta\left(w; kp^*, kd^*\right)$, where $w = s^{1/v}$. Then, one root of Δ will cross through w^* from the left to the right of the $\Gamma-$boundary as $\mathbf{k}$ crosses the stability crossing curve $\mathcal{T}$ through $\mathbf{k}^*$, in the increasing direction of k_χ for $\chi \in \{p, d\}$ if:

$$S_\chi > 0, \tag{4.28}$$

where S_χ is defined as

$$S_\chi := \langle \Gamma_\chi, \hat{\boldsymbol{u}} \rangle, \tag{4.29}$$

with Γ_χ and $\hat{\mathbf{u}} \in \mathbb{R}^2$ are defined as:

$$\Gamma_\chi = \begin{bmatrix} \Re\left\{ \left.\frac{dw}{dk_\chi}\right|_{(w^*, \mathbf{k}^*)} \right\} \\ \Im\left\{ \left.\frac{dw}{dk_\chi}\right|_{(w^*, \mathbf{k}^*)} \right\} \end{bmatrix}, \hat{\boldsymbol{u}} = \begin{bmatrix} \sin(\frac{\pi}{2v}) \\ -\cos(\frac{\pi}{2v}) \end{bmatrix}. \tag{4.30}$$

Proof. Let $\chi \in \{p, d\}$, w^* be a point on the $\Gamma-$boundary and let $\mathbf{k}^*$ be the corresponding gain. Thus, it is clear to see that a solution $w\left(\mathbf{k}\right)$ will cross from the LHP to the RHP of the $\Gamma-$boundary in the increasing direction of k_χ if the following inequality holds:

$$\Re\left\{ e^{j\frac{v-1}{2v}\pi} \frac{dw}{dk_\chi} \right\} > 0.$$

Now, by the *Implicit Function Theorem* we know that

$$\frac{dw}{dk_\chi} = -\frac{\frac{\partial \Delta}{\partial k_\chi}}{\frac{\partial \Delta}{\partial w}}.$$

Let us define

$$\alpha + j\beta := \left.\frac{dw}{dk_\chi}\right|_{(w^*,\mathbf{k}^*)},$$

and observe that

$$e^{j\frac{v-1}{2v}\pi} = \sin\left(\tfrac{\pi}{2v}\right) + j\cos\left(\tfrac{\pi}{2v}\right).$$

Thus, the proof follows straightforwardly by noticing that

$$\Re\left\{(\alpha + j\beta)\left(\sin\left(\tfrac{\pi}{2v}\right) + j\cos\left(\tfrac{\pi}{2v}\right)\right)\right\} \equiv \langle \Gamma_\chi, \hat{\boldsymbol{u}}\rangle .$$

□

Corollary 4.0.1

Let $u = 1$ and $k_d \neq 0$ then one root of the characteristic equation (4.9) will cross from the LHP to the RHP of the complex plane through the origin as $\mathbf{k}$ crosses the stability crossing curve $\mathcal{T}_0$, in the increasing direction of k_p if:

$$k_d < 0, \tag{4.31}$$

otherwise, it will cross from the RHP to the LHP.

Proof. We have to compute the crossing direction S_p when $\omega = 0$. In this fashion, from the fact that (4.9) is equivalent to the w-transformed characteristic equation at $s = 0$. Then, for $w \in \mathbb{C}$ we can express (4.9) as

$$\Delta_r(w, k_p, k_d) := \frac{Q(w)}{P(w)} + (k_p + k_d w^u)e^{-w^v\tau} = 0. \tag{4.32}$$

Now, according to the *Implicit function theorem*, we know that

$$\tfrac{dw(k_p,k_d)}{dk_p} = -\left(\tfrac{\partial\Delta_r(w,k_p,k_d)}{\partial k_p}\right) / \left(\tfrac{\partial\Delta_r(w,k_p,k_d)}{\partial w}\right), \tag{4.33}$$

where

$$\tfrac{\partial\Delta_r(w,k_p,k_d)}{\partial k_p} = e^{-w^v\tau}, \tag{4.34}$$

$$\tfrac{\partial\Delta_r(w,k_p,k_d)}{\partial w} = \tfrac{P(w)Q'(w)-Q(w)P'(w)}{P(w)^2} + k_d u w^{u-1}e^{-\tau w^v} - v\tau w^{v-1}e^{-\tau w^v}\left(k_d w^u + k_p\right), \tag{4.35}$$

and the condition

$$\tfrac{\partial\Delta_r(0,k_p,k_d)}{\partial w} \neq 0, \tag{4.36}$$

must be satisfied in order to compute $\frac{dw(k_p,k_d)}{dk_p}|_{w=0}$.

From the fact that $\mu := \frac{u}{v} \in (0,1)$ and $u, v \in \mathbb{N}$ where $v > u$. Condition (4.36) is satisfied for $k_d \neq 0$ if and only if $u = 1$. Then, for $k_d \neq 0$ and $u = 1$ we have that

$$\left.\tfrac{dw(k_p,k_d)}{dk_p}\right|_{w=0} = -\left(\tfrac{\partial\Delta_r(0,k_p,k_d)}{\partial k_p}\right) / \left(\tfrac{\partial\Delta_r(0,k_p,k_d)}{\partial w}\right) = -\tfrac{1}{k_d}, \tag{4.37}$$

consequently

$$\operatorname{sgn}\left[\left.\tfrac{dw(k_p,k_d)}{dk_p}\right|_{w=0}\right] = \operatorname{sgn}\left[-k_d\right]. \tag{4.38}$$

By (4.38) we derive (4.31), which completes the proof. □

Remark 4.0.6. *By Corollary 4.0.1 we conclude that the w-transformed characteristic equation (4.32) has a root at the origin with multiplicity of at least u. Hence, for $k_d \neq 0$ and $u > 1$ we should derive at least u-times such a characteristic equation to find $\Delta_r(0, k_p, k_d) \neq 0$. Furthermore, for $k_d, k_p = 0$ it has a root at the origin with multiplicity of at least v.*

Stability index determination

Let $\mathbf{k}^\star := \left[k_p^\star, k_d^\star\right]^T$ to be a chosen point on the $k_p - k_d$ parameters plane such that $\mathbf{k}^\star \notin \mathcal{T}$ and η the invariant number of roots in a given region of the parameter space. Besides, let η_0 be the number of roots for $\mathbf{k} = [0, 0]^T$. We propose a linear path for $\mathbf{k}$ from the origin (at which $\eta = \eta_0$) to $\mathbf{k}^\star$. Let us define the set Ω_s as the set of all $\omega \in \Omega$ for which the vector $\mathbf{k}^\star$ intersects $\mathcal{T}_\omega$. This set corresponds to all $\omega \in \Omega$ such that the following expression holds

$$k_p^\star k_d(\omega) - k_d^\star k_p(\omega) = 0, \tag{4.39}$$

and satisfies at least one of the following conditions:

$$0 \leq \frac{k_p(\omega)}{k_p^\star} < 1, \qquad 0 \leq \frac{k_d(\omega)}{k_d^\star} < 1. \tag{4.40}$$

Besides, there can only exist an intersection between $\mathbf{k}^\star$ and $\mathcal{T}_0$ if and oly if (4.24) holds for $\mathbf{k} = \epsilon\mathbf{k}^\star$ where $\epsilon \in (0, 1)$. This brings to the definition of the indicative function $\mathcal{J}_\epsilon$ as follows

$$\mathcal{J}_\epsilon := \begin{cases} 1 & \text{if } \epsilon \in (0,1), \\ 0 & \text{if } \epsilon \notin (0,1), \end{cases} \tag{4.41}$$

where ϵ is computed as

$$\epsilon = -\frac{q_0}{k_p^\star p_0} \quad \forall \quad k_d^\star \in \mathbb{R}. \tag{4.42}$$

$\mathcal{J}_\epsilon$ establishes the existence of an intersection between $\mathbf{k}^\star$ and $\mathcal{T}_0$ if and only if $\mathcal{J}_\epsilon = 1$.

The situation when $\mathcal{T}_\omega$ or $\mathcal{T}_0$ crosses at the origin of the parameter space, is related to the existence of roots on the imaginary axis of the open-loop characteristic equation. Such a case must be treated separately, and for that reason we define the sets Ω_{c_0} and Ω_{c_+}, as

$$\Omega_{c_0} := \{\omega \in \{0\} \quad | \quad Q(j\omega) = 0\}\,. \tag{4.43}$$

and the set

$$\Omega_{c_+} := \{\omega \in \Omega_+ \quad | \quad Q(j\omega) = 0\}\,. \tag{4.44}$$

Finally, considering Proposition 4.0.4 and Corollary 4.0.1; we construct the functions ∇ and ∇_0 as

$$\nabla_0(\mathbf{k}) \quad := \quad \operatorname{sgn}(-k_d) \tag{4.45}$$

$$\nabla(\mathbf{k}, \omega) \quad := \quad \operatorname{sgn}(S_\chi), \tag{4.46}$$

it is neccesary that $\mu = \alpha$ to use expression (4.45).

According to Proposition 4.0.2 the origin of the parameter-space place $\mathbf{k} = [0, 0]$ can be located as in the three cases depicted in Figs. 4.2, 4.3 and 4.4.

Based on the previous lines, consider the following result:

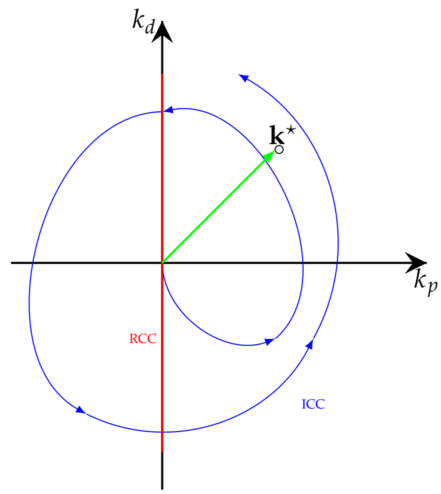

Figure 4.2: Position of the point $\mathbf{k} = [0,0]^T$. Case (i)

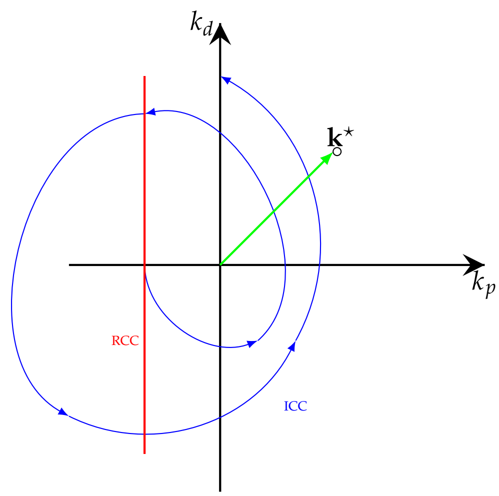

Figure 4.3: Position of the point $\mathbf{k} = [0,0]^T$. Case (ii)

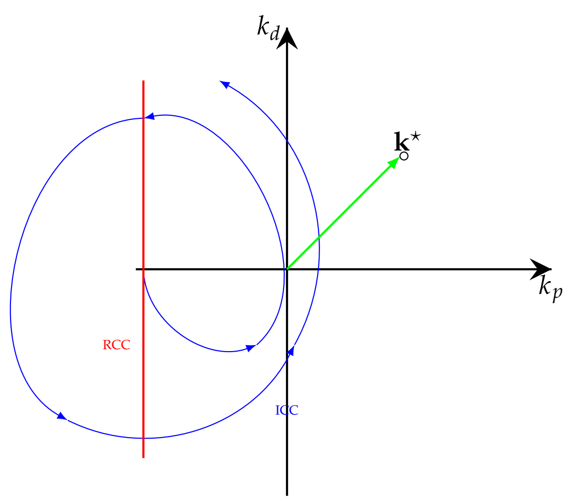

Figure 4.4: Position of the point $\mathbf{k} = [0,0]^T$. Case (iii)

Proposition 4.0.5

Let G be a transfer function defined as (4.4) with $\deg Q > \deg P$, $\tau \in \mathbb{R}^+$ and $\mu = \alpha$ be fixed values and let $\mathbf{k}^\star := \left[k_p^\star, k_d^\star\right]^T \in \mathcal{R}^\star \subset \mathbb{R}^2$ such that $\mathbf{k}^\star \notin \mathcal{T}$. If $\Omega_{c_0} = \emptyset$, then $\forall \quad \mathbf{k} \in \mathcal{R}$ the number of roots η on the RHP of the complex plane of the w-transformed of (4.9) can be computed by

$$\eta = \eta_0 + \mathcal{J}_\epsilon \nabla_0(\mathbf{k}) + 2 \sum_{\omega \in \Omega_s} \nabla(\mathbf{k}, \omega), \tag{4.47}$$

besides, when $\Omega_{c_0} \neq \emptyset$

$$\eta = \eta_0 + \nabla_0(\delta \mathbf{k}^\star) + 2\,\mathrm{sgn}(\omega) \sum_{\omega \in \Omega_s} \nabla(\mathbf{k}, \omega), \tag{4.48}$$

where $\delta \approx 0$.

Proof. Consider the fixed values $\mathbf{k}^\star$, η_0 and ϵ, as well as he sets Ω_s, Ω_t, Ω_{c_0} and Ω_{c_+}, and the functions $\mathcal{J}_\epsilon$, $\nabla_0(\mathbf{k})$ and $\nabla(\mathbf{k}, \omega)$, as defined above.

In order to determine η, we need to observe the behaviour of the roots of the w-transformed characteristic equation of (4.9) as $\mathbf{k}$ varies from the origin to $\mathbf{k}^*$. As we have shown in Figs. 4.2, 4.3 and 4.4, we have three possible escenarios for locating $\mathbf{k} = [0, 0]^T$ into the parameters space D-partition. These escenarios are of interest to analyze the behaviour of the roots as $\mathbf{k}$ varies along the vector $\mathbf{k}^*$, such escenarios can be described as follows:

(i) The point $\mathbf{k} = [0, 0]^T$ is located at the stability crossing curve formed by $\mathcal{T}_0 \cap \mathcal{T}_\omega$.

(ii) The point $\mathbf{k} = [0, 0]^T$ is not at $\mathcal{T}$.

(iii) The point $\mathbf{k} = [0, 0]^T$ is at $\mathcal{T}_\omega$.

Evidently, for case (ii) $\eta = \eta_0$ at $\mathbf{k} = 0$. Then starting from such a point, we can analyze the behaviour of the roots when $\mathbf{k}$ varies along the vector $\mathbf{k}^\star$ by means of (4.47).

Now, for case (iii) because (4.40) consider the case when $\mathbf{k} = \left[k_p(\omega), k_d(\omega)\right]^T = 0$ we can use (4.47) yet for this case. Finally for case (i), because $\mathbf{k} = 0 \in \mathcal{T}_0 \cap \mathcal{T}_\omega$ we can analyze the crossing direction by choosing a $\mathbf{k} = \delta \mathbf{k}^\star$ in ∇_0 and not considering ∇ in $\omega = 0$. This completes the proof. $\square$

Definition 4.0.3: Stability Region

The stability region in the parameter space $k_p - k_d$ is the set of all $\mathbf{k} \in \mathcal{R} \subset \mathbb{R}^2$ such that the number of roots in the RHP of the complex plane $\eta = 0$.

Characterization of stability regions algorithm

In the spirit of deriving an algorithm to characterize the stability regions by a number of unstable roots (invariant in each region), let's assume that we have $\ell-$regions $\mathcal{R}_1$, $\mathcal{R}_2, \ldots, \mathcal{R}_\ell$, with $\ell \geq 2$. Without any loss of generality, assume that $\mathcal{R}_1$ and $\mathcal{R}_2$ are the first two neighboring regions (relabeled if necessary) of interest (for instance, closest to the origin), let $\mathbf{k}^{(j)}$ be a point on the boundary of regions $\mathcal{R}_j$ and $\mathcal{R}_{j+1}$ and N_j denote the number of roots of (4.9) for $\mathcal{R}_j$. S_χ corresponds to the crossing direction sign (pointing in the increasing direction) passing through a given $\mathbf{k}^{(j)}$ found by means of Proposition 4.0.4. Then, we have the algorithm described in 1.

Algorithm 1: Stability Regions Characterization

Input: $\ell \in \mathbb{N}$ regions with $\ell \geq 2$, r roots of $Q(s)$ in the RHP
Output:

```
StabilityRegionsC(ℓ,r,𝒯_ω)
j := 0
N_0 := 0
k^(0) := [0,0]^T
if (k^(0) ∈ 𝒯_ω) then
    if (k^(0) ∈ 𝒯_0) then
        Select k^(0) := [0,k*_d] where k*_d ≠ 0
        N_0 := r − sgn(k*_d)
    else
        N_0 = r + 2 sgn(S_χ)
else
    N_0 := r
repeat
    Compute S_χ for k^(j+1)
    if (k^(j+1) ∉ 𝒯_0) then
        N_{j+1} := N_j + 2 sgn(S_χ)
    else
        Choose a k*_d ≠ 0 such that k^(j+1) := [−q_0/p_0, k*_d]
        N_{j+1} := N_j − sgn(k*_d)
    j := j + 1
until (j ⩾ ℓ)
```

Remark 4.0.7. *Algorithm 1, describes a step by step process of analyzing the root crossing directions to identify the stability region. This process has been summarized with expresions (4.47) and (4.48) in Proposition 4.0.5.*

Fragility of Fractional$-PD^{\mu}$ Controllers

An important issue in control design is the analysis concerning to the control fragility which give a measure of the robustness of the closed-loop system against parametrical uncertainties in the control gains. This consists of computing the maximum controller parameters deviation d of a given stabilizing controller $\bar{\mathbf{k}} := (\bar{k}_p, \bar{k}_d)^T$, such that the closed-loop system remains stable, as long as the controller parameters $\mathbf{k}$ satisfy the inequality:

$$\sqrt{(k_p - \bar{k}_p)^2 + (k_d - \bar{k}_d)^2} < d. \tag{4.49}$$

In order to address this problem, let $\mathbf{k}(\omega) = \left[k_p(\omega), k_d(\omega)\right]^T$ as given in Proposition 1 and the function $\xi : \mathbb{R}^+ \to \mathbb{R}^+$ to be defined as

$$\xi(\omega) := \sqrt{(k_p(\omega) - \bar{k}_p)^2 + (k_d(\omega) - \bar{k}_d)^2}. \tag{4.50}$$

We have the following:

Proposition 4.0.6: Fragility Determination

Let $\bar{\mathbf{k}}$ be a stabilizing controller. Then, the maximum parameter deviation d of $\mathbf{k}$, such that the closed-loop system remains stable, is given by

$$d := \min\{\tilde{d}, d_0\}, \tag{4.51}$$

where $\tilde{d}$ and d_0 are given by:

$$\tilde{d} := \min_{\omega \in \Omega_f} \{\xi(\omega)\}, \tag{4.52}$$

$$d_0 := \tfrac{q_0}{p_0} + \bar{k}_p, \tag{4.53}$$

where Ω_f denote the set of all roots of $f(\omega)$ defined as

$$f(\omega) := \left\langle \mathbf{k}(\omega) - \bar{\mathbf{k}}, \tfrac{d\mathbf{k}(\omega)}{d\omega} \right\rangle. \tag{4.54}$$

Proof. By assumption, $\bar{\mathbf{k}}$ is located inside some stability region delimited by some appropriate stability crossing curves, thus, the closed-loop system is unstable if the controller $\bar{\mathbf{k}}$ has a parameter deviation such that it crosses for at least one of its boundaries. Therefore, the objective is to compute the minimal distances between $\bar{\mathbf{k}}$ and the different boundaries of the stability region. In order to compute the minimal distance between a point $\bar{\mathbf{k}}$ and the stability crossing curves with $\omega \neq 0$, we need to identify the points $\mathbf{k}(\omega)$ at which the tangent vectors to the curve are orthogonal to $\mathbf{k}(\omega) - \bar{\mathbf{k}}$. In other words, to find points in which ω is a root of (4.54). Therefore, the minimum distance $\tilde{d}$ to a stability crossing curve with $\omega \neq 0$ is given by (4.52). In addition, we can note that the boundaries of the stability crossing curve related to $\omega = 0$ are described by (4.24). Thus, the minimum distance to this line can be computed as follows:

Substituting (4.24) in (4.50) leads to

$$\xi(0) = \sqrt{(\tfrac{q_0}{p_0} + \bar{k}_p)^2 + (k_d - \bar{k}_d)^2}, \tag{4.55}$$

the gain k_d at which $\xi(0)$ attains its minimum, is given by the solution of the following equation:

$$\tfrac{d\xi^2(0)}{dk_d} = 2k_d - 2\bar{k}_d = 0. \tag{4.56}$$

Then, this value is defined as d_0 and can be obtained by substituting the solution of (4.56) into (4.55). Finally, the proof ends by noticing that the minimal distance d can be computed by means of (4.51). $\square$

Numerical and Experimental Results

Inverted Pendulum

Consider the linear normalized transfer function of an inverted pendulum given by

$$G(s) = \frac{e^{-s\tau}}{s^2 - 1}, \tag{4.57}$$

where we consider a delayed input u as the acceleration of the pivot and the output as the pendulum angle θ.

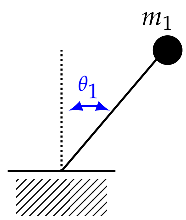

Figure 4.5: Inverted pendulum.

Now, in order to illustrate the proposed results we analyze the system subject to the PD^{μ} controller given by (4.6). First, we found the ICC and the RCC of the closed-loop system by following Propositions 4.0.1 and 4.0.3. Next, by using the w-transformation of the closed-loop characteristic polynomial we apply Proposition 4.0.4 to compute the crossing directions. Finally, in order to ilustrate how Proposition 4.0.4 in conjunction with Algorithm 1 can be used to identify the stability regions avoiding unnecessary computations let us consider the points $\mathbf{k}^{(1)}$, $\mathbf{k}^{(2)}$, $\mathbf{k}^{(3)}$ and $\mathbf{k}^{(4)}$ of the parameter space, besides, the fixed parameters $\mu = 1/5$ and $\tau = 1/7$ (sec.). The results are summarized in Fig. 4.6 and Table .

Crossing Directions

Point	k_p	k_d	ω	$\mathbf{x}$	$S_{\mathbf{x}}$	sgn
$\mathbf{k}^{(1)}$	0.9455	0.154703	0.237682	p	0.536718	+
$\mathbf{k}^{(2)}$	1.053	0.629733	0.797508	d	-0.00946026	-
$\mathbf{k}^{(3)}$	1.053	2.03733	1.491597	d	0.00333839	+
$\mathbf{k}^{(4)}$	0.8391	2.92063	1.75329	d	0.00503787	+

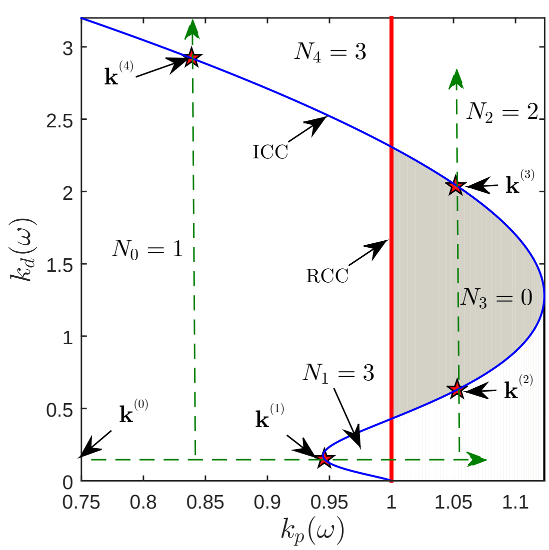

Figure 4.6: Crossing Directions Analysis.

First order time delay system

Consider the first order time delay system described by

$$G(s) = \frac{k}{Ts+1}e^{-sL}, \tag{4.58}$$

where k represents the steady-state gain of the plant, L represents the time delay, and T represents the time constant of the plant taken from (Caponetto, 2010).

This simple system region stability canbe analyzed by means of Proposition 4.0.4 to obtain the red-shaded region shown in figure 4.7.

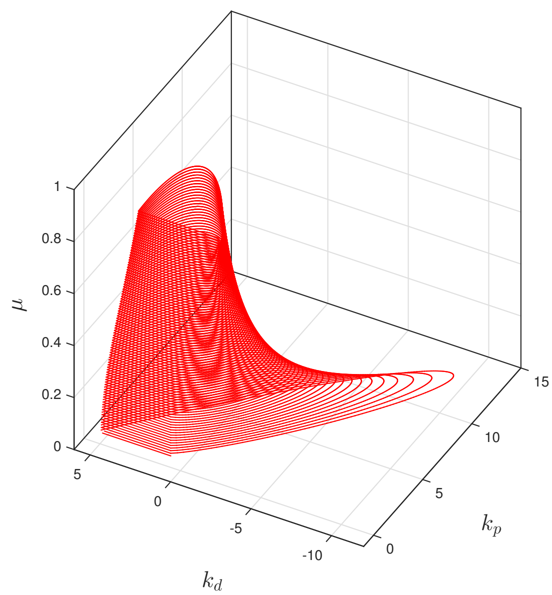

Figure 4.7: Stability region fractional order PD^μ controller for $k=1$, $T=2$ and $L=1.2$.

Fractional order system with time delay

Consider the fractional order system taken from (Hamamci, 2008) adding a constant time delay τ

$$G(s) = \frac{s^{3.8}+2s^{2.8}+39s^{1.9}+48s^{1.1}-4}{s^5+2s^{4.1}+31s^{3.1}+35s^{2.2}+49s^{0.9}+92}e^{-s\tau}. \tag{4.59}$$

Let $\tau = 0.5$seg and $\mu = 0.5$. By using Proposition 4.0.4 we obtain the results shown in Fig. 4.8.

Networked mechanical system

Its demostrated that the inifite binary tree of springs and dampers shown in Fig. 4.9 has a fractional order behaviour.(Goodwine, 2016) Besides, this scheme can be used to represent the interactions in a robot formation. The fractional dynamics of the netwoked mechanical system is proved to be valid for at least 4 generations in the binary tree (Leyden and Goodwine, 2016).

Acording to (Goodwine, 2016) the transfer function relating the last position $x_{last}(t)$ with the first position $x_{1,1}(t)$ in Fig. 1.8 when adding a constant time delay τ is given by

$$G(s) = \frac{\sqrt{kb}}{m_{last}s^{1.5}+\sqrt{kb}}e^{-s\tau}. \tag{4.60}$$

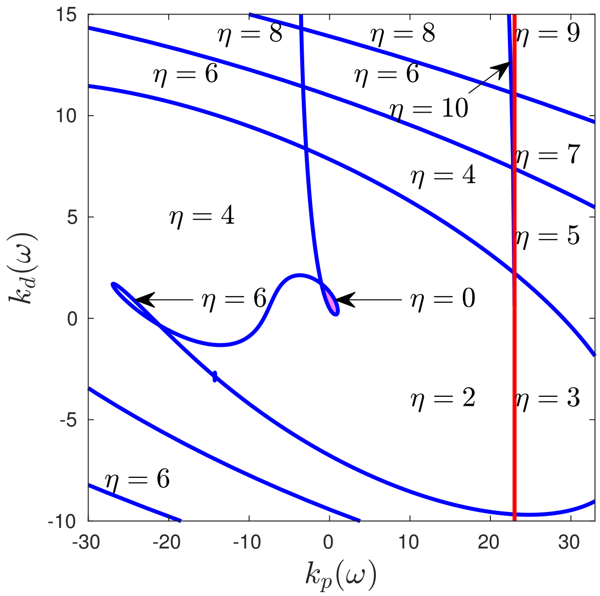

Figure 4.8: Stability region analysis for system (4.59).

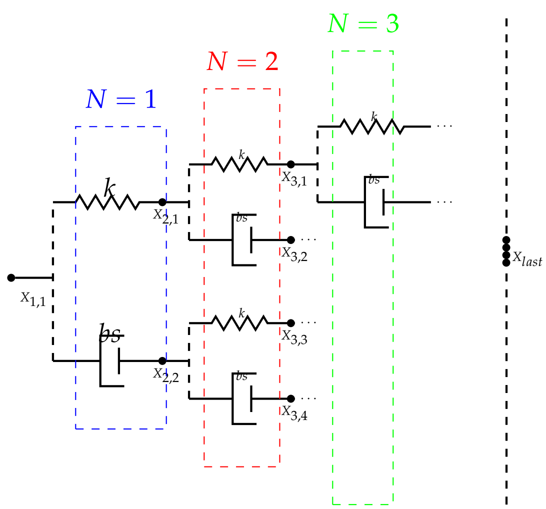

Figure 4.9: Networked mechanical system.

We aim to design a fractional PD^{μ} controller to system (4.60). Hence, we can write the closed-loop w-transformed characteristic equation as

$$\Delta(w, k_p, k_d) := m_{last} w^3 + \sqrt{kb} + \sqrt{kb} e^{-w^2 \tau} \left(k_p + k_d w\right) \tag{4.61}$$

Now by means of Proposition 4.0.5, consider the points $\mathbf{k}_1$ and $\mathbf{k_2}$ which are the points where the choosen vector $\mathbf{k}^{\star}$ crosses to $\mathcal{T}$. Because, $\mathbf{k} = [0,0]^T \notin \mathcal{T}$ we deal with case (ii) of Fig. 4.3 and hence we can use expression (4.47) to find the number of roots η in the RHP of the complex plane for each enclosed region of

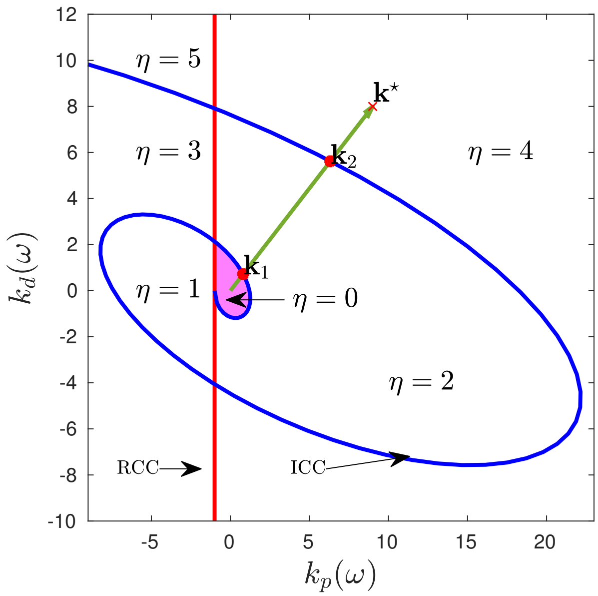

Figure 4.10: Stability region detection for networked mechanical system.

the parameter space. The results can be seen in the following picture:

Fractional PI^λ controller design

Consider now Problem 2. To apply the same ideas discussed for the PD^μ controller design we have to consider the following:

Note 4.0.1: System restrictions

The fractional w-transformed closed-loop characteristic equation when using the PI^λ-controller is given by

$$\Delta_t(w; k_p, k_d) = \frac{Q(w)}{P(w)} + e^{-\tau w^v} \left(k_p + k_i w^{-u}\right) = 0. \tag{4.62}$$

Then, by multiplying (4.62) by w^u we get

$$\Delta_t(w; k_p, k_d) = \frac{Q(w) w^u}{P(w)} + e^{-\tau w^v} \left(k_p w^u + k_i\right) = 0, \tag{4.63}$$

which, when $k_p = k_i = 0$ shows to have a zero of multiplicity u at the origin. For the actual algorithm the following system restrictions must be considered

1. $u = 1$.
2. $Q((j\omega)^\alpha) > 0$ for $\omega = 0$.
3. $|P((j\omega)^\alpha)| > 0\ \forall \omega \in \mathbb{R}$.
4. if $Q((j\omega^*)^\alpha) = 0$, then $|Q'((j\omega^*)^\alpha)| > 0$, $\omega^* \in \mathbb{R} \backslash \{0\}$).

Hence, even when we are talking about a PI^{λ} controller our methods discussed for PD^{μ} controllers design can be also applied to this type of controllers as we will see in further applications and so we will not write the same statements declared for fractional PD^{μ} controllers using the PI^{λ} controller.

5
Practical applications of fractional-order controllers

Fractional PD^{μ} Controller for Transparent Bilateral Control Scheme for Local Teleoperating System

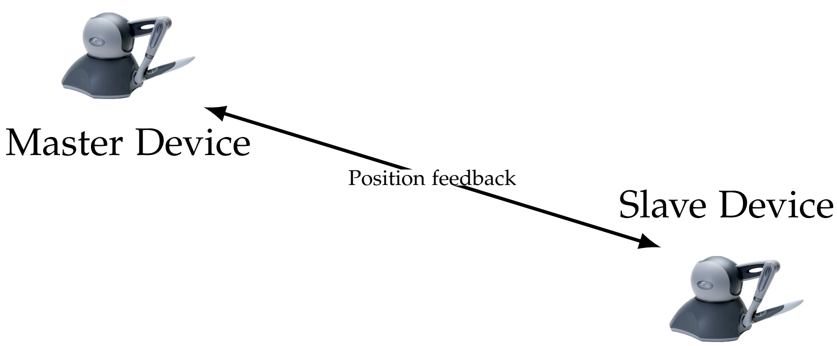

Figure 5.1: Conceptual Control Scheme for local teleoperating system.

Influenced by the contributions of (Liacu et al., 2013) and (Tavakoli et al., 2003), we outline in this example a bilateral control scheme using two Phantom Omni Haptic devices (see, Fig. 5.1) whose dynamics can be described as a decoupled time-invariant linear model formed by three mechanical admittances of each joint given by:

$$P(s) := \frac{\Theta(s)}{\Lambda(s)} = \frac{1}{s(ms+b)}. \tag{5.1}$$

where each mechanical admittance $P(s)$ is described by the transfer function from each torque input $\Lambda(s)$ to its respectively angular position $\Theta(s)$ and depicts the behavior of each mechanical joint. The main goal of the proposed control scheme is to achieve a perfect bilateral position tracking under the interaction of the exogenous forces of the human and the remote environment on the master and slave device, respectively.

The bilateral control scheme proposed is shown in Fig. 5.1 and 5.2 where τ_p is considered as the delay due to signal processing, Λ_h and Λ_ℓ are the exogenous torques related to the human operator and the remote environment, respectively. P_M and P_S are the mechanical admittances of the master and the slave device, respectively: furthermore, a similar notation is used for the controllers C_M and C_S and the angular positions Θ_M and Θ_S. This scheme is a variation presented in (Hernández-Díez et al., 2016) of the one used in (Liacu et al., 2013) for haptic-virtual systems, however here, instead of using a PD or a $P-\delta$ controller, a fractional-PD^{μ} controller is proposed.

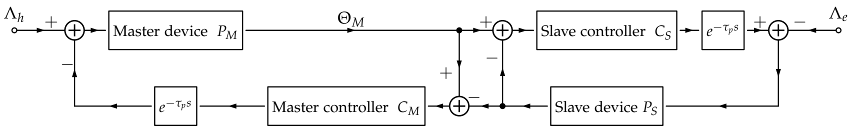

Figure 5.2: Control diagram of the bilateral control scheme.

From (Hernández-Díez et al., 2016), the characteristic equation of the closed-loop system can be written as follows:

$$2P(s)C(s)e^{-\tau_p s} + 1 = 0 \tag{5.2}$$

Stability Analysis

In the sequel, whitout any loss of generality, we can say that the analysis presented in this paper can be used in any of the decoupled time-invariant systems of each joint (5.1). The characteristic function $\Delta : \mathbb{C} \to \mathbb{C}$, of the system (5.2) can be rewritten as:

$$\Delta(s; k_p, k_d) := ms^2 + bs + 2e^{-\tau_p s}\left(k_p + k_d s^{\mu}\right). \tag{5.3}$$

The system parameters are taken from (Hernández-Díez et al., 2016), where the estimated used delay is $\tau_p = 0.001$ seconds and considering only Joint 1 for the sake of brevity, its parameters are $m = 0.0131$ and $b = 0.0941$. Then, we have the following:

Stability crossing curves

Let $\theta_1, \theta_2, \theta_3 \in \mathbb{R}$ here to be defined as $\theta_1 := \tau\omega$, $\theta_2 := \frac{\mu\pi}{2}$, and $\theta_3 := \frac{\pi\mu}{2} - \tau\omega$, respectively. Then by using the ideas of Proposition 4.0.3 we find that the RCC is given by

$$k_p = 0, \tag{5.4}$$

and using steps in Proposition 4.0.1 the ICC is described by:

$$\begin{aligned} k_p(\omega) &:= \frac{1}{2}\omega(\cos(\theta_1)(b\cot(\theta_2) + m\omega) + \sin(\theta_1)(b - m\omega\cot(\theta_2))), \\ k_d(\omega) &:= \frac{1}{2}\omega^{1-\mu}\csc(\theta_2)(m\omega\sin(\theta_1) - b\cos(\theta_1)). \end{aligned}$$

Crossing Directions

Following the procedure given by Proposition 4.0.4 we show a simulation in Fig. 5.3 of the S_χ behavior when changing the parameters k_p or k_d and its correspondent $k_p - k_d$ parameters plot.

By inspection of $\mathrm{sgn}(S_\chi)$, we conclude that the $k_p - k_d$ parameters stability region corresponds to the gray shaded region in Fig. 5.4.

Fragility

Using the scheme given by Proposition 4.0.6 we chose two stabilizing controllers $\mathbf{k}_1^*$ and $\mathbf{k}_2^*$ and show the results in Fig. 5.4 and Table , respectively:

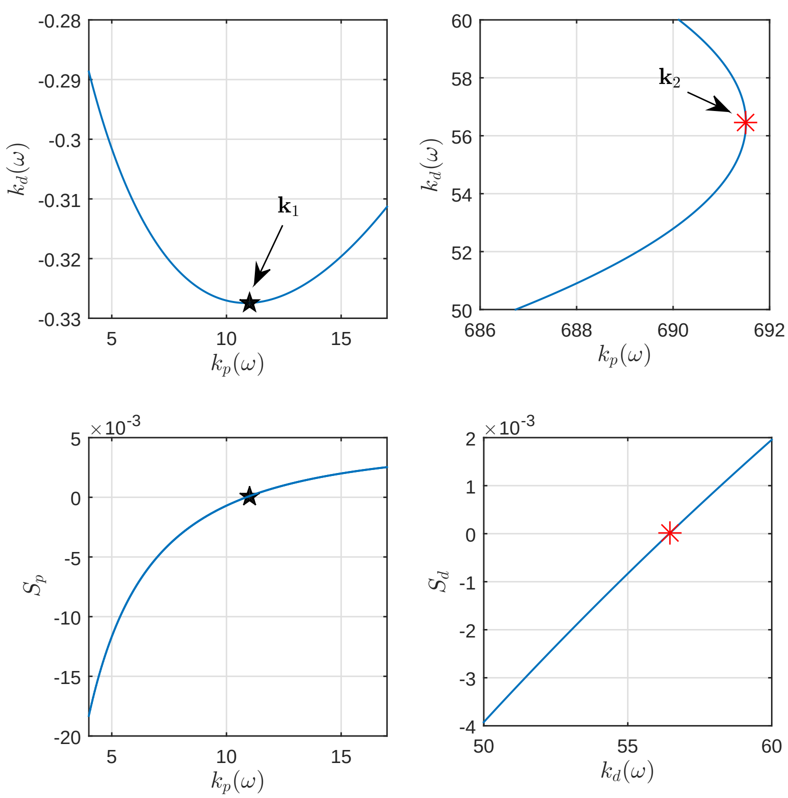

Figure 5.3: Stability region analysis for Joint 1. $\mathbf{k}_1$ and $\mathbf{k}_2$ are the points where condition (4.28) starts to hold.

Fragility Results						
$\mathbf{k}$	k_p	k_d	ω	d_ℓ	d_0	d
$\mathbf{k}_1^*$	100	80	$\{129.638, 531.717, 775.909\}$	59.0678	100	59.0678
$\mathbf{k}_2^*$	600	60	$\{415.574, 633.24, 531.7041\}$	26.4114	600	26.4114

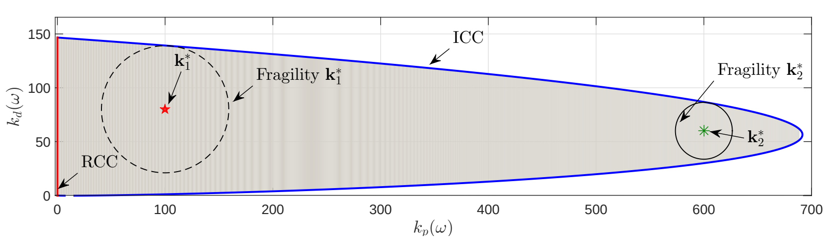

Figure 5.4: Stability Region for Joint 1.

Experimental results

See audiovisual evidence: `https://youtu.be/AwWq6prKfbw`

In order to illustrate how the PD^μ controller works experimentally, we use the transparent bilateral control scheme example in a experimental setup implemented by means of two Phantom Omni devices and the Matlab-Simulink toolkits Phansim (Mohammadi et al., 2008) and

Ninteger (Valerio and da Costa, 2004). Now, using the stability analysis, we show the control response taking $\mu = 0.5$ and the controller's gains as $\mathbf{k} = [5, 1]^T$, $\mathbf{k} = [11, 2]^T$ and $\mathbf{k} = [5, 0.5]^T$ for the joint one, two and three, respectively. Furthermore, we propose an experimental test perceiving a plastic sphere. This test consists of manipulating the master device in order to "feel" the plastic sphere in a remote environment, where the slave device is located. The experimental results are illustrated in Fig. 5.5, which shows how the control scheme implemented drives the trajectory of the master device which is also guided by the human operator but restricted by the plastic sphere. Fig. 5.6 illustrates the same experiment but using a classical PD controller with $\mathbf{k} = [5, 1]^T$, $\mathbf{k} = [5, 1]^T$ and $\mathbf{k} = [5, 0.5]^T$ as the controller's gains for joint one, two and three, respectively.

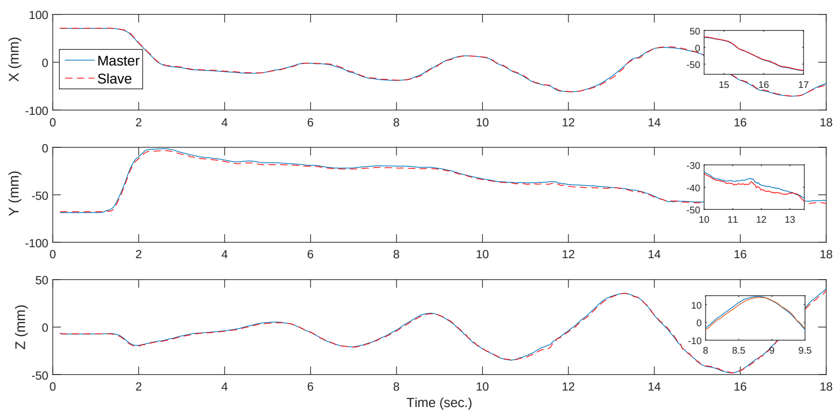

Figure 5.5: Master-Slave comparison using fractional-PD^{μ} controller.

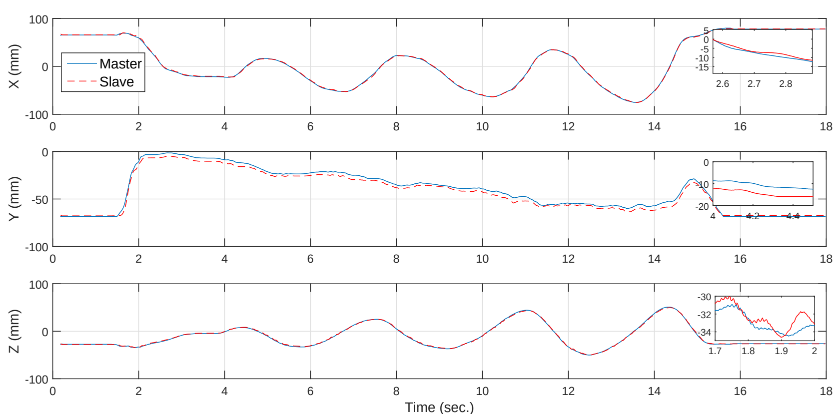

Figure 5.6: Master-Slave comparison using a classical PD control.

Fractional PI^{λ} controller for current-mode control for boost power converters

The commonly used PI-controller is well known to cope with steady state error. Meanwhile, the fractional-PI^{λ} controller sometimes may lead to not desirable performances when applied to integer-order systems. In this sense, it would be of interest to analyze some other desirable characteristics of the PI^{λ} controller.

In this section we contemplate the application of a fractional-PI^{λ} controller to a *current-mode control for boost power converters*[1] (see, (Langarica-Cordoba et al., 2017)) as an illustrative example of the utilization of our design methodology. The application considers the following control diagram

[1] This work was an attempt of a colaboration with Dr. Diego Langarica-Cordoba at Instituto Potosino de Investigación Científica y Tecnológica.

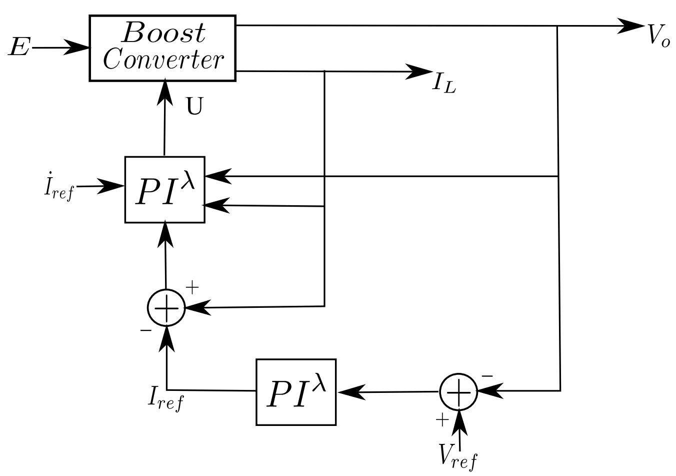

Figure 5.7: Block diagram of the proposed closed-loop system.

for the conventional boost converter system set-up shown in Fig. 5.8.

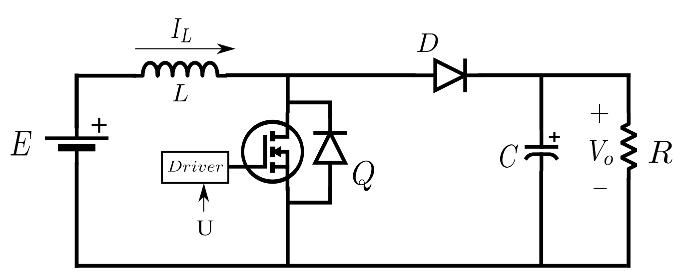

Figure 5.8: Conventional boost converter system set-up.

The non-linear average model of the Boost converter is given by

$$\begin{aligned} \dot{I}_L &= \frac{1}{L}\left[-(1-\mathrm{U})V_o + E\right], \\ \dot{V}_o &= \frac{1}{C}\left[(1-\mathrm{U})I_L - \frac{V_o}{R}\right]. \end{aligned} \tag{5.5}$$

Let

$$\begin{aligned} I_L &= \bar{I}_L + \tilde{i}_L, && (5.6) \\ V_o &= \bar{V}_o + \tilde{v}_o, && (5.7) \\ \mathrm{U} &= \bar{u} + \tilde{u}, && (5.8) \end{aligned}$$

then, the linear model is given by

$$\begin{bmatrix} \dot{\tilde{i}}_L \\ \dot{\tilde{v}}_o \end{bmatrix} = \begin{bmatrix} 0 & -\frac{(1-\bar{u})}{L} \\ \frac{(1-\bar{u})}{C} & -\frac{1}{RC} \end{bmatrix} \begin{bmatrix} \tilde{i}_L \\ \tilde{v}_o \end{bmatrix} + \begin{bmatrix} \frac{\bar{V}_o}{L} \\ -\frac{\bar{I}_L}{C} \end{bmatrix} \tilde{u}. \tag{5.9}$$

Here, we will only deal with the transfer function relating the input as the control signal $\tilde{u}$ with the inductor current $\tilde{i}_L$ as the output (which corresponds to the inner loop of Fig. 5.7. A similar analysis must be done for the outer loop in Fig. 5.7). Such a transfer function is described as

$$\frac{\tilde{i}_L(s)}{\tilde{u}(s)} = \frac{\bar{V}_o}{(1-\bar{u})^2} \frac{1 - \frac{L}{R(1-\bar{u})^2} s}{\frac{LC}{(1-\bar{u})^2} s^2 + \frac{L}{R(1-\bar{u})^2} s + 1}. \tag{5.10}$$

The proposed PI^λ controller is defined as

$$C(s) = k_p + k_i s^{-\lambda}. \tag{5.11}$$

Thus, in order to consider a more realistic escenario we will borrow the system parameter values from (Langarica-Cordoba et al., 2017), where according to this work such values are given as follows

$$\begin{aligned} C &= 518\mu F, & \bar{V}_o &= 24V, \\ L &= 55\mu H, & \bar{u} &= 0.5, \\ E &= 12V, & R &= 4.5\Omega. \end{aligned}$$

Now, in order to derive the $\mathcal{D}$-decomposition curves in the remaining part of the text we will take $\lambda = \frac{1}{2}$. Hence, the closed-loop characteristic function will be given as

$$R\left(Cs\left(k_i\bar{V}_o s^{-\lambda} + k_p\bar{V}_o + Ls\right) + (\tilde{u}-1)^2\right) + 2\bar{V}_o\left(k_i s^{-\lambda} + k_p\right) + Ls = 0. \tag{5.12}$$

Therefore, by applying the results derived in the previous chapter we obtain the stability crossing curves depicted in Fig. 5.9

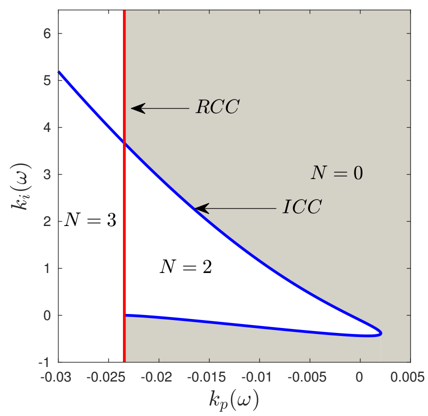

Figure 5.9: Stability region analysis. N stands for the number of roots in the RHP.

According to Fig. 5.9, all parameters belonging to the shaded region are stabilizing controllers. Hence, by taking $k_p = 0.01$ and $k_i = 2$ we obtain the response illustrated in Fig. 5.10 (all simulations consider the nominal values $\bar{V}_o = 24$ V, and $\bar{I}_L = 10.666$ A).

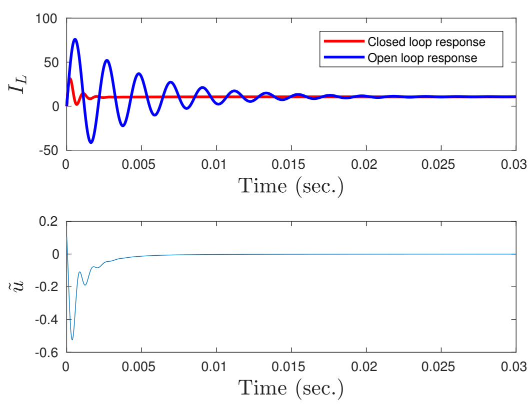

Figure 5.10: Current I_L and control $\tilde{u}$ response, using $k_p = 0.01$, $k_i = 2$ and $\lambda = 0.5$.

The results depicted in Fig. 5.10 show a highly acceptable closed-loop system response in comparison with the open loop system behavior. Now, according to our previous results if follows that choosing gains k_p, k_i in a zone where $N > 0$ in Fig. 5.9 we must obtain an unstable behavior. Such cases are illustrated in Figs. 5.11 and 5.12 where we have chosen, the parameter gains $(k_p, k_i) = (-0.15, 1)$ and $(k_p, k_i) = (-0.027, 3)$.

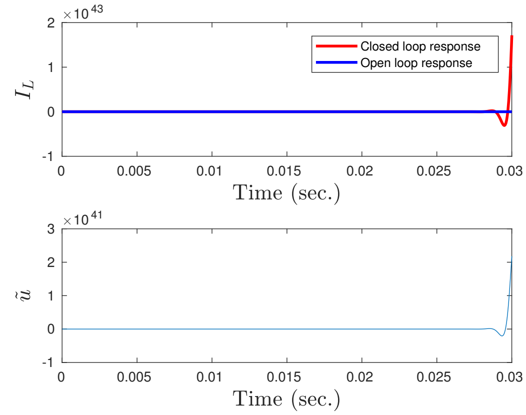

Figure 5.11: Current I_L and control $\tilde{u}$ response, using $k_p = -0.015$ and $k_i = 1$.

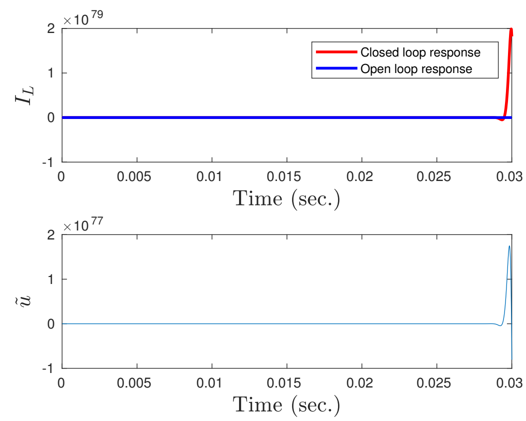

Figure 5.12: Current I_L and control $\tilde{u}$ response, using $k_p = -0.027$ and $k_i = 3$.

Conclusions

Our main goal by considering this example was to show how our methodology can be applied straighforwardly in this kind of systems. It is worth mentioning that a second PI^{λ} controller must be designed for the voltage loop in Fig. 5.7.

For future work we plan to complete the analysis of this application in deeper details. Besides, we persuit to implement the PI^{λ} controller by using a *dSpace*-platform in a real scenario.

Conclusions

In this work fractional calculus has been used to provide a different method to describe physical phenomena and a new tool to develope feedback control techniques.

We have arrived to the conclusion of an existent connection between *infinite-dimensional* order systems and fractional order systems by using the *Laplace*-transform and hence a complex variable analysis in various proposed physical phenomena. We have added a comparison between the infinite order model with the finite generations model for a special system, demostrating the usefulness of the propositions when modeling high order systems. Nevertheless, we have left as a future work the control design analysis for this type of systems but we have exemplified how the multivalued nature of this type of functions in the complex domain must be included as an important part in our future analysis.

Besides, the use of the fractional $PI^{\lambda}D^{\mu}$-type feedback control technique has been discussed and implemented experimentally. We propose that the fractional derivative properties and its implementation methods permit us to use it as a high-frequency noise filter meanwhile it works as a stabilizing controller, but deeper experimental analysis must be done as a future work to have a stronger conclusion. Eventhough, we have focused in the design of fractional PD^{μ} controllers we have considered the same methodology for the design of fractional PI^{λ} controllers. Such a methodology can be easily extended to the fractional $PI^{\lambda}D^{\mu}$ controller and we have considered that case as part of future work.

From the results obtained experimentally, fractional order controllers still have much to be improved in terms of its implementation. Hence, implementing fractional order controllers is concluded to be a research area with many gaps and could be a part of our forthcoming interests. Digital technology limits are an obstacle for implementing fractional derivatives and integrals due to its definitions itself. The definition of a non-integer order derivative or integral is still an issue for the *Fractional Calculus* community and hence a great obstacle and open problem in the area.

Therefore, *Fractional Calculus* has a significat amount of open problems. Our main future work will consists in trying to find systems which should or can be modeled by means of this mathematical tool. There is a great interest in using *Fractional Calculus* to provide better models for non-linear, distribuided-parameters, large-scale or cyber-physical systems, to mention some of them.

Finally, we conclude that the aims of this work were achieved and we are aware of the proportions of our contribution, this permit us think about continuing working in this research area and bring out more possible applications and solutions to the actual problems in engineering.

6 Bibliography

Abu-Saris, R. and Al-Mdallal, Q. (2013). On the asymptotic stability of linear system of fractional-order difference equations. *Fractional calculus and applied analysis*, 16(3).

Adams, J. L., Veillette, R. J., and Hartley, T. T. (2012). Conjugate-order systems for signal processing: stability, causality. boundedness, compactness. *Signal, Image and Video Processing*.

Arfken, G. (2005). *Mathematical methods for physicists*. Elsevier academic press.

Astrom, K. J. and Kumar, P. R. (2014). Control: A perspective. *Automatica*, 50:3–43.

Baleanu, S. J. P., Ranjbar, A., Ghaderi, R., and Abdeljawad, T. (2010). Mittag-leffler stability theorem for fractional nonlinear systems with delay. *Abstract and applied analysis*.

Bar-Yam, Y. (1997). *Dynamics of complex systems*. Addison-Wesley.

Bellman, R. and Cooke, K. L. (1963). *Differential-difference equations*. Academic Press.

Bhattacharyya, S. P., Chapellat, H., and Keel, L. H. (1995). *Robust control: the parametric approach*. New Jersey, NJ: Prentice Hall.

Bonnet, C., Fioravanti, A. R., and Partington, J. R. (2009). Stability of neutral systems with multiple delays and ppole asymptotic to the imaginary axis. In *48th IEEE conference on decision and control and 28th chinese control conference*, pages 269–273.

Bonnet, C. and Partington, J. R. (2000). Coprime factorizations and stability of fractional differential systems. *Systems and Control Letters*, 41:167–174.

Bonnet, C. and Partington, J. R. (2002). Analysis of fractional delay systems of retarded and neutral type. *Automatica*, 38:1133–1138.

Boudjehem, B. and Boudjehem, D. (2016). Fractional pid controller design based on minimizing performance indices. *IFAC-PapersOnLine*, 49(9):164 – 168. 6th IFAC Symposium on System Structure and Control SSSC 2016.

Buslowicz, M. (2008). Stability of linear continuous-time fractional order systems with delays of the retarted type. *Bulletin of the Polish Academy of Sciences*, 56(4):319–324.

Caponetto, R. (2010). *Fractional Order Systems: Modeling and Control Applications*. World Scientific Series on Nonlinear Science: Series A. World Scientific.

Caputo, M. and Fabrizio, M. (2015). A new definition of fractional derivative without singular kernel. *Progr. Fract. Differ. Appl*, 1(2):1–13.

Cohen, H. (2007). *Complex analysis with application in science and engineering*. Springer.

Cohn, H. (1967). *Conformal Mapping On Riemann Surfaces*. McGraw-Hill.

Coimbra, C. F. M. (2003). Mechanics with variable-order differential operators. *Annalen der physik*, 12(11-12):692–703.

Curtain, R. F. (1992). *A Synthesis of Time and Frequency Domain Methods for the Control of Infinite-Dimensional Systems: A System Theoretic Approach*, chapter 5, pages 171–223. Frontiers in Applied Mathematics.

Curtain, R. F. and Zwart, H. (1995). *An Introduction to Infinite-Dimensional Linear Systems Theory*, volume 21. Texts in Applied Mathematics.

de Oliveira, E. C. and Machado, J. A. T. (2014). A review of definitions for fractional derivatives and integral. *Mathematical problems in engineering*.

Deng, W., Li, C., and L´u, J. (2007). Stability analysis of linear fractional differential system with multiple time delays. *Nonlinear Dynamics*.

Dorčák, L., Valsa, J., Gonzalez, E., Terpák, J., Petráš, I., and Pivka, L. (2013). Analogue realization of fractional-order dynamical systems. *Entropy*, 15(10):4199–4214.

Dulău, M., Gligor, A., and Dulău, T.-M. (2017). Fractional order controllers versus integer order controllers. *Procedia Engineering*, 181:538–545.

Farkas, H. M. and Kra, I. (1980). *Riemann Surfaces*, volume 71 of *Graduate Texts in Mathematics*. Springer.

Fioravanti, A. R., Bonnet, C., ´Ozbay, H., and Niculescu, S.-I. (2010). A numerical method to find stability windows and unstable poles for linear neutral time-delay systems. *IFAC Proceedings Volumes*, 43(2):183 – 188. 9th IFAC Workshop on Time Delay Systems.

Galvao, R. K. H., Hadjiloucas, S., Kienitz, K. H., Paiva, H. M., and Afonso, R. J. M. (2013). Fractional order modeling of large three-dimensional rc networks. *IEEE Transactions on Circuits and Systems I: Regular Papers*, 60(3):624–637.

Genin, R. and Calvez, L. C. (1970). Existence of an overshoot in the step-function response of a linear circuit. *Electronics Letters*, 6(3):55–56.

Gómez-Aguilar, J., Razo-Hernández, R., and Granados-Lieberman, D. (2014). A physical interpretation of fractional calculus in observables terms: analysis of the fractional time constant and the transitory response. *Revista mexicana de física*, 60(1):32–38.

Gómez-Aguilar, J. F., Yépez-Martínez, H., Calderón-Ramón, C., Cruz-Orduña, I., Escobar-Jiménez, R. F., and Olivares-Peregrino, V. H. (2015). Modeling of a mass-spring-damper system by fractional derivatives with and without a singular kernel. *Entropy*, 17(9):6289–6303.

Goodwine, B. (2014). Modeling a multi-robot system with fractional-order differential equations. *IEEE International Conference on Robotics & Automation*.

Goodwine, B. (2016). Fractional-order approximations to implicitly-defined operators for modeling and control of networked mechanical systems. In *2016 IEEE International Symposium on Intelligent Control (ISIC)*, pages 1–7.

Goodwine, B. (2018). Approximations for implicitly-defined dynamics of networks of simple mechanical components. In *26th Mediterranean Conference on Control and Automation*.

Gorenflo, R., Kilbas, A. A., Mainardi, F., and Rogosin, S. V. (2014). *Mittag-Leffler Functions, Related Topics and Applications*. Springer Monographs in Mathematics.

Gryazina, E. N. (2004). The d-decomposition theory. *Automation and Remote Control*, 65(12):1872–1884.

Gryazina, E. N., Polyak, B. T., and Tremba, A. A. (2008). D-decomposition technique state-of-the-art. *Automation and Remote Control*, 69(12):1991–2026.

Gu, K., Kharitonov, V. L., and Chen, J. (2003). *Stability of time-delay systems*. Birkh´auser Boston.

Guel-Cortez, A.-J., Méndez-Barrios, C.-F., Romero, J., Ramírez-Rivera, V., and González-Galván, E. (2018). Fractional$-pd^{\mu}$ controllers design for lti-systems with time-delay. a geometric approach. In *2018-5th International Conference on Control, Decision and Information Technologies*.

Hamamci, S. E. (2007). An algorithm for stabilization of fractional-order time delay systems using fractional-order pid controllers. *IEEE Transactions on Automatic Control*.

Hamamci, S. E. (2008). Stabilization using fractional-order pi and pid controllers. *Nonlinear Dynamics*, 51(1):329–343.

Hernández-Díez, J.-E., Niculescu, S.-I., Méndez-Barrios, C.-F., and González-Galván, E. (2016). A transparent bilaterla control scheme for a local teleoperation system using proportional-delayed controllers. *AMRob Journal, Robotics: Theory and Applications*, 49(2):1–7.

Heymans, N. and Bauwens, J.-C. (1994). Fractal rheological models and fractional differential equations for viscoelastic behavior. *Rheologica Acta*, 33:210–219.

Ho, M.-T., Datta, A., and Bhattacharyya, S. (1999). Generalizations of the hermite–biehler theorem. *Linear Algebra and its Applications*, 302:135–153.

Ho, M.-T., Datta, A., and Bhattacharyya, S. (2000). Generalizations of the hermite–biehler theorem: the complex case. *Linear Algebra and Its Applications*, 320(1-3):23–36.

Hollkamp, J. P., Sen, M., and Semperlotti, F. (2018). Model-order reduction of lumped parameter systems via fractional calculus. *Journal of Sound and Vibration*, 419:526–543.

Holmgren, H. (1867). Omdiffedifferentiation med indices af havd natur som helst. *Kungliga svenska ventenkaps-akadamiens*, 5(11):1–83.

Jacob, J. A., Tare, A. V., Vyawahare, V. A., and Pande, V. N. (2016). A review of time domain, frequency domain and stability analysis of linear complex-order systems. In *IEEE International WIE conference on electrical and computer engineering*.

Karci, A. (2015). The physical and geometrical interpretation of fractional order derivatives. *Universal journal of engineering science*, 3(4):53–63.

Koeller, R. C. (1984). Applications of fractional calculus to the theory of viscoelasticity. *Journal of Applied Mathematics*, 51.

Kolmanovskii, V. and Nosov, V. (1986). *Stability of Functional Differential Equations*. Mathematics in Science and Engineering. Elsevier Science.

Langarica-Cordoba, D., Leyva-Ramos, J., Diaz-Saldierna, L. H., and Ramirez-Rivera, V. M. (2017). Non-linear current-mode control for boost power converters: a dynamic backstepping approach. *IET Control Theory and Applications*, 11(14):2261–2269.

Lenka, I. K. and Banerjee, S. (2018). Sufficient conditions for asymptotic stability and stabilization of autonomous fractional order systems. *Nonlinear science and numerical simulation*, 56:365–379.

LePage, W. R. (1980). *Complex Variables and the Laplace Transform for Engineers*. New York: Dover Publications.

Leyden, K. and Goodwine, B. (2016). Fractional-order system identification for health monitoring of cooperating robots*. In *IEEE International Conference on Robotics and Automation*.

Li, C., Qian, D., and Chen, Y. (2011). On riemann-liouville and caputo derivatives. *Discrete Dynamics in Nature and Society*.

Li, Y., Chen, Y., and Podlubny, I. (2009). Mittag-leffler stability of fractional order nonlinear dynamic systems. *Automatica*, 45:1965–1969.

Li, Y., Chen, Y., and Podlubny, I. (2010). Stability of fractional-order nonlinear dynamic systems: Lyapunov direct method and generilized mittag-leffler stability. *Computers and Mathematics with Applications*, 59:1810–1821.

Liacu, B., Koru, A., Özbay, H., Niculescu, S.-I., and Andriot, C. (2013). Optimizing low-order controllers for haptic systems under delayed feedback. *Control Engineering Practice, vol. 21, pp. 655-668*.

Liouville, J. (1832). Mémoire sur quelques quéstions de géometrie et de mécanique, et sur un nouveau genre de calcul pour résoudre ces quéstions. *J. Ecole Polytech*, 13:1–69.

Lundstrom, B. N., Higgs, M. H., Spain, W. J., and Fairhall, A. L. (2008). Fractional differentiation by neocortical pyramidal neurons. *Nature neuroscience*, 11(11).

Magin, R. L. (2006). *Fractional calculus in bioengineering*. Begell House Redding.

Marsden, J. and Hoffman, M. (1999). *Basic Complex Analysis*. W. H. Freeman.

Martínez-García, M., Gordon, T., and Shu, L. (2017). Extended crossover model for human-control of fractional order plants. *IEEE Access*, 5:27622–27635.

Matignon, D. (1996). Stability results for fractional differential equations with applications to control processing. In *Computational engineering in systems applications*, volume 2, pages 963–968. IMACS, IEEE-SMC Lille, France.

Matignon, D. (1998). Stability properties for generalized fractional differential systems. In *ESAIM: proceedings*, volume 5, pages 145–158. EDP Sciences.

Mayes, J. and Sen, M. (2011). Approximation of potential-driven flow dynamics in large-scale self-similar tree networks. *Proceedings of the royal society a mathematical, physical and engineering sciences*, 467(2134):2810–2824.

Meerschaert, M. M., Mcgough, R. J., Straka, P., and Zhou, Y. (2012). Fractional calculus models for medical ultrasound. In *4th International Conference on Porous Media*.

Mendiola-Fuentes, J. and Melchor-Aguilar, D. (2018). Modification of mikhailov stability criterion for fractional commensurate order systems. *Journal of the Franklin Institute*, pages 1–12.

Merrikh-Bayat, F. and Afshar, M. (2008). Extending the root-locus method to fractional-order systems. *Journal of applied mathematics*.

Merrikh-Bayat, F. and Karimi-Ghartemani, M. (2008). On the essential instabilities caused by fractional-order transfer functions. *Mathematical Problems in Engineering*.

Michiels, W. and Niculescu, S.-I. (2007). *Stability and stabilization of time-delay systems. An eigenvalue-based approach*. Society for Industrial and Applied Mathematics.

Miller, K. and Ross, B. (1993). *An Introduction to the Fractional Calculus and Fractional Differential Equations*. Wiley.

Mohammadi, A., Tavakoli, M., and Jazayeri, A. (2008). Phansim: A simulink toolkit for the sensable phantom haptic device. In *23rd CANCAM*.

Monje, C., Chen, Y., Vinagre, B., Xue, D., and Feliu-Batlle, V. (2010). *Fractional-order Systems and Controls: Fundamentals and Applications*. Advances in Industrial Control. Springer London.

Moornani, K. A. and Haeri, M. (2011). Neccesary and sufficient conditions for bibo-stability of some fractional delay systems of neutral type. *transactions on automatic control*, 56(1):125–128.

Moslehi, L. and Ansari, A. (2016). Some remarks on inverse laplace trnasforms involving conjugate branch points with applications. *UPB Scientific Bulleting, Series A: Applied Mathematics and Physics*, 78(3):107–118.

Mussat, L. (2017). The era of automatic control. *CNRS Le Journal*.

Nakagawa, M. and Sorimachi, K. (1992). Basic characteristics of a fractance device. *IEICE Transactions on Fundamentals of Electronics, Communications and Computer Science*, E75-A(12).

Needham, T. (1997). *Visual Complex Analysis*. Clarendon Press, Oxford.

Neimark, J. (1949). D-subdivisions and spaces of quasi-polynomials. *Prinkl. Math. Mech., vol. 10, pp. 349-380*.

Neto, J. P., Coelho, R. M., Valério, D., Vinga, S., Sierouciuk, D., Malesza, W., Macias, M., and Dzieliński, A. (2017). Variable order differential models of bone remodelling. *IFAC-PapersOnLine*, 50:8066–8071.

Nguyen, L. H. V. and Bonnet, C. (2012). Stability analysis of fractional neutral time-delay systems with multiple chains of ppole asymptotic to soame points in the imaginary axis. In *Conference on desicion and control*, pages 6891–6895.

Oldham, K. B. and Spanier, J. (2006). *The fractional calculus. Theory and applications of differentiation and integration to arbitrary order*. Dover publications, inc.

Oprzędkiewicz, K. and Dziedzic, K. (2017). A tuning of a fractional order pid controller with the use of particle swarm optimization method. In *Artificial Intelligence and Soft Computing*, pages 394–407. Springer International Publishing.

Ortigueira, M. D. and Machado, J. A. T. (2015). What is a fractional derivative? *Journal of Computational Physics*, 293:4–13.

Petráš, I. (2011a). Fractional derivatives, fractional integrals, and fractional differential equations in matlab. In Assi, A., editor, *Engineering Education and Research Using MATLAB*, chapter 10. InTech, Rijeka.

Petráš, I. (2011b). *Fractional-order nonlinear systems. Modeling, analysis and simulation*. Springer.

Podlubny, I. (1994). Fractional-order systems and fractional-order controllers. *Slovak Academy of Science, Institute of Experimental Physics, UEF 03-94, Kosice*, pages 1–18.

Podlubny, I. (1999). *Fractional Differential Equations*. Mathematics in science and engineering. Academic Press.

Podlubny, I. (2001). Geometric and physical interpretation of fractional integration and fractional differentiation. *arXiv preprint math/0110241*.

Podlubny, I., Petraš, I., Vinagre, B. M., O'leary, P., and Dorčák, L. (2002). Analogue realizations of fractional-order controllers. *Nonlinear dynamics*, 29(1):281–296.

Pontryagin, L. S. (1955). On the zeros of some elementary trascendental functios. *American Mathematical Society Translations*, 1(2):95–110.

Radwan, A. G., Soliman, A., Elwakil, A. S., and Sedeek, A. (2009). On the stability of linear systems with fractional-order elements. *Chaos, Solitons & Fractals*, 40(5):2317–2328.

Riemann, B. (1847). Versuch einer auffassung der integration und differentiation. *Gesammelte Werke*, pages 331–334.

Sabatier, J. and farges, C. (2012). Onthestsystems of commensurate fractional order systems. *International journal of bifurcation and chaos*, 22(4).

Sen, M., Hollkamp, J. P., Semperlotti, F., and Goodwine, B. (2018a). Implicit and fractional-derivative operators in infinite networks of integer-order components. *Chaos, Solitons & Fractals*, 114:186–192.

Sen, M., P. Hollkamp, J., Semperlotti, F., and Goodwine, B. (2018b). Implicit operators for networked mechanical and thermal systems with integer-order components.

Shah, P. and Agashe, S. (2016). Review of fractional pid controller. *Mechatronics*, 38:29–41.

Sigdell, J. E. (1967). On the existence of an overshoot in the step-function response of a linear circuit. *Electronics Letters*, 3(2):66–68.

Simpson, R., Jaques, A., nez, H. N., and Almonacid, A. (2012). Fractional calculus as a mathematical tool to improve the modeling of mass transfer phenomena in food processing. *Food Engineering Reviews*, 5(1).

Singal, A. (2013). The paradox of power loss in a lossless infinite transmission line.

Singla, A. (2013). Vibration suppression of a cart-flexible pole system using a hybrid controller. In *1st international conference on machines and mechanisms*.

Stojic, M. and Siljak, D. (1965). Generalization of hurwitz, nyquist, and mikhailov stability criteria. *IEEE Transactions on Automatic Control*, 10(3):250–254.

Tavakoli, M., Patel, R., Moallem, M., and Aziminejad, A. (2003). *Haptics for Teleoperated Surgical Robotic Systems*. World Scientific Publishing Company.

Tavassoli, M. . H., Tavassoli, A., and Rahimi, M. R. O. (2013). The geometric and physical interpretation of fractional order derivatives of polynomial functions. *Differential geometry-dynamical systems*, 15:93–104.

Tavazoei, M. S. (2010). Notes on integral performance indices in fractional-order control systems. *Journal of Process Control*, 20:285–291.

Tavazoei, M. S. (2011). Overshoot in the step response of fractional-order control systems. *Journal of Process Control*.

Tavazoei, M. S. (2012). From traditional to fractional pi control: A key for generalization. *IEEE Industrial Electronics Magazine*, 6(3):41–51.

Tavazoei, M. S. (2014). Time response analysis of fractional-order control systems: a survey on recent results. *Fractional calculus and applied analysis*, 17(2).

Tavazoei, M. S. and Haeri, M. (2009). A note on the stability of fractional order systems. *Mathematics and computers in simulation*, 79:1566–1576.

Uchaikin, V. V. (2013). *Fractional Derivatives for Physicists and Engineers: Volume I Background and Theory*. Nonlinear Physical Science. Springer Berlin Heidelberg.

Valerio, D. and da Costa, J. S. (2004). Ninteger: a non-integer control toolbox for matlab. In *Fractional Differential Applications, Bordeaux*.

Valério, D. and da Costa, J. S. (2013). *An Introduction to Fractional Control*. Control, Robotics and Sensors Series. Institution of Engineering and Technology.

van Enk, S. J. (2000). Paradoxical behavior of an infinite ladder network of inductors and capacitors. *American Journal of Physics*, 68(9).

Wall, H. S. (1967). *analytic theory of continued fractions*. Chelsea publishing company. Bronx, N. Y.

Westerlund, S. and Ekstam, L. (1994). Capacitor theory. *IEEE Transactions on Dielectrics and Electrical Insulation*, 1(5).

Wyrwas, M. and Mozyrska, D. (2015). On mittag-leffler stability of fractional order difference systems. In *Latawiec K. et al. (eds) Advances in Modelling and Control of Non-integer-Order Systems. Lecture Notes in Electrical Engineering*.

Xiao, M., Zheng, W. X., Jiang, G., and Cao, J. (2017). Stability and bifurcation of delayed-order dual congestion control algorithms. *IEE transactions on automatic control*, 62(9):4819–4826.

Zagórowska, M., Baranowski, J., Bauer, W., Dziwiński, T., Piatek, P., and Mitkowski, W. (2015). Lyapunov direct method for non-integer order systems. In *Latawiec K. et al. (eds) Advances in Modelling and Control of Non-integer-Order Systems. Lecture Notes in Electrical Engineering*.

Zemanian, A. H. (1988). Infinite electrical networks: a reprise. *IEEE Transactions on circuits and systems*, 35(11):1346–1358.

Zhang, F. and Li, C. (2011). Stability analysis of fractional differential systems with order lying in (1,2). *Advances in Difference Equations*.

Zhao, D. and Luo, M. (2017). General conformable fractional derivative and its physical interpretation. *Calcolo*, 54(3):903–917.